



National Library  
of Canada

Acquisitions and  
Bibliographic Services Branch

395 Wellington Street  
Ottawa, Ontario  
K1A 0N4

Bibliothèque nationale  
du Canada

Direction des acquisitions et  
des services bibliographiques

395, rue Wellington  
Ottawa (Ontario)  
K1A 0N4

*Your file - Votre référence*

*Our file - Notre référence*

## NOTICE

The quality of this microform is heavily dependent upon the quality of the original thesis submitted for microfilming. Every effort has been made to ensure the highest quality of reproduction possible.

If pages are missing, contact the university which granted the degree.

Some pages may have indistinct print especially if the original pages were typed with a poor typewriter ribbon or if the university sent us an inferior photocopy.

Reproduction in full or in part of this microform is governed by the Canadian Copyright Act, R.S.C. 1970, c. C-30, and subsequent amendments.

## AVIS

La qualité de cette microforme dépend grandement de la qualité de la thèse soumise au microfilmage. Nous avons tout fait pour assurer une qualité supérieure de reproduction.

S'il manque des pages, veuillez communiquer avec l'université qui a conféré le grade.

La qualité d'impression de certaines pages peut laisser à désirer, surtout si les pages originales ont été dactylographiées à l'aide d'un ruban usé ou si l'université nous a fait parvenir une photocopie de qualité inférieure.

La reproduction, même partielle, de cette microforme est soumise à la Loi canadienne sur le droit d'auteur, SRC 1970, c. C-30, et ses amendements subséquents.

Canada

**THE UNIVERSITY OF ALBERTA**

**FLUOROMETRY OF QUIN-2, FURA-2, AND THEIR  
CALCIUM COMPLEXES**

**By**

**Shahla Shakerinia**

**A THESIS**

**SUBMITTED TO THE FACULTY OF GRADUATE STUDIES AND RESEARCH  
IN PARTIAL FULFILLMENT OF THE REQUIREMENTS FOR THE DEGREE  
OF MASTER OF SCIENCE**

**DEPARTMENT OF CHEMISTRY**

**EDMONTON, ALBERTA**

**FALL 1994**



National Library  
of Canada

Acquisitions and  
Bibliographic Services Branch

395 Wellington Street  
Ottawa, Ontario  
K1A 0N4

Bibliothèque nationale  
du Canada

Direction des acquisitions et  
des services bibliographiques

395, rue Wellington  
Ottawa (Ontario)  
K1A 0N4

*Vostra lib. - Votre référence*

*Our lib. - Notre référence*

**The author has granted an irrevocable non-exclusive licence allowing the National Library of Canada to reproduce, loan, distribute or sell copies of his/her thesis by any means and in any form or format, making this thesis available to interested persons.**

**L'auteur a accordé une licence irrévocable et non exclusive permettant à la Bibliothèque nationale du Canada de reproduire, prêter, distribuer ou vendre des copies de sa thèse de quelque manière et sous quelque forme que ce soit pour mettre des exemplaires de cette thèse à la disposition des personnes intéressées.**

**The author retains ownership of the copyright in his/her thesis. Neither the thesis nor substantial extracts from it may be printed or otherwise reproduced without his/her permission.**

**L'auteur conserve la propriété du droit d'auteur qui protège sa thèse. Ni la thèse ni des extraits substantiels de celle-ci ne doivent être imprimés ou autrement reproduits sans son autorisation.**

ISBN 0-315-95110-9

**Canada**

Name Shahla Shakerina

Dissertation Abstracts International is arranged by broad, general subject categories. Please select the one subject which most nearly describes the content of your dissertation. Enter the corresponding four-digit code in the spaces provided.

0486

U.M.I

SUBJECT TERM

SUBJECT CODE

## Subject Categories

### THE HUMANITIES AND SOCIAL SCIENCES

#### COMMUNICATIONS AND THE ARTS

Architecture	0729
Art History	0377
Cinema	0900
Dance	0378
Fine Arts	0357
Information Science	0723
Journalism	0391
Library Science	0369
Mass Communications	0708
Music	0413
Speech Communication	0459
Theater	0465

#### EDUCATION

General	0515
Administration	0514
Adult and Continuing	0516
Agricultural	0517
Art	0273
Bilingual and Multicultural	0282
Business	0688
Community College	0275
Curriculum and Instruction	0727
Early Childhood	0518
Elementary	0524
Finance	0277
Guidance and Counseling	0519
Health	0680
Higher	0745
History of	0520
Home Economics	0278
Industrial	0521
Language and Literature	0279
Mathematics	0280
Music	0522
Philosophy of	0998
Physical	0523

Psychology	0525
Reading	0535
Religious	0527
Sciences	0714
Secondary	0533
Social Sciences	0534
Sociology of	0340
Special	0529
Teacher Training	0530
Technology	0710
Tests and Measurements	0288
Vocational	0747

#### LANGUAGE, LITERATURE AND LINGUISTICS

Language	
General	0679
Ancient	0289
Linguistics	0290
Modern	0291
Literature	
General	0401
Classical	0294
Comparative	0295
Medieval	0297
Modern	0298
African	0316
American	0591
Asian	0305
Canadian (English)	0352
Canadian (French)	0355
English	0593
Germanic	0311
Latin American	0312
Middle Eastern	0315
Romance	0313
Slavic and East European	0314

#### PHILOSOPHY, RELIGION AND THEOLOGY

Philosophy	0422
Religion	
General	0318
Biblical Studies	0321
Clergy	0319
History of	0320
Philosophy of	0322
Theology	0469

#### SOCIAL SCIENCES

American Studies	0323
Anthropology	
Archaeology	0324
Cultural	0326
Physical	0327
Business Administration	
General	0310
Accounting	0272
Banking	0770
Management	0454
Marketing	0338
Canadian Studies	0385
Economics	
General	0501
Agricultural	0503
Commerce-Business	0505
Finance	0508
History	0509
Labor	0510
Theory	0511
Folklore	0358
Geography	0366
Gerontology	0351
History	
General	0578

Ancient	0579
Medieval	0581
Modern	0582
Black	0328
African	0331
Asia, Australia and Oceania	0332
Canadian	0334
European	0335
Latin American	0336
Middle Eastern	0333
United States	0337
History of Science	0585
Law	0398
Political Science	
General	0615
International Law and Relations	0616
Public Administration	0617
Recreation	0814
Social Work	0452
Sociology	
General	0626
Criminology and Penology	0627
Demography	0938
Ethnic and Racial Studies	0631
Individual and Family Studies	0628
Industrial and Labor Relations	0629
Public and Social Welfare	0630
Social Structure and Development	0700
Theory and Methods	0344
Transportation	0709
Urban and Regional Planning	0999
Women's Studies	0453

### THE SCIENCES AND ENGINEERING

#### BIOLOGICAL SCIENCES

Agriculture	
General	0473
Agronomy	0285
Animal Culture and Nutrition	0475
Animal Pathology	0476
Food Science and Technology	0359
Forestry and Wildlife	0478
Plant Culture	0479
Plant Pathology	0480
Plant Physiology	0817
Range Management	0777
Wood Technology	0746

#### Biology

General	0306
Anatomy	0287
Biostatistics	0308
Botany	0309
Cell	0379
Ecology	0329
Entomology	0353
Genetics	0369
Limnology	0793
Microbiology	0410
Molecular	0307
Neuroscience	0317
Oceanography	0416
Physiology	0433
Radiation	0821
Veterinary Science	0778
Zoology	0472

#### Biophysics

General	0786
Medical	0760

#### EARTH SCIENCES

Biogeochemistry	0425
Geochemistry	0996

Geodesy	0370
Geology	0372
Geophysics	0373
Hydrology	0388
Mineralogy	0411
Paleobotany	0345
Paleoecology	0426
Paleontology	0418
Paleozoology	0985
Palynology	0427
Physical Geography	0368
Physical Oceanography	0415

#### HEALTH AND ENVIRONMENTAL SCIENCES

Environmental Sciences	0768
Health Sciences	
General	0566
Audiology	0300
Chemotherapy	0992
Dentistry	0567
Education	0350
Hospital Management	0769
Human Development	0758
Immunology	0982
Medicine and Surgery	0564
Mental Health	0347
Nursing	0569
Nutrition	0570
Obstetrics and Gynecology	0380
Occupational Health and Therapy	0354
Ophthalmology	0381
Pathology	0571
Pharmacology	0419
Pharmacy	0572
Physical Therapy	0382
Public Health	0573
Radiology	0574
Recreation	0575

Speech Pathology	0460
Toxicology	0383
Home Economics	0386

#### PHYSICAL SCIENCES

##### Pure Sciences

Chemistry	
General	0485
Agricultural	0749
Analytical	0486
Biochemistry	0487
Inorganic	0488
Nuclear	0738
Organic	0490
Pharmaceutical	0491
Physical	0494
Polymer	0495
Radiation	0754
Mathematics	0405
Physics	
General	0605
Acoustics	0986
Astronomy and Astrophysics	0606
Atmospheric Science	0608
Atomic	0748
Electronics and Electricity	0607
Elementary Particles and High Energy	0798
Fluid and Plasma	0759
Molecular	0609
Nuclear	0610
Optics	0752
Radiation	0756
Solid State	0611
Statistics	0463

##### Applied Sciences

Applied Mechanics	0346
Computer Science	0984

#### Engineering

General	0537
Aerospace	0538
Agricultural	0539
Automotive	0540
Biomedical	0541
Chemical	0542
Civil	0543
Electronics and Electrical	0544
Heat and Thermodynamics	0348
Hydraulic	0545
Industrial	0546
Marine	0547
Materials Science	0794
Mechanical	0548
Metallurgy	0743
Mining	0551
Nuclear	0552
Packaging	0549
Petroleum	0765
Sanitary and Municipal	0554
System Science	0790
Geotechnology	0428
Operations Research	0796
Plastics Technology	0795
Textile Technology	0994

#### PSYCHOLOGY

General	0621
Behavioral	0384
Clinical	0622
Developmental	0620
Experimental	0623
Industrial	0624
Personality	0625
Physiological	0989
Psychobiology	0349
Psychometrics	0632
Social	0451

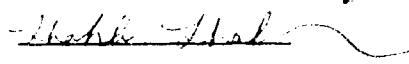


**THE UNIVERSITY OF ALBERTA**  
**RELEASE FORM**

NAME OF AUTHOR: Shahla Shakerinia  
TITLE OF THESIS: Fluorometry of Quin-2, Fura-2, and their  
Calcium Complexes  
DEGREE: Master of Science  
YEAR THIS DEGREE  
GRANTED: 1994

Permission is hereby granted to THE UNIVERSITY OF ALBERTA LIBRARY to reproduce single copies of this thesis and to lend or sell such copies for private, scholarly or scientific research purposes only.

The author reserves other publication rights, and neither the thesis nor extensive extracts from it may be printed or otherwise reproduced without the author's written permission.

  
(Student's Signature)

Permanent Address;  
# 2403, 8-Banyay Ave.  
Kitimat, British Colombia

DATE: Sept 28/1994

**THE UNIVERSITY OF ALBERTA**

**FACULTY OF GRADUATE STUDIES AND RESEARCH**

The undersigned certify that they have read, and recommend to the Faculty of Graduate Studies and Research for acceptance, a thesis entitled **FLUOROMETRY OF QUIN-2, FURA-2, AND THEIR CALCIUM COMPLEXES** submitted by **SHAHLA SHAKEKINIA** in partial fulfillment of the requirements for the degree of **MASTER OF SCIENCE**.

B. Kratochvil

**B. Kratochvil, Supervisor**

James A. Plambeck

**J. Plambeck**

Peter Sporns

**P. Sporns, External Examiner**

**Date:** Sept 28 / 1994

*To my Family  
and  
my Husband*

## **Abstract**

In this work the UV-visible absorption and fluorescence properties of two calcium indicator dyes, quin-2 and fura-2, and their calcium complexes were studied. The quantum efficiencies of the dyes were determined to be 0.03 for quin-2 and 0.22 for fura-2 using quinine sulfate as standard. Also, the effect of variation in environmental conditions such as temperature, pH and ultraviolet radiation on the quantum yields were examined.

The stoichiometries of quin-2/Ca<sup>2+</sup> and fura-2/Ca<sup>2+</sup> were determined to be 1:1 from slopes of plots of the normalized fluorescence intensity of a series of calcium-dye solutions against the ionic calcium concentration on a logarithmic scale. The calcium-dye calibration solutions were prepared using Ca-EGTA buffers. The conditional association constant of Ca<sup>2+</sup>(quin-2) was determined to be about  $2 \times 10^7$  at physiological conditions and that for Ca<sup>2+</sup>(fura-2) was determined to be  $5 \times 10^6$  to  $8 \times 10^6$ . The affinities of these dyes for calcium were studied at various temperatures, ionic strengths and physiological pH values. The conditional association constants of Ca<sup>2+</sup>(quin-2) and Ca<sup>2+</sup>(fura-2) were also determined in the presence of 1 millimolar free magnesium to be  $8 \times 10^7$  and  $4 \times 10^7$  respectively. Ca-Mg-EGTA buffers were used for preparation of the calibration solutions.

Because of the high affinity of quin-2 and fura-2 for calcium, the fluorescence signals of the dyes saturate at [Ca<sup>2+</sup>] greater than 1 to 10 micromolar. This makes the dyes quite suitable for intra-cellular [Ca<sup>2+</sup>] measurements but not for the extra-cellular media (biological fluids) in which free calcium concentrations fall in the millimolar range. Hence EDTA, which is a strong chelating agent for calcium and magnesium, was used for the



determination of total calcium in a milk diffusate (obtained by dialysis) by masking magnesium, an interfering cation, and buffering the calcium to submicromolar levels. Unfortunately, the presence of other ligands in the milk diffusate (citrate and phosphate) makes determination of ionic calcium by this method difficult. Concentrations of EDTA to be added were estimated by approximating the total calcium and magnesium in the diffusate from literature values. To provide additional background, total calcium and magnesium were also determined by ICP atomic emission spectroscopy.

## **Acknowledgments**

I would like to express my deepest appreciation and gratitude to Dr. B. Kratochvil for his supervision and encouragement throughout the course of this thesis.

Special thanks to Dr. M. Palcic for providing her laboratory facilities and her helpful recommendations.

The author is grateful to the staff of the Chemistry Department Machine Shop, especially Mr. R. Lipiecki, for the design and construction of the thermostated sample holder for the fluorometer.

Appreciation also goes to Ms. D. Mahlow and Ms. A. Dunn in micro-analytical laboratory for their assistance in weighing the dye samples

I would also like to thank the research group for their help and support, especially Mr. K. Donkor for his generous assistance and Mr. H. Ren for his assistance in operation of the ICP - AES.

Finally, I extend my gratitude to the University of Alberta Chemistry Department for financial support and assistance.

## **Table of Contents**

<b>Chapter</b>	<b>Page</b>
1. Introduction.....	1
1. Background on Ionic Calcium Measurements.....	1
1.1 Methods for ionic calcium determination in biological fluid.....	2
1.1.1 Ion-selective electrode potentiometry.....	2
1.1.2 Spectrophotometry using indicator dyes.....	2
1.1.3 Ion-exchange chromatography.....	4
1.2 Methods for intra-cellular free calcium determination.....	5
1.2.1 Ion-selective microelectrodes (ISM).....	5
1.2.2 Calcium-activated photoproteins.....	6
1.2.3 Bis-azo indicator dyes.....	7
1.2.4 Tetracarboxylate chelating fluorescent dyes.....	7
2. Fluorometry.....	12
2. Characterization of Quin-2 and Fura-2 Dyes.....	18
1. Background.....	18
1.1 Excitation and emission spectra.....	18
1.2 Fluorescent quantum efficiency.....	19
1.2.1 Oxygen and impurity quenching.....	19
1.2.2 Concentration quenching.....	20
1.2.3 Refractive index.....	20
1.2.4 Temperature quenching.....	21
1.2.5 Photochemical decomposition.....	21
1.2.6 Effects of pH on fluorescence of compounds.....	22

2. Experimental.....	23
2.1 Reagents and solutions.....	23
2.2 Apparatus.....	26
2.3 Procedure.....	26
2.3.1 General procedure for obtaining the excitation and emission spectra of the dyes.....	26
2.3.2 Procedure for determination of fluorescent quantum yield of the dyes and testing the effect of concentration..	27
2.3.3 Procedure for testing the effect of temperature.....	29
2.3.4 Procedure for evaluation of photochemical decomposition.....	29
2.3.5 Procedure for testing the effect of pH.....	30
3. Results and discussion.....	31
3.1 Calculation of quantum yields of the dyes.....	32
3.2 Oxygen quenching.....	32
3.3 Concentration quenching.....	32
3.4 Temperature effect.....	34
3.5 Photodecomposition effect.....	35
3.6 Effect of pH on quantum yield of the dyes.....	37
3. Complexation of Free Calcium(II) in Solution with Quin-2 and fura-2 under Physiological Conditions.....	73
1. Background.....	73
2. Experimental.....	78
2.1 Reagents, solutions and Apparatus.....	78
2.2 Procedure.....	80
2.2.1 Stoichiometry of quin-2 and fura-2 with calcium.....	81

2.2.2 Effect of environmental conditions on the binding affinity of quin-2 and fura-2 for calcium(II).....	82
2.2.3 Effect of magnesium(II) on the complexation of quin-2 and fura-2 by calcium(II).....	83
3. Results and Discussion.....	83
3.1 Derivation of expressions for calculation of free calcium(II) concentrations from fluorescence measurements.....	85
3.2 Stoichiometry of calcium to quin-2 and fura-2 in the calcium-dye complexes.....	86
3.3 Conditional association constants of $\text{Ca}^{2+}$ (quin-2) and $\text{Ca}^{2+}$ (fura-2).....	87
3.4 Effect of environmental conditions on affinity of quin-2 and fura-2 for calcium.....	88
3.5 Binding affinity of quin-2 and fura-2 for calcium in the presence of 1 millimolar magnesium(II).....	89
4. Fluorometric Determination of Calcium in Milk Diffusate Using Quin-2 and Fura-2.....	117
1. Background.....	117
1.1 Measurement of extra-cellular ionic calcium.....	117
1.2 Calcium in milk.....	119
2. Experimental.....	120
2.1 Solutions and reagents.....	120
2.2 Apparatus.....	120
2.3 Procedure.....	121
3. Results and discussion.....	122
5. Conclusions and Future Work.....	131

<b>5. Conclusions and Future Work.....</b>	<b>131</b>
<b>1. Conclusions.....</b>	<b>131</b>
<b>2. Future Work.....</b>	<b>132</b>
<b>Bibliography.....</b>	<b>133</b>
<b>Appendix A.....</b>	<b>138</b>

## **List of Tables**

<b>Table</b>	<b>Page</b>
2-1 Calculated quantum yield of quin-2 and fura-2 at room temperature.....	41
2-2 Effect of self absorption and concentration quenching on quantum yield of quin-2.....	42
2-3 Effect of self absorption and concentration quenching on quantum yield of fura-2.....	43
2-4 Effect of temperature on quantum efficiency of quin-2.....	50
2-5 Effect of temperature on quantum efficiency of fura-2.....	51
2-6 Photochemical decomposition of quin-2 at excitation and emission slit widths of 5 and 10 nm respectively.....	54
2-7 Photochemical decomposition of quin-2 at excitation and emission slit widths of 10 and 10 nm respectively.....	55
2-8 Photochemical decomposition of quin-2 at excitation and emission slit widths of 15 and 15 nm respectively.....	56
2-9 Photochemical decomposition of fura-2 at excitation and emission slit widths of 5 and 10 nm respectively.....	57
2-10 Photochemical decomposition of fura-2 at excitation and emission slit widths of 10 and 10 nm respectively.....	58
2-11 Photochemical decomposition of quin-2 at excitation and emission slit widths of 15 and 15 nm respectively.....	59
2-12 Photochemical decomposition of quin-2 as a result of exposure to the laboratory lights.....	65
2-13 Photochemical decomposition of fura-2 as a result of exposure to the laboratory lights.....	66

2-14	Variation of quantum yield of quin-2 with pH.....	69
2-15	Variation of quantum yield of fura-2 with pH.....	70
3-1	Stokes shifts for quin-2 and fura-2 at varying $[Ca^{2+}]$ .....	93
3-2	Variation in the normalized fluorescence intensity of 25 micromolar quin-2 with $[Ca^{2+}]$ at 25°C, pH 7.2 and ionic strength of 0.2.....	94
3-3	Variation in the normalized fluorescence intensity of 1 micromolar fura-2 with $[Ca^{2+}]$ at 25°C, pH 7.2 and ionic strength of 0.2.....	95
3-4	Variation in the normalized fluorescence intensity of 25 micromolar quin-2 with $[Ca^{2+}]$ at 18, 25 and 37°C, pH 7.2 and ionic strength of 0.2.....	100
3-5	Variation in the normalized fluorescence intensity of 1 micromolar fura-2 with $[Ca^{2+}]$ at 18, 25 and 37°C, pH 7.2 and ionic strength of 0.2.....	101
3-6	Variation in the normalized fluorescence intensity of 25 micromolar quin-2 with $[Ca^{2+}]$ at 25°C, pH 6.7, 7.2, 7.6 and ionic strength of 0.2.....	104
3-7	Variation in the normalized fluorescence intensity of 1 micromolar fura-2 with $[Ca^{2+}]$ at 25°C, pH 6.7, 7.2, 7.6 and ionic strength of 0.2.....	105
3-8	Variation in the normalized fluorescence intensity of 25 micromolar quin-2 with $[Ca^{2+}]$ at 25°C, pH 7.2 and ionic strength of 0.1, 0.2 and 0.4.....	108
3-9	Variation in the normalized fluorescence intensity of 1 micromolar fura-2 with $[Ca^{2+}]$ at 25°C, pH 7.2 and ionic strength of 0.1, 0.2 and 0.4.....	109
3-10	Calculated values for the activity coefficient of a tetravalent ion as	



	function of ionic strength.....	112
3-11	Effect of $[Ca^{2+}]$ on the normalized intensity of solutions of 25 micromolar quin-2 and 1 micromolar fura-2 at 25°C, pH 7.2 and ionic strength of 0.2 M in the presence of 1 millimolar $Mg^{2+}$ .....	114
4-1	Concentrations of total Na, K, Mg and Ca in samples of milk diffusate obtained with ICP measurements.....	125
4-2	Variation of the normalized fluorescence intensity of 25 micromolar quin-2 and 1 micromolar fura-2 with $[Ca^{2+}]$ at 37°C, pH 6.68 and ionic strength of 0.065.....	126
4-3	Result of the analysis of milk diffusate samples for calcium using fluorometric technique and quin-2 dye.....	127
4-4	Results of the analysis of milk diffusate samples for calcium using fluorometric technique and fura-2 dye.....	128
A-1	Thermodynamic association constants for EGTA at 20°C and ionic strength of 0.1.....	143

## **List of Figures**

<b>Figure</b>	<b>Page</b>
1-1 Molecular structure of EGTA.....	10
1-2 Molecular structure of BAPTA.....	10
1-2 Molecular structure of quin-2.....	11
1-4 Molecular structure of fura-2.....	11
1-5 Transitions involved in molecular fluorescence and phosphorescence..	15
1-6 Block diagram of a typical fluorescence spectrometer.....	16
2-1a Excitation spectrum of quin-2.....	39
2-1b Emission spectrum of quin-2.....	39
2-2a Excitation spectrum of fura-2.....	40
2-2b Emission spectrum of fura-2.....	40
2-3a Effect of concentration on fluorescence intensity of quin-2.....	44
2-3b Effect of concentration on absorbance of quin-2.....	45
2-3c Effect of concentration on quantum efficiency of quin-2.....	46
2-4a Effect of concentration on fluorescence intensity of fura-2.....	47
2-4b Effect of concentration on absorbance of fura-2.....	48
2-4c Effect of concentration on quantum efficiency of fura-2.....	49
2-5 Variation of quantum efficiency of quin-2 with temperature.....	52
2-6 Variation of quantum efficiency of fura-2 with temperature.....	53
2-7 Effect on quantum yield of exposure of quin-2 to radiation from the 150 W xenon source lamp of the fluorometer over 75 minutes.....	60
2-8b Variation of quantum yield of fura-2 with time as a result of exposure of the dye to radiation from 150 W xenon source lamp at excitation and emission slit widths of 5 and 10 nm respectively.....	61

2-8b	Variation of quantum yield of fura-2 with time as a result of exposure of the dye to radiation from 150 W xenon source lamp at excitation and emission slit widths of 10 and 10 nm respectively.....	62
2-8c	Variation of quantum yield of fura-2 with time as a result of exposure of the dye to radiation from 150 W xenon source lamp at excitation and emission slit widths of 15 and 15 nm respectively.....	63
2-8d	Effect on quantum yield of exposure of fura-2 to radiation from 150 W xenon source lamp over 75 minutes at three sets of excitation and emission slit widths.....	64
2-9	Effect of conventional fluorescence laboratory illumination on quantum yield of quin-2 over a period of 96 hours.....	67
2-10	Effect of conventional fluorescence laboratory illumination on quantum yield of fura-2 over a period of 96 hours.....	68
2-11	Variation in quantum yield of quin-2 as a function of pH.....	71
2-12	Variation in quantum yield of fura-2 as a function of pH.....	72
3-1	Excitation and emission spectra of 25 micromolar quin-2 at $[Ca^{2+}]$ of 0 to 1 millimolar at 25°C, pH 7.2 and ionic strength of 0.2.....	91
3-2	Excitation and emission spectra of 1 micromolar fura-2 at $[Ca^{2+}]$ of 0 to 1 millimolar at 25°C, pH 7.2 and ionic strength of 0.2.....	92
3-3	Variation of the normalized fluorescence intensity of quin-2 with $[Ca^{2+}]$ in logarithmic scale.....	96
3-4	Variation in the normalized fluorescence intensity of fura-2 with $[Ca^{2+}]$ in logarithmic scale.....	97
3-5	Variation in the normalized fluorescence intensity of 25 micromolar quin-2 over a $[Ca^{2+}]$ range of 0 to 2 micromolar at 25°C, pH 7.2 and ionic strength of 0.2.....	98

3-6	Variation in the normalized fluorescence intensity of 1 micromolar fura-2 over a $[Ca^{2+}]$ range of 0 to 2 micromolar at 25°C, pH 7.2 and ionic strength of 0.2.....	99
3-7	Effect of temperature on conditional association constant of $Ca^{2+}$ -(quin-2).....	102
3-8	Effect of temperature on conditional association constant of $Ca^{2+}$ -(fura-2).....	103
3-9	Effect of pH on conditional association constant of $Ca^{2+}$ -(quin-2).....	106
3-10	Effect of pH on condition association constant of $Ca^{2+}$ -(fura-2).....	107
3-11	Effect of ionic strength on conditional association constant of $Ca^{2+}$ -(quin-2).....	110
3-12	Effect of ionic strength on conditional association constant of $Ca^{2+}$ -(fura-2).....	111
3-13	Variation in the activity coefficient of a tetravalent ion with ionic strength.....	113
3-14	Variation in the normalized fluorescence intensity of 25 micromolar quin-2 with $[Ca^{2+}]$ at 25°C, pH 7.2 and ionic strength of 0.2, in the presence of 1 millimolar $Mg^{2+}$ .....	115
3-15	Variation in the normalized fluorescence intensity of 1 micromolar fura-2 with $[Ca^{2+}]$ at 25°C, pH 7.2 and ionic strength of 0.2 M, in the presence of 1 millimolar $Mg^{2+}$ .....	116
4-1	Calibration curve for the determination of $[Ca^{2+}]$ in solutions containing milk diffusate samples using quin-2 indicator dye.....	129
4-2	Calibration curve for the determination of $[Ca^{2+}]$ in solutions containing milk diffusate samples using fura-2 indicator dye.....	130

## **Chapter 1**

### **Introduction**

#### **1. Background on Ionic Calcium Measurements**

Calcium has been a topic of attention in a vast number of chemical and biological researches. It exists in both ionic and bound forms in biological fluids. Calcium binds to proteins<sup>1</sup> and ligands such as citrate, phosphate, sulphate and oxalate<sup>2,3</sup>. A variety of techniques has been used for the measurement of total calcium in biological fluids. Inductively coupled plasma (ICP)<sup>4,5</sup> and atomic absorption spectrophotometry<sup>6,7</sup> are the two most widely accepted methods for this purpose because of their high accuracy and speed. Titrimetric analysis has also been used; in most cases ethylenediamine-tetraacetic acid (EDTA) has been employed as the titrant<sup>8,9</sup>.

At the same time, other methods have been developed for ionic calcium measurements in biological fluids and biological cells. Knowledge of ionized calcium concentrations in urine<sup>10</sup> and blood serum<sup>11,12</sup> is quite important in many medical areas such as for the diagnosis of urinary tract or kidney stone diseases. The most common methods for calcium analysis in these systems are potentiometry using ion-selective electrodes<sup>13-17</sup>, spectrophotometry using indicator dyes<sup>18-21</sup> and ion-exchange chromatography using ion-exchange resins<sup>22</sup>. Cytoplasmic free calcium has a very important role as a key regulator for many cellular functions<sup>23,24</sup>. The most employed methods for intra-cellular ionic calcium ( $[Ca^{2+}]_i$ ) measurement involve the use of ion-selective micro-electrodes<sup>25,26</sup>, calcium-activated photoproteins<sup>27-29</sup>, bis-azo dyes<sup>30,31</sup> and tetracarboxylate chelating fluorescent dyes<sup>32-37</sup>.

## **1.1 Methods for ionic calcium determination in biological fluids**

### **1.1.1 Ion-selective electrode potentiometry**

The first calcium ion-selective electrode (ISE) was designed in 1967 by Ross<sup>38</sup>. The original concept was to measure the potential difference across a porous membrane where calcium ion concentration was held constant on one side and the potential varied with the concentration on the other side. The porous membrane was saturated with a water immiscible organic solvent in which was dissolved a ligand that selectively complexed calcium ions.

In order to measure free calcium concentration using an ISE, the standards must be very similar to the sample. Variations in terms of pH and ionic strength are much higher in urine than in blood, therefore, the present-day calcium ISE's are mainly used to measure  $[Ca^{2+}]$  in blood rather than in urine, and they are developed in such a way to eliminate the problems which are associated with measurements in blood<sup>13,14</sup>.

Another problem arising from the use of these electrodes is the interferences, especially contamination from proteins<sup>39</sup>. Sometimes the electrode is used with a dialysis membrane attached over the tip in order to avoid protein poisoning<sup>40</sup>.

### **1.1.2 Spectrophotometry using indicator dyes**

Indicator dyes have also been used for the analysis of ionic calcium in biological fluids. The dye is usually a weak calcium binding ligand which binds a small fraction of the ionized calcium without perturbing the sample equilibria. The concentration of  $Ca^{2+}$ -indicator complex is determined using Beer's law. The concentration of the free calcium is then calculated using the complexation

constant of the  $\text{Ca}^{2+}$ -indicator chelate, concentration of the free dye and the concentration of the  $\text{Ca}^{2+}$ -indicator complex.

Murexide and tetramethylmurexide (TMMA) have been the most commonly used indicators for free calcium determination in biological fluids. This area has been extensively reviewed by Hewavitharana<sup>22</sup>. Murexide was first used in 1951 for the determination of free calcium in milk ultrafiltrate and urine because of its good selectivity for calcium in the presence of citrate. There were, however, problems associated with the use of murexide, such as its pH dependence and interferences from sodium and proteins. To reduce these problems, TMMA was introduced in 1962, and since then has been recommended for calcium determinations in plasma and urine. TMMA is pH insensitive within the range of 4 to 9 but there are still some interferences from proteins for  $[\text{Ca}^{2+}]$  measurements in blood, and so it can only be used for plasma ultrafiltrate and not for whole blood. Proteins are not usually a problem because they do not normally appear in urine, but the inherent color of urine can interfere. Ways to overcome this problem have included running blanks or using charcoal for decolorization.

Another problem in using TMMA arises from the fact that its response is sensitive to sodium ion concentration and ionic strength, and therefore, samples and standards must be matched in terms of both sodium and ionic strength. To overcome this problem some workers applied a correction factor taken from empirically derived tables according to the sodium-calcium ratio and the ionic strength of the urine sample. Also, calibration curves based on activity and not the concentration of calcium have been used.

In general, the TMMA colorimetric method is more sensitive than ion-selective potentiometry, but it is not the best technique for measurements in

colored fluids. Also, addition of an indicator dye to the sample slightly disturbs the equilibria of the system.

### **1.1.3 Ion-exchange chromatography**

An ion-exchange chromatographic method has been developed for measurement of trace free ion concentrations in solutions. This method is based on the equilibration of solute ions between solvent and fixed charged sites on a stationary ion exchange resin phase. The most important advantage to using this method for biological fluids is that it is possible to obtain equilibrium between the ion-exchanger and the sample fluid without disturbing the equilibria in the system. This is done by using a small amount of exchanger compared to the volume of the fluid and passing fresh sample over the exchanger until the influent and effluent are identical.

This method has been used for speciation of calcium in milk and milk ultrafiltrate.<sup>41-43</sup> The reproducibility is quite good. The main disadvantage of this technique compared to ion-selective potentiometric and spectroscopic methods is the lack of speed.

A recent study was done on the determination of free calcium and magnesium in urine using a quantitative ion-exchange column equilibrium method with atomic absorption detection<sup>22</sup>. Originally this method was developed for free calcium measurement, but since magnesium in urine was found to interfere with the calcium measurements, the method was modified to develop a simultaneous analysis for both of these ions by using equations for the species in solutions containing sodium and potassium at urine-like concentrations. The method is quite selective for both free metal ions in the presence of phosphate, citrate and sulphate, and has been applied for free calcium and magnesium



determination in a standard urine sample (SRM 2670 from NIST). The standard is certified only for total and not for free ion concentrations, however so the results could not be compared.

## **1.2 Methods for intra-cellular free calcium determination**

### **1.2.1 Ion-selective microelectrodes (ISM)**

The first ISM for  $[Ca^{2+}]_i$  was designed in 1976<sup>44</sup> using di[P-(1,1,3,3-tetramethylbutyl)phenyl]phosphoric acid. Later electrodes with sensors based on the neutral carrier N,N'-di(11-ethoxycarbonyl)undecyl-N,N',4,5-tetramethyl-3,6-dioxaoctane diacid diamide (ETH1001) were used in preference to the original one, because of the smaller size of the tip and better  $Mg^{2+}$  rejection<sup>26</sup>.

In spite of good selectivity for calcium,  $Ca^{2+}$ -ISM's suffer from a number of problems<sup>25</sup>. (1) Even with all the progress made in reducing the tip size, there is still a great deal of difficulty in studying small cells. (2) Another problem is the seal between the electrode exterior and the cell membrane. Because of the large gradient of  $Ca^{2+}$ , the slightest leak can raise  $[Ca^{2+}]_i$  near the tip of the electrode. (3) At the submicromolar level the electrode response time to changes in  $[Ca^{2+}]_i$  is too slow for many problems involving cellular calcium function. The slowness of the response time is mainly due to diffusional and ion-binding kinetics, which are not easy to speed up. (4) The microelectrode measures  $[Ca^{2+}]_i$  at only the point where the electrode tip is placed. Since it is often not clear where the tip is located in relation to other cell structures, this point-sample nature of the signal yields some uncertainty.

### **1.2.2 Calcium-activated photoproteins**

Calcium-activated photoproteins have been important in the investigation of temporal and spatial changes in calcium ion concentration involved in the regulation of cellular functions. These photoproteins are precharged bioluminescent proteins that emit light upon binding  $\text{Ca}^{2+}$  or certain other inorganic ions. Unlike most classical bioluminescence systems, in which an enzyme catalyses the oxidation of an organic substrate with formation of an excited state and the emission of light, the reaction of photoproteins with calcium ion does not require molecular oxygen or any other cofactor. The emitted light is only derived from the precharged photoprotein, thus the molecule can only react once and does not "turn over" as an enzyme does<sup>27,28</sup>.

The first photoprotein found to be sensitive to  $[\text{Ca}^{2+}]_i$  was aequorin. Aequorin was isolated from luminescent marine coelenterates in 1961 by Shimomura et al<sup>45</sup>. In the initial investigations it was found that aequorin had high sensitivity and relative specificity for  $\text{Ca}^{2+}$ , and activity at physiological pH values which gave it considerable promise as a calcium indicator for biological research<sup>45,46</sup>. Later studies involved the application of aequorin to free calcium determination in various types of cells<sup>47-50</sup>.

Although other calcium-activated photoproteins have been isolated (reviewed by Blinks, Prendergast and Allen<sup>28</sup>), including halisaurin, obelin, mnemiopsin and berovin, the most known and applied one has been aequorin, partly because it was the first to be discovered but more importantly because of its relative availability.

The properties that make aequorin and other calcium sensitive photoproteins useful for intra-cellular free calcium determination are<sup>29,30</sup>: (1) high sensitivity to low  $[\text{Ca}^{2+}]$ , (2) relative specificity to calcium, (3) ease of signal

detection, (4) non-toxicity. At the same time, there are certain difficulties accompanied with the use of these photoproteins<sup>29,31</sup>. These include: (1) consumption of the protein during the luminescent reaction makes it unclear whether a decline of luminescence is due to a decline in free calcium concentration or depletion of the photoprotein from some intracellular compartment, (2) the uncertainty of the stoichiometry for the calcium-photoprotein binding reaction and its dependency on environmental conditions, and (3) the slowness of the luminescent reaction, which makes it difficult to follow rapid changes of  $[Ca^{2+}]$ .

### **1.2.3 Bis-azo indicator dyes**

The best known dyes in this category are arsenazo III and antipyrilazo III. The absorbance spectrum for the arsenazo III-calcium complex shows two maxima between 575 and 675 nm, which is distinguishable from the spectrum of arsenazo- $Mg^{2+}$  with only one maximum. Antipyrilazo III also shows maxima beyond 650 nm which are more effected by  $Ca^{2+}$  binding than by  $Mg^{2+}$  binding or deprotonation<sup>30</sup>.

The major drawback in the use of these dyes is the fact that neither of them have a simple 1:1 stoichiometry with calcium. The apparent 1:1 complexation constant varies according to the concentration of the dye, increasing as the dye concentration increases<sup>51,52</sup>. In order to fit the data, simultaneous equilibria between 1:1, 2:2, and 1:2 Ca:dye complexes are required. These equilibria are further complicated by competition with  $Mg^{2+}$  and  $H^+$ .

### **1.2.4 Tetracarboxylate chelating fluorescent dyes**

Recent studies (since early 1980's) for cytoplasmic free calcium determination have applied the use of a group of calcium indicator fluorescent dyes

with backbones similar to that of ethylene glycol-bis-(beta-aminoethyl)-N,N,N',N'-tetraacetic acid (EGTA)<sup>32-37,53</sup>. These molecules are able to chelate calcium with high affinity and specificity. They contain aromatic rings that interact electronically and sterically with the chelating backbone. As a result of chelation with calcium, the wavelength maximum of absorbance and fluorescence of the molecule shifts.

EGTA (Fig. 1-1) is a chelating agent with high selectivity for  $\text{Ca}^{2+}$  over  $\text{Mg}^{2+}$ . This effect is produced because the binding cavity of EGTA is the right size for  $\text{Ca}^{2+}$  but cannot constrict further to hold  $\text{Mg}^{2+}$  snugly (the carboxyl groups at each end start butting into each other). The nitrogens bind protons with  $\text{pK}_a$ 's of approximately 9 and 10, making the  $\text{Ca}^{2+}$ -buffering action of EGTA strongly dependent on pH variation near 7. They also slow down the chelation and release of  $\text{Ca}^{2+}$  such that they may take seconds to happen<sup>32,54</sup>.

The fluorescent dyes were designed and synthesized as derivatives of EGTA by replacing the methylene groups between N and O with benzene rings. This substitution leaves the cavity more or less the same size and shape as EGTA but shifts the protonated nitrogen  $\text{pK}_a$ 's to more acidic values of 5 or 6. Cation affinities for these molecules can be varied by placing appropriate electron withdrawing or donating substituents on the benzene rings and/or modification of the ether linkage. For example, in quin-2, one of the first dyes in this group to be synthesized, an ether oxygen has been replaced by an  $\text{sp}^2$  heterocyclic nitrogen (figure 1-3). Because of the higher basicity of nitrogen over oxygen, quin-2 has higher affinity for calcium than the original compound (BAPTA, figure 1-2), but the methoxy group meta to the 8-amino group exerts an electron withdrawing effect and lowers the affinity of the dye for calcium about 0.3 to 0.5 log unit<sup>54</sup>.

These dyes are recommended over other indicator dyes, photoproteins and ISM's for intra-cellular determination of  $\text{Ca}^{2+}$  mainly because<sup>32,54</sup>: (1) they are highly selective against competing cations, particularly  $\text{H}^{+}$  and  $\text{Mg}^{2+}$ ; (2) they have simple stoichiometries of interaction with  $\text{Ca}^{2+}$ ; (3) because of their high affinity for  $\text{Ca}^{2+}$ , only a small amount of dye is needed, which means there is less danger of toxic side effects on the system; and (4) controlled amounts of the dye are easily trapped in the cytoplasm of a large population of small cells, so there is no need for microinjection, fusing or lysing the cells<sup>50</sup>. Instead, the four carboxylate groups are esterified by acetoxymethyl groups. The resulting hydrophobic esters readily permeate cell membranes. In the cell cytoplasmic esterases cut the masking groups off and restore the chelators to their original  $\text{Ca}^{2+}$ -binding forms.

In this work, the behavior of two of these dyes, quin-2 and fura-2 (figures 1-3 & 1-4) and their complexibility with calcium under different environmental conditions have been studied for the purpose of extra-cellular calcium measurements, using fluorescence spectrometry. Although these dyes have been widely studied for intra-cellular free  $\text{Ca}^{2+}$  measurements, they have not been reported for determination of free calcium outside of cells in either biological or other fluids. We were also interested in whether they could be applied to the measurement of  $\text{Ca}^{2+}$  at concentrations higher than the  $10^{-5}$  M levels typically encountered in cells.

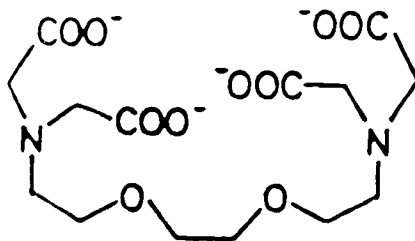


**Figure 1-1** EGTA: ethylene glycol bis(beta-aminoethyl ether)-N,N,N',N'-tetraacetic acid

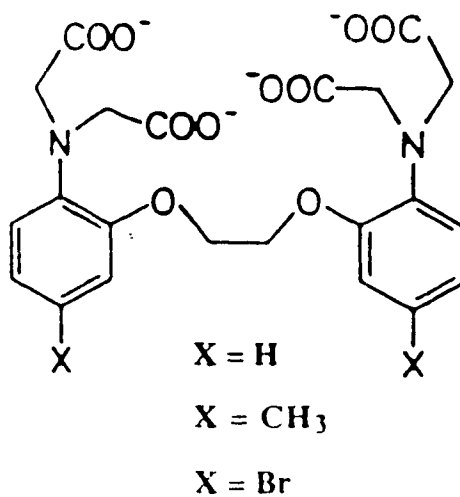


**Figure 1-2** BAPTA: 1,2-bis(o-aminophenoxy)-ethane-N,N,N',N'-tetraacetic acid

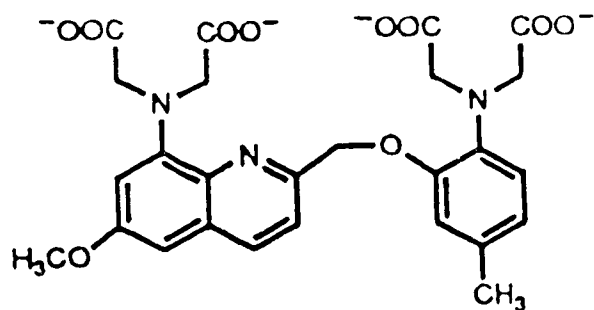


**Figure 1-3** Quin-2: 2-{[2-bis(carboxymethyl)-amino-5-methylphenoxy]-methyl}-6-methoxy-8-bis-(carboxymethyl)-aminoquinoline

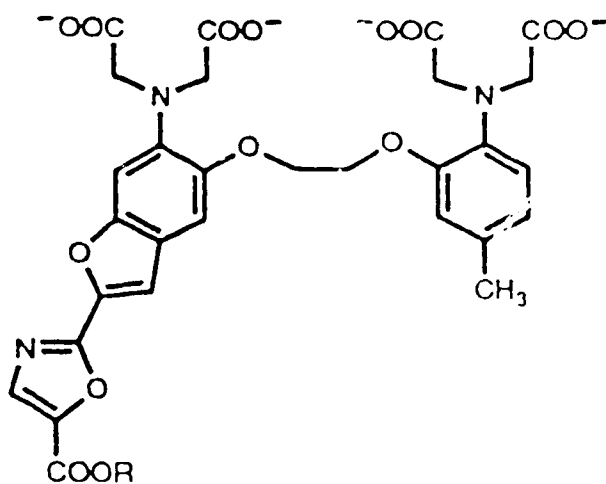


**Figure 1-4** Fura-2: 1-[2-(5-carboxyoxazol-2-yl)-6-aminobenzofuran-5-oxy]-2-(2'-amino-5'-methylphenoxy)-ethane-N,N,N',N'-tetraacetic acid

## **2. Fluorometry**

Fluorescence spectroscopy is quite useful in chemical and biological researches, especially for the study of molecular structure, molecular interaction, and localization of molecules (especially in biological systems), as well as for many types of trace analysis. Fluorescence is usually defined as a rapid emission of radiant energy in the UV-visible region from a photo-excited species, or fluorophor.

In general, a molecule absorbing radiation is initially in its electronic ground state  $S_0$ . During the excitation process it acquires vibrational as well as electronic energy and is promoted to some vibrational sublevel of an excited electronic state  $S_1$ . The process of excitation takes about  $10^{-15}$  s, thus is essentially instantaneous. Before returning to the ground electronic state by emission of a photon, the molecule drops to its base level  $S_1$ . This is why the energy of a fluorescence transition is usually less than the absorption transition and, therefore, why molecular fluorescence is usually observed at a longer wavelength than that of the absorbed radiation (excitation). If the molecule is, however, in the lower one or two vibrational sub-levels of the ground state  $S_0$ , and is excited to an  $S_1$  state (figure 1-5), then even though most of the fluorescent emission is at a longer wavelength than the excitation, a portion of the emitted radiation will appear at a shorter wavelength than the longest wave of the excitation spectrum. This usually results in some degree of overlap between excitation and emission spectra. The time required for the transition from  $S_1$  to  $S_0$  is about  $10^{-8}$  s<sup>55-59</sup>.

An excited molecule can also lose its excess energy through processes other than fluorescence. In one process (figure 1-5) intersystem crossing from the lowest excited singlet state ( $S_1$ ) to the lowest triplet state ( $T_1$ ) occurs, and the



molecule in the triplet state emits radiation in the form of phosphorescence ( $T_1 \rightarrow S_0$ ). The lifetime of phosphorescence is much longer than that of fluorescence ( $\sim 10^{-3}$  to  $10^{-2}$  s)<sup>55,56</sup>.

Figure 1-6 shows a schematic diagram of the general instrumentation for fluorescence spectroscopy. Light from the source, usually a mercury arc or a xenon arc lamp, falls on the first monochromator, where the wavelength of excitation is selected. The sample is then excited by the selected radiation. The emitted radiation from the sample is examined with a second monochromator positioned at a  $90^\circ$  angle to the incident light. The monochromators are set at a  $90^\circ$  angle from each other so that incident radiation that strikes the detector can be kept as low as possible. The selected emitted beam is then received by the detector (photomultiplier), converted to an electronic signal, and the signal sent to a recorder<sup>60,61</sup>.

The relationship between the fluorescence intensity of a dilute sample and its concentration can be simply derived from the Beer-Lambert law of absorption. The Beer-Lambert law is shown as<sup>56</sup>:

$$I_t = I_0 10^{-\epsilon bc} \quad (1.1)$$

where  $I_0$  is the intensity of the incident light and  $I_t$  is the intensity of the transmitted light,  $\epsilon$  is the molar absorptivity of the compound,  $b$  is the path length of the light in the cuvette in cm, and  $c$  the molar concentration of the sample.

Equation (1.1) can be transformed to:

$$I_a = I_0 (1 - 10^{-\epsilon bc}) \quad (1.2)$$

where  $I_a$  is the intensity of the absorbed light ( $I_a = I_0 - I_t$ ). The intensity of the fluorescence is given by  $I_a \phi_f$ , where  $\phi_f$  is the fluorescence quantum efficiency, defined as the ratio of the total energy emitted as photons per unit time to quanta of energy absorbed per unit time. The fluorescence intensity is then shown as:

$$I_f = I_0 \phi_f (1 - 10^{-\epsilon bc}) \quad (1.3)$$

$$I_f = I_0 \phi_f \{1 - [1 - 2.303 \epsilon bc + (2.303 \epsilon bc)^2 / 2! \dots]\} \quad (1.4)$$

If  $bc \leq 0.05$ , equation 1.4 can be simplified to:

$$I_f = 2.303 I_0 \phi_f \epsilon bc \quad (1.5)$$

Molecular fluorescence is quite advantageous over many other analytical techniques because of its extreme sensitivity and good selectivity<sup>58</sup>. Its sensitivity is mainly due to the fact that the emitted radiation is measured directly and can be increased or decreased by altering the intensity of the exciting radiant energy. In fluorometric methods, an increase in signal over a zero background is measured, whereas in absorption spectroscopic methods absorbed radiation is measured indirectly as the difference between incident and the transmitted beam. This small decrease in the intensity of a large signal leads to a corresponding loss in sensitivity. The selectivity of fluorescence is the result of two main factors: (a) Fewer compounds fluoresce than absorb radiation. In order for a compound to fluoresce, it must absorb radiation, so all fluorescent compounds must absorb light. But not all compounds that absorb light reemit it. (b) Two compounds that absorb light at the same wavelength may fluoresce at two different wavelengths.

Therefore, compared to spectrophotometric methods, in which only one wavelength is used, there is less chance of interference from other compounds or elements.

At the same time there are limitations to the fluorescence technique<sup>58</sup>. A main disadvantage of fluorescence as an analytical tool is its dependence on environmental variations such as temperature, pH and viscosity. In a practical sense, environmental conditions must be kept constant during the measurements in order for maximum precision and accuracy to be achieved. Also, the fluorescent intensity of a compound can be subject to quenching by high temperature, intense radiation, high concentration and dissolved oxygen.

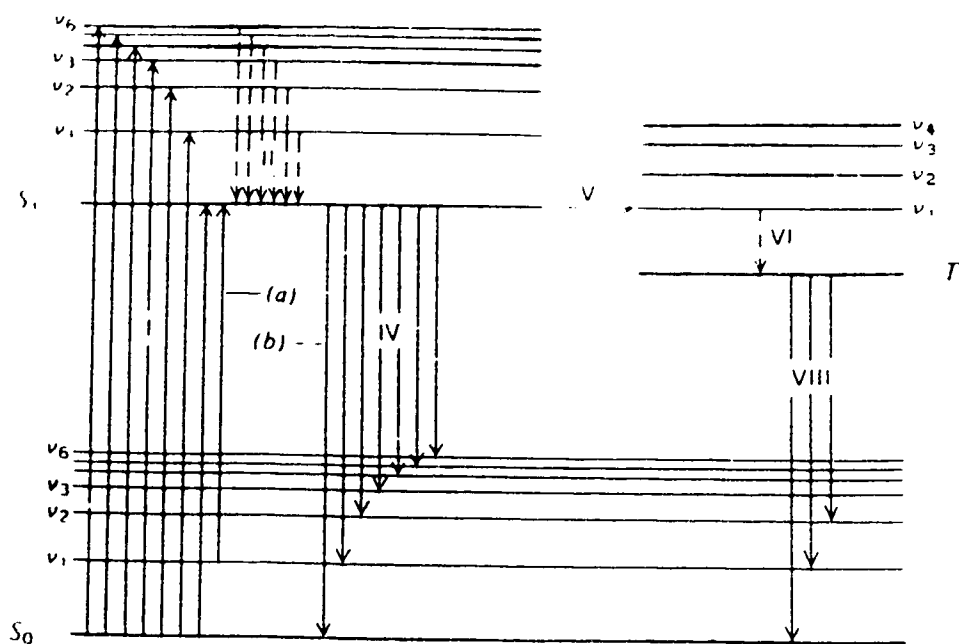


**Figure 1-5** Transitions involved in molecular fluorescence and phosphorescence.

During process I, the molecules acquire vibrational as well as electronic energy and end up in some vibrational sub-level of  $S_1$  electronic state. Then they lose their energy through collisions and drop to the lowest sub-level of  $S_1$  (process II). A number of these molecules return directly to the ground state by emitting a photon (fluorescence, process IV). Some shift to a metastable triplet level by intersystem crossing (processes V, VI) before return to the ground state (process VI). The transition marked (a) is responsible for the overlap of excitation and fluorescence spectra, as it is less energetic than transition (b). (Drawing adapted from fig. 6-1 in reference 70)

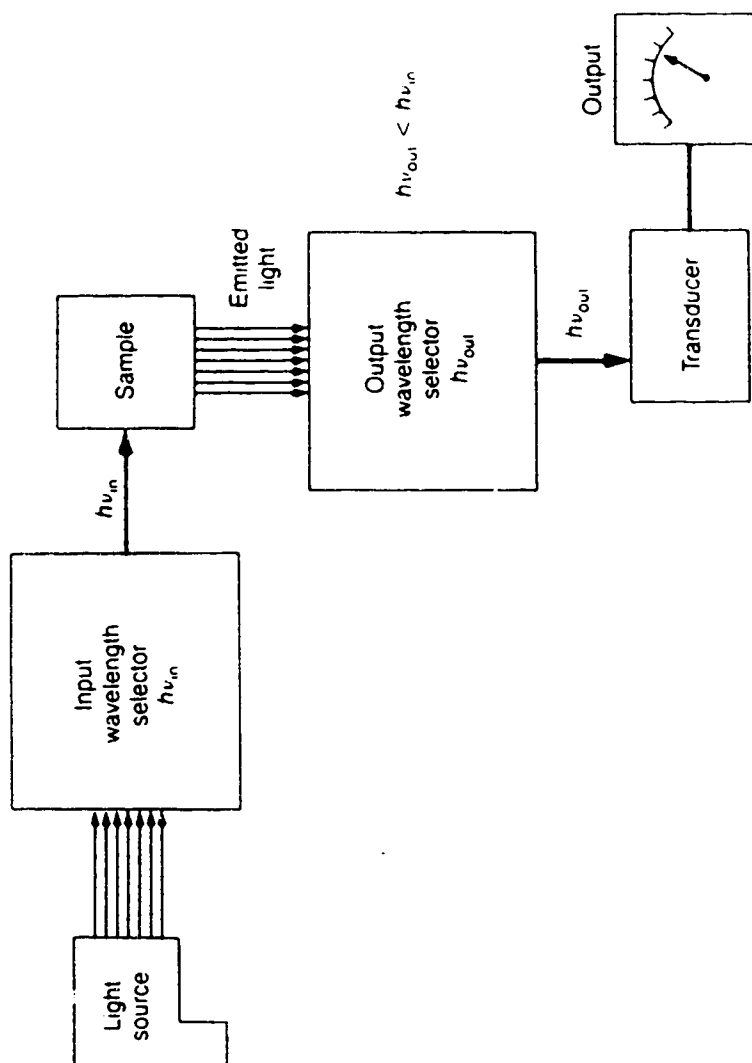


**Figure 1-6** Block diagram of a fluorescence spectrophotometer.  
(Drawing adapted from fig. 17-9 in reference 76)

## **Chapter 2**

### **Characterization of Quin-2 and Fura-2 Dyes**

#### **1. Background**

##### **1.1 Excitation and emission spectra**<sup>58,62</sup>

Fluorescent molecules have two characteristic spectra: the excitation spectrum, which is the relative efficiency of different wavelengths of exciting radiation, and the emission spectrum, which is the relative intensity of radiation emitted at various wavelengths. The excitation spectrum is obtained by holding the wavelength of maximum emission ( $\lambda_{em}$ ) constant and varying the excitation wavelength. For some compounds more than one excitation peak may be observed. In that case, in order to minimize decomposition effects, the longest wavelength radiation is normally chosen for excitation. The emission spectrum of a compound is the result of reemission of radiation absorbed during the excitation process, and is obtained by holding the excitation wavelength ( $\lambda_{ex}$ ) fixed and scanning the emitted radiation spectrum. Excitation and emission spectra of a compound are approximately mirror images of each other. Fluorescent peaks other than the mirror image of the absorption band correspond to scattering or the presence of impurities.

The difference between the maxima of the excitation ( $\lambda_{ex}$ ) and emission ( $\lambda_{em}$ ) wavelengths of a molecule is a physical constant called the Stokes shift. It indicates the energy dissipated during the lifetime of the excited state before return to the ground state.

$$\text{Stokes shift} = 10^7 (1/\lambda_{ex} - 1/\lambda_{em}) \quad (2.1)$$

The Stokes shift is of interest to analytical chemists because of possible shifts of the emission wavelength as a result of varying the form of the molecule being excited.

### **1.2 Fluorescent quantum efficiency<sup>56,58</sup>**

Fluorescence quantum yield or quantum efficiency is defined as the ratio of the photons of emitted radiation to the photons of absorbed radiation.

$$\phi_f = \frac{\text{number of quanta emitted}}{\text{number of quanta absorbed}}$$

The greater the value of  $\phi_f$ , the higher is the fluorescence of a compound. This value for a non-fluorescent compound is zero. The quantum efficiency of a molecule provides information on radiationless processes and purity of molecules. It also aids in the assignment of electronic transitions.

A series of factors may affect the quantum yield of a molecule. Some of them are listed below.

#### **1.2.1 Oxygen and impurity quenching<sup>58,63</sup>**

The presence of oxygen in solution normally reduces the fluorescence intensity of a compound. The degree of quenching varies for different compounds; it ranges from less than 1% for a compound with a strong first absorption band to 95% for a long lived fluorescer. Oxygen quenching may be eliminated by de-aerating the samples and standards with a nonquenching gas such as nitrogen prior to measurements

Impurities in samples and solvents can also lead to some degree of quenching. Fluorometry can be a very sensitive and specific technique with no

chemical interferences if measurements are made in dilute solutions that contain only trace amounts of quenching substances. At moderate concentrations, however, impurities may lead to some interferences. One of the major impurity interferences comes from heavy metals. These effects can often be eliminated by addition of a chelating agent to the sample solution. They may also be reduced by dilution as long as the chemical equilibrium of the system is not disturbed.

### **1.2.2 Concentration quenching**<sup>58,61</sup>

Fluorescence intensity usually has a linear relationship with concentration only at low concentrations (very dilute solutions). At higher concentrations problems such as inner filter effects and self absorption may occur, especially if there is a considerable overlap between excitation and emission spectra. Because of its applicability over a larger range of analyte concentrations and its higher sensitivity, luminescence spectroscopy may seem preferable to absorption spectroscopy where both techniques can be used. Overall the problem of self absorption is a major drawback to the use of fluorometry in quantitative analysis.

### **1.2.3 Refractive index**<sup>56</sup>

When a beam of light travels between two media ( e.g., a liquid solvent and air ), it bends away or toward the normal and a change in its intensity occurs at the interface. The angle of refraction varies for different liquids at different concentrations. Therefore, when different solvents are used for standards and samples, a correction for differences in refractive indices may be required. The following correction factor is applied for the effects of emitted light traversing different refractive indices with a 90 degree viewing angle.



$$I_o = \frac{I_i \cos \theta}{n_i (n_i^2 - \sin^2 \theta)^{1/2}} \quad (2.2)$$

Here  $I_o$  is the intensity of the light in air,  $I_i$  is the intensity of the light in the second medium,  $n_i$  is the refractive index of that medium, and  $\theta$  is the angle of deviation of light from the normal. In fluorometric techniques, if it is assumed that the angle of deviation is zero, equation (2.2) can be condensed to:

$$I_o = \frac{I_i}{n_i^2} \quad (2.3)$$

#### **1.2.4 Temperature quenching**<sup>56,58</sup>

For many compounds the fluorescence yield and decay time decreases with increasing temperature. The degree of temperature dependence varies for different compounds. Elevation of temperature decreases the viscosity of the solvent, which causes an increase in the number of molecular collisions and hence removes energy from an excited molecule as kinetic energy.

In a practical sense, all solutions should be kept at a constant temperature for maximum precision to be achieved. The heat from the radiation source may also cause fluorescence quenching during excitation, hence a shutter should be used between measurements to protect the solution from thermal decomposition.

#### **1.2.5 Photochemical decomposition**<sup>56,58</sup>

The energetic ultraviolet radiation used for excitation usually causes some degree of photochemical decomposition in a molecule. This effect appears as a gradual decrease in the fluorescence intensity of the compound. Photodecomposition is a more pronounced problem in dilute solutions. In

concentrated solutions the amount of decomposed sample is often minor compared to the total amount.

In a practical sense, in order to minimize the effect of photodecomposition, the samples and standards should be protected from sunlight and ultraviolet radiation by storing in dark bottles. Also, where possible the longest wavelength radiation (lowest excitation energy) should be employed and the fluorescent measurements taken as quickly as feasible.

#### **1.2.6 Effects of pH on fluorescence of compounds<sup>58,62</sup>**

The fluorescent spectra of most aromatic compounds containing acidic or basic functional groups are very sensitive to pH variations. Variation in pH alters the charge and resonance of the chromophores by protonation or deprotonation of functional groups and hence varies the fluorescence of the compound in terms of intensity or wavelength shift.

#### **1.3 Background of work described in this chapter**

In this chapter the fluorescence properties of the compounds quin-2 and fura-2 are examined. Their quantum yields and excitation and emission spectra recorded, and the effects of temperature, concentration, pH, and other variables studied.

## **2. Experimental**

### **2.1 Reagents and solutions**

All chemicals were reagent grade and used as supplied. Distilled deionized water (DDW) was used for the preparation of all solutions.

**Quin-2.** The 95% tripotassium salt of quin-2 (Sigma Chemical Company) was supplied in a dark sealed vial to minimize photodecomposition. Upon arrival the salt was stored in a desiccator in a refrigerator at 3°C. To minimize deterioration, a fresh solution of quin-2 was prepared for each set of experiments by dissolving the appropriate amount of the dye in DDW. These solutions were used within a week.

**Fura-2.** The 93% pentasodium salt of fura-2 (Calbiochem Company) was also supplied in a dark sealed vial. Since weighing the required amount for each experiment caused some difficulties and led to wasting of a considerable amount of the dye (due to the small mass of the supplied material, i.e. 1 mg), the whole amount in each vial was weighed, dissolved in 5 ml of DDW, and divided into portions of 0.47 ml. Each portion was then stored in a small sealed polyethylene vial and kept frozen until the time of use. These solutions were of the order of 0.26 to 0.27 mM.

**Standard EGTA solution.** A 0.04768 M solution of  $K_2H_2EGTA$  was prepared by dissolving 9.5042 g of EGTA (Sigma Chemical Company) and approximately 3.5 g of KOH pellets (BDH) in DDW and diluting to 500 ml. Since the KOH pellets contained about 20%  $K_2CO_3$  and moisture, the calculated amount based on assumption of 100% purity was not enough. Therefore, pellets were continually added until all the EGTA dissolved. The resulting solution was

standardized against 0.1027 M  $\text{Ca}(\text{NO}_3)_2$  solution using a 0.02 percent calcein solution as indicator.

Standard  $\text{Ca}(\text{NO}_3)_2$  solution. 10.27 g of  $\text{CaCO}_3$  (Fisher Scientific Company), previously dried at  $80^\circ\text{C}$  for 24 hours to evaporate the absorbed moisture, was added to 100 ml of 2 M  $\text{HNO}_3$  and diluted to 1 liter with DDW to produce a 0.1027 M solution.

Calcein indicator solution. 25 ml of DDW was added to 19.56 mg of calcein (Fisher Scientific Company) and a small amount of potassium hydroxide was added to dissolve all the solid. Then it was diluted to 100 ml with DDW to make a 0.02 percent solution.<sup>64</sup> To reduce deterioration, the solution was transferred into a polyethylene bottle and kept in refrigerator. For prolonged storage, small portions of calcein solution were stored frozen in small polyethylene vials.

0.05 M MOPS buffer solution. 5.287 g of 4-morpholinepropanesulfonic acid (MOPS, Aldrich Chemical Company Inc.) was dissolved in 400 ml of DDW and the pH adjusted to  $7.2 \pm 0.1$  by dropwise addition of standard KOH solution. Then it was diluted to 500 ml with DDW.

0.05 M HEPES buffer solution. 1.3021 g of the sodium salt of N-[2-Hydroxy-ethylpiperazine-N']-[2-ethanesulfonic acid] (HEPES, Sigma Chemical Company) was dissolved in 70 ml of DDW and the pH of the solution was adjusted to  $7.5 \pm 0.1$  by dropwise addition of concentrated KOH solution. Then it was diluted to 100 ml with DDW.

0.05 M MES buffer solution. 1.039 g of 4-morpholineethane sulfonic acid (MES, Aldrich Chemical Company Inc.) was dissolved in 70 ml of DDW and the pH of the solution adjusted to  $6.1 \pm 0.1$  by dropwise addition of concentrated KOH solution. Then it was diluted to 100 ml with DDW.

NH<sub>3</sub> / NH<sub>4</sub>Cl buffer solution of pH 10. 23 ml of 14.8 M NH<sub>4</sub>OH (BDH) were added to 5 ml of 10.14 M HCl and diluted to 500 ml with DDW to make a buffer of 0.56 M NH<sub>4</sub>Cl and 0.1 M NH<sub>3</sub>.

CH<sub>3</sub>COONa / CH<sub>3</sub>COOH buffer solution of pH5. 26 ml of 0.8 M NaOH and 2 ml of 17.4 M CH<sub>3</sub>COOH (American Scientific & Chemical) were added to 72 ml of DDW to make 100 ml of a solution of 0.19 M CH<sub>3</sub>COONa and 0.1 M CH<sub>3</sub>COOH.

CH<sub>3</sub>COONa / CH<sub>3</sub>COOH buffer solution of pH 4. 122 ml of 0.8 M NaOH and 34 ml of 17.4 M CH<sub>3</sub>COOH were added to 344 ml of DDW to make a buffer solution of 0.19 M CH<sub>3</sub>COONa and 1 M CH<sub>3</sub>COOH.

0.83 M NaOH solution. Approximately 4 g of NaOH pellets (BDH) were dissolved in 50 ml of DDW and diluted to 100 ml. The resulting solution was roughly standardized against 12.4 M HCl solution using phenolphthalein as indicator.

8.1 M standard KOH solution. Approximately 56 g of KOH pellets (BDH) were dissolved in 50 ml of DDW and diluted to 100 ml. This solution was roughly standardized against 12.4 M HCl solution using phenolphthalein as indicator.

5 micromolar solution of quinine sulfate in 0.1 N H<sub>2</sub>SO<sub>4</sub>. A 1000 ppm solution of quinine sulfate monohydrate was prepared by dissolving 1.1024 g of 90% quinine sulfate monohydrate (Aldrich Chemical Company) in 1 liter of 0.1 N H<sub>2</sub>SO<sub>4</sub>. A 0.348 ml portion of this solution was diluted to 100 ml with 0.1 N H<sub>2</sub>SO<sub>4</sub>. The remaining 10% was reported by Aldrich to be hydroquinine, which was assumed to have the same fluorescence properties as quinine.

## **2.2 Apparatus**

All pH values were measured with a Fisher-Accumet (model 520 digital) pH/Ion meter equipped with an Accu-pHast combination electrode. This electrode pair was found to provide excellent stability. The pH meter was calibrated against two standard buffers (Fisher Scientific Company): 0.05 M potassium phosphate monobasic-sodium hydroxide (pH 7.00 at 25°C) and 0.05 M potassium biphthalate (pH 4.00 at 25°C). Calibration was done before each pH measurement.

Fluorescent spectra were recorded using a Shimadzu RF-5000 spectrofluorophotometer. Absorption spectra were collected on a Hewlett Packard 8451 diode array spectrophotometer.

During fluorescence measurements the sample compartment temperature was controlled to  $\pm 0.1$  degree with a K-4/RD Lauda/Brinkmann circulating water bath by circulation of water through a jacketed cell compartment designed and constructed by Mr. R. Lipiecki in the machine shop of the department of chemistry.

## **2.3 Procedure**

### **2.3.1 General procedure for obtaining the excitation and emission spectra of the dyes**

All glassware was soaked in 10% nitric acid for 24 hours, then rinsed with DDW. Solutions of 10 millimolar MOPS / 10 millimolar EGTA / 5 micromolar quin-2 and 10 millimolar MOPS / 10 millimolar EGTA / 5 micromolar fura-2 were prepared by dissolving the appropriate amounts of the dyes in small amount of DDW, pipeting 5.243 ml of EGTA (to mask calcium and heavy metal ions that exist in trace amounts in the solutions and that may cause interference by binding

with the dyes)<sup>65</sup>, adding 5.00 ml of MOPS buffer, and diluting to 25 ml. The pH of each solution was adjusted to  $7.20 \pm 0.01$  by dropwise addition of concentrated KOH solution. The solutions were then passed through a 0.2 micron filter to prevent scattering of the radiation beam by dust and other particles. Finally nitrogen gas was bubbled through the solutions for 10 minutes to remove dissolved oxygen which may cause quenching of the fluorescent signal. To avoid evaporation of solvent from the sample solutions, the nitrogen gas was pre-saturated with water vapor.

Excitation spectra of quin-2 and fura-2 were obtained by setting the emission monochromator at 492 nm for quin-2 and 512 nm for fura-2,<sup>68</sup> and scanning from 200 nm to 800 nm, using excitation and emission band widths of 5 and 10 nm respectively. Emission spectra were obtained by holding the excitation wavelengths at their peak maxima (360 nm for quin-2 and 365 nm for fura-2) and scanning through the emitted radiation. The excitation spectra were collected again after the maximum  $\lambda_{em}$  had been identified.

During measurement the solutions were kept at  $24.0 \pm 0.1^\circ\text{C}$  by means of water pumped through a thermostated cell holder connected to a water bath. The exciting radiation was blocked from the sample solutions between measurements to avoid photodecomposition. All measurements were made in triplicate. The same procedure was repeated without de-aeration of the solutions to examine the extent of oxygen quenching.

### **2.3.2 Procedure for determination of fluorescent quantum yield of the dyes and testing the effect of concentration**

There are several methods for determining the quantum efficiency of a fluorescent compound. We use here a simple comparative method based on the

fact that if two compounds are studied in the same apparatus and using the same incident light intensity, the integrated areas under fluorescence spectra of the unknown sample and the standard ( $F_{\text{unk}}$  &  $F_{\text{std}}$ ) are related as follows:

$$\frac{F_{\text{std}}}{F_{\text{unk}}} = \frac{\phi_{\text{std}}}{\phi_{\text{unk}}} \frac{A_{\text{std}}}{A_{\text{unk}}} \frac{n_{\text{unk}}^2}{n_{\text{std}}^2} \quad (2.4)$$

where the  $\phi$  terms are quantum efficiencies, the A values are absorbances at the respective excitation wavelength maxima, and the n terms refer to the refractive indices of the solvents. The term  $\frac{n_{\text{unk}}^2}{n_{\text{std}}^2}$  is equal to 1, if the same solvent is used for

both standard and the unknown samples.<sup>56,63</sup>

The fluorescent spectra of 5 micromolar quinine sulfate in 0.1 N  $\text{H}_2\text{SO}_4$ , 5 micromolar fura-2, and 5 micromolar quin-2 were obtained using the RF-5000 spectrofluorophotometer ( $\lambda_{\text{ex}}$  for quinine sulfate is 350 nm). Because the Shimadzu RF-5000 instrument does not have an absorption mode, absorption spectra were obtained using the HP 8451 diode array spectrophotometer. Quinine sulfate was run as standard.<sup>56</sup> No correction for refractive index was made. Since n for 1 N  $\text{H}_2\text{SO}_4$  at 24°C is 1.36<sup>66</sup> and that for water at this temperature is 1.33<sup>67</sup>, the value of n for 0.1 N  $\text{H}_2\text{SO}_4$  was estimated to be approximately 1.333. Considering the uncertainties in the A and F values, this small difference in n was not expected to affect the calculation of quantum yield for the dyes to an appreciable extent.

To test the effect of concentration quenching, solutions of 0, 0.05, 0.01, 0.02, 0.05, 0.1, 0.25, 0.5, 0.75, and 1 millimolar quin-2, and 0, 1, 2, 5, 7, 10, 12.5, 25 and 50 micromolar fura-2 were prepared and their absorbance and fluorescence spectra were collected. All measurements were made in triplicate.



### **2.3.3 Procedure for testing the effect of temperature**

The fluorescence and absorption spectra of 5 micromolar quin-2 and 5 micromolar fura-2 were recorded over a temperature range of 14°C to 55°C (starting with the lowest temperature) using a K-4/RD Lauda/Brinkmann circulator to adjust the temperature. The pH of each solution was readjusted at each temperature using concentrated KOH and HCl solutions. Sample solutions were placed in the cell holder for 10 minutes before each measurement to allow equilibration at the new temperature. During this time the source shutter was closed to protect the sample from radiation. All measurements were made in triplicate.

### **2.3.4 Procedure for evaluation of photochemical decomposition**

The extent of photodecomposition of the dyes was studied both by exposing the dye solutions directly to conventional fluorescent laboratory illumination, and by irradiating them with the 150 W xenon lamp of the fluorometer at the wavelength of maximum absorption of each dye over a range of excitation and emission slit widths.

Solutions of 5 micromolar fura-2 and 5 micromolar quin-2 in pyrex glassware were exposed on the bench-top to the standard room fluorescent lighting for 96 hours. Fluorescence and absorbance spectra were recorded every half hour for the first 6 hours, then at 20, 24, 30, 44, 48, 54, 68, 72, 78, 92 and 96 hours after the starting time. The fluorescence spectra were recorded at excitation and emission slit widths of 5 and 10 nm respectively.

Fresh solutions of the same concentrations were exposed to the exciting radiation from the xenon lamp of the fluorometer for 75 minutes and the

fluorescence intensity and absorbance values recorded every three minutes. The radiation intensity was controlled by varying the excitation slit width from 5 nm to 10 to 15nm. All measurements were made in triplicate.

### **2.3.5 Procedure for testing the effect of pH**

Ten solutions of 10 micromolar fura-2 and of 10 micromolar quin-2 were prepared using the appropriate buffers and adjusted to the desired pH values by dropwise addition of concentrated KOH or HCl solutions. All pH measurements were made with a Fisher-Accumet (model 825 MP) pH meter equipped with a Accu-pHast combination electrode.

- Solution (1): 10 micromolar quin-2 / 10 millimolar EGTA / 10 millimolar (CH<sub>3</sub>COONa / CH<sub>3</sub>COOH) buffer of pH 4, adjusted to pH  $4.20 \pm 0.01$ .
- Solution (2): 10 micromolar quin-2 / 10 millimolar EGTA / 10 millimolar (CH<sub>3</sub>COONa / CH<sub>3</sub>COOH) buffer of pH 5, adjusted to pH  $5.00 \pm 0.01$ .
- Solution (3): 10 micromolar quin-2 / 10 millimolar EGTA / 10 millimolar MES buffer, adjusted to pH  $5.90 \pm 0.01$ .
- Solution (4): 10 micromolar quin-2 / 10 millimolar EGTA / 10 millimolar MES buffer, adjusted to pH  $6.20 \pm 0.01$ .
- Solution (5): 10 micromolar quin-2 / 10 millimolar EGTA / 10 millimolar MOPS buffer, adjusted to pH  $6.80 \pm 0.01$ .
- Solution (6): 10 micromolar quin-2 / 10 millimolar EGTA / 10 millimolar MOPS buffer, adjusted to pH  $7.00 \pm 0.01$ .
- Solution (7): 10 micromolar quin-2 / 10 millimolar EGTA / 10 millimolar MOPS buffer, adjusted to pH  $7.20 \pm 0.01$ .

**Solution (8): 10 micromolar quin-2 / 10 millimolar EGTA / 10 millimolar HEPES buffer, adjusted to pH  $7.60 \pm 0.01$ .**

**Solution (9): 10 micromolar quin-2 / 10 millimolar EGTA / 10 millimolar HEPES buffer, adjusted to pH  $8.00 \pm 0.01$ .**

**Solution (10): 10 micromolar quin-2 / 10 millimolar EGTA / 10 millimolar ( $\text{NH}_3/\text{NH}_4\text{Cl}$ ) buffer, adjusted to pH  $10.00 \pm 0.01$ .**

A similar set of solutions was prepared for fura-2. The absorption and fluorescence spectra of all the solutions were obtained and the quantum yields of the dyes were calculated. All measurements were made in triplicate.

### **(3) Results and discussion**

The excitation and emission spectra of 5 micromolar solutions of quin-2 and fura-2 are presented in figures 2-1 and 2-2. The spectra obtained indicate that  $\lambda_{em}$  for quin-2 and for fura-2 are at 490 and 510 nm respectively, while  $\lambda_{ex}$  for quin-2 is 360 nm with a shoulder at 274 nm and that for fura-2 is 365 nm with a shoulder at 263 nm. The small difference between the  $\lambda_{em}$  values here and those reported in the literature<sup>54</sup> ( 492 nm for quin-2 and 512 for fura-2) is due to a bias in the calibration of the emission monochromator of the fluorometer used in this work. This shift was of the order of 2 nm, which is within the specifications of the instrument.

The Stokes shifts for quin-2 was  $10^7 ( 1/360 - 1/490 ) = 7370 \text{ nm}^{-1}$  and that for fura-2 was  $10^7 ( 1/365 - 1/510 ) = 7789 \text{ nm}^{-1}$ . As will be shown later, these values are subject to change upon chelation of the dyes to calcium and some other metals.

### **3.1 Calculation of quantum yields of the dyes**

The integrated areas under the fluorescence spectra, the peak absorbances, and quantum efficiencies of the samples and the standards are shown in table 2-1, along with relative standard deviations based on triplicate measurements. Quantum yields were calculated using equation (2.4).

### **3.2 Oxygen quenching**

The ratios of fluorescence peak areas in aerated and non-aerated solutions ( $F_0/F$ ), determined as described earlier, were 1.2 for quin-2 and 1.1 for fura-2. The fact that this ratio is slightly larger for quin-2 may suggest a longer fluorescence lifetime for quin-2. This was not investigated further.

Oxygen quenching is a type of excited state quenching. Oxygen can decrease the fluorescence of these dyes either by chemical oxidation, or by promoting intersystem crossing through collisions with excited dye molecules and formation of a transitory charge transfer complex.<sup>62</sup>

### **3.3 Concentration quenching**

Figures 2-3a,b and c show the calibration curves of fluorescence, absorbance and quantum yield of quin-2 in the concentration range of 0 to 1 millimolar. Up to ~50 micromolar, where the absorbance is less than 0.3, there is a linear relationship between fluorescence intensity and concentration. At higher concentrations, the excitation radiation intensity is no longer evenly distributed as it passes into the solution. The portion of the solution facing the light source absorbs a higher percentage of the radiation compared to the rest of the solution. As a result, considerable excitation occurs at one side of the cell and much less throughout the rest of the solution. This phenomena is called the inner-filter

effect.<sup>73</sup> Also, at high concentrations part of the fluorescent radiation can be reabsorbed by the sample. This process is called self-absorption.<sup>61</sup> As a result of self-absorption, less emitted radiation will reach the detector than expected. Both the inner-filter effect and self-absorption effect may contribute to the shape of the fluorescence calibration curve of quin-2 at high concentrations. It should be noted that, since there are two possible concentrations for each relative fluorescence value, in case of an unknown, one must dilute the sample and repeat the measurements to ensure that the sample concentration is in the linear portion of the calibration plot having a positive slope.

The absorbance curve for quin-2 (figure 2-3b) shows linearity up to 250 micromolar and then slightly curves down. This deviation from linearity could be due to the emitted fluorescence at high concentration adding to the transmitted radiation, thereby causing the absorbance to appear as a lower value than expected.

In the linear region of the fluorescence intensity plot the quantum efficiency of fura-2 is about seven times larger than that of quin-2 and its extinction coefficient is about four times higher. As a result the fluorescence intensity of fura-2 is about 25 to 30 times greater than the intensity of quin-2 (tables 2-2 & 2-3). Therefore in order for the same sensitivity to be achieved, a concentration range about 20 to 30 times lower was used for fura-2.

Figure 2-4a shows the fluorescence variation of fura-2 over a concentration range of 0 to 50 micromolar. Between 10 and 12.5 micromolar the plot starts to curve. As with quin-2, self absorption and inner-filter effects are the most probable cause of this behavior. However, because of the lower concentration the deviation from linearity is smaller. At higher concentrations the effect would be expected to be more pronounced.

The effect of concentration quenching on quantum yield of the dyes is presented in figures 2-3c and 2-4c. It is not surprising that in the linear region (low concentration range)  $\phi_f$  values remain constant, then decrease drastically as the quenching effect becomes more pronounced.

### **3.4 Temperature effect**

The fluorescence quantum efficiency of a compound as a function of temperature ( $\phi_f$ ) can be calculated over a wide temperature range using the following equation:<sup>56</sup>

$$\phi_f(T) = \phi_f^o \frac{\int_0^{\infty} F(\bar{\nu}, T) d\bar{\nu}}{\int_0^{\infty} F_o(\bar{\nu}) d\bar{\nu}} \frac{A_o}{A(T)} \frac{n^2(T)}{n_o^2} \quad (2.5)$$

Here  $\phi_f^o$  is the quantum yield at room temperature,  $F$  corresponds to the fluorescence spectrum in terms of the number of quanta per unit wavenumber,  $A$  is the absorbance at the excitation wavelength, and  $n$  is the refractive index of the solvent.

The change in absorbance with temperature is mainly due to variation in density of the solvent, spectral shifts and transition probabilities of the absorption peaks. The refractive index term corrects for the temperature variations in the angles of emerging emission from the plane of the cuvette-air interface. This term decreases with elevation of temperature, i.e., with decreasing solvent density for most solvents over the temperature range studied.

The integrated fluorescence emission and absorbance values, literature values of refractive indices<sup>67</sup> and the calculated quantum yields at various

temperatures are shown in table 2-4 for quin-2 and table 2-5 for fura-2. The experimental data indicate that the variation in absorbances over the temperature range of 14 to 50 °C is within 6.5% for quin-2 and 4.8% for fura-2 of absorbance values at room temperature (24°C). Variation in the refractive index of water over this temperature range is within 0.2% of the  $n$  values at room temperature. The integrated areas under the fluorescent peaks of the dyes are, however, affected much more by variation in temperature. An important reason for temperature quenching is a decrease in viscosity of the solvent with increase of temperature, which leads to an increase in the rate of collisional deactivation of the excited state. The extent of temperature quenching varies from compound to compound. Figures 2-5 and 2-6 show plots of quantum efficiency versus temperature for quin-2 and fura-2. Drop in quantum efficiency of quin-2 over the temperature range of 14 to 50°C is almost twice as large as that for fura-2. Also, temperature changes have little effect on fura-2 over the range of 14 to 24°C. Above 24°C a steady decrease is seen with increasing temperature.

### **3.5 Photodecomposition effect**

Figures 2-7 and 2-8 show the effect of xenon lamp radiation at  $\lambda_{ex}$ , 360 and 365 nm, on the quantum yields of quin-2 and fura-2 respectively. It can be seen that the rate of decomposition of both dyes increases with increasing excitation slit width. While the irradiation power of the lamp remains constant, a larger portion of the solution is exposed to a broader band of radiation at larger slit widths. The reason for testing the effect of different slit widths is that at low concentration of the dyes or in the presence of quenchers, the fluorescence intensity using the smallest set of slit sizes (Ex: 5, Em: 10 nm) shows a

considerable amount of noise. Hence, to achieve reasonable sensitivity, the slit widths must be increased.

No appreciable variation in absorbance was observed for either of these dyes over the range of slit widths investigated. Therefore, the quantum yields of the dyes were estimated from fluorescence values only.

Using the first set of slit widths (5, 10 nm), the decrease in fluorescence intensity of quin-2 over a period of 75 minutes is very gradual, with the quantum yield dropping to 91% of the original value. At 10 and 10 nm slit widths this value drops to 71% of the original value, and at 15 and 15 nm slit widths to 66%.

The drops in quantum yield for fura-2 using the narrowest set of slit widths is hardly noticeable, with a decrease after 75 minutes of only 5%. The decrease is, as for quin-2, larger with wider slits; the drop is 23% for 10 nm slit widths and 24% for 15 nm slit widths. But unlike quin-2, photodecomposition is not constant over time. Between 25 and 40 minutes the quantum yield actually rises again. Two possible explanations for this type of behavior were considered: (1) During the excitation only a small portion of the solution is irradiated directly and is subject to photodecomposition. Since the solution was not stirred, convection and diffusion might have caused replacement of decomposed molecules with new material. (2) As a result of photochemical processes fura-2 is converted to one or more new products with higher quantum yield. Since this behavior was not observed for quin-2 the first explanation seems unlikely. The second explanation, however, appears more reasonable because a slight shift in the wavelength of the fluorescence maximum of fura-2, from 510 nm to 507 nm, was also observed. At the same time one might expect some change in the absorbance of the product relative to the original dye, although it is possible that the new product might have the same absorbance as the original fura-2.



Figures 2-9 and 2-10 show the effect of laboratory fluorescent lights on quin-2 and fura-2 over a period of 96 hours. The drop of quantum efficiency is 55% for quin-2 and 28% for fura-2. Similar to the previous study of decomposition at  $\lambda_{ex}$ , the quantum yield of fura-2 shows some small increases at some points throughout the time period. Decomposition of the dyes could also be partially due to hydrolysis and interactions in the solutions. In order to isolate the effect of the fluorescent lights, two identical sets of solutions may be prepared, one to be kept in the dark and the other to be exposed to the fluorescent lights for the same period of time and the measurements to be taken at the same intervals. Then the results obtained from the solutions in the dark (blanks) could be subtracted from those obtained from the solutions exposed to light. This kind of parallel experiment was not done here.

### 3.6 Effect of pH on quantum yield of the dyes

Figures 2-11 and 2-12 show the variation in quantum yield of quin-2 and fura-2 as a function of pH. Neither of the dyes show sensitivity to pH in the pH range of 7 to 8. The fluorescence intensity of quin-2 drops steadily with increasing acidity below pH 7. This effect may be due to protonation of amine nitrogens on the aromatic rings. If it is assumed that the aromatic nitrogen in quin-2 has a  $pK_a$  similar to that of aniline (4.6)<sup>65</sup>, it would become progressively protonated as pH values dropped below 7. Hence the lone electron pair of the nitrogen would no longer be delocalized and the cation would have a resonance form similar to benzene. This would lead to a decrease in fluorescence and a shift in  $\lambda_{ex}$  and  $\lambda_{em}$  toward shorter wavelengths (benzene exhibits fluorescence only in the ultraviolet region)<sup>62</sup>. The same argument could be used for protonation of the amino nitrogen on the other side of the molecule, where the structure is similar

to that of 8-aminoquinoline, which has a  $pK_a$  of 4.04<sup>65</sup>. Protonation of the amino nitrogen here would prevent delocalization of the electron pair and hence this portion of the molecule may have only the resonance of quinoline.

The behavior of fura-2 as a function of pH is exactly opposite to that of quin-2, i.e., the fluorescence intensity of the dye increases with the acidity of the solution. The reason for this behavior is not clear. It seems that even with protonation of nitrogen atoms on both sides of the molecule, because of a higher degree of conjugation on the left side of the molecule in figure 1-4 compared with quin-2, there will be still some delocalization of the electron lone pair over the heterocyclic groups and hence the fluorescence intensity will not drop as it does in the case of quin-2. The small shift of the fluorescence wavelength for fura-2 could be due to protonation of the amino nitrogen on the right side of the molecule, leaving the aromatic group with only the resonance of benzene, which fluoresces at shorter wavelengths.

The absorbances of the dyes show no variation over the pH range of 4.2 to 10 (see tables 2-14 & 2-15), therefore quantum yield values were estimated directly from the integrated fluorescence areas. The absorption wavelength of quin-2, however, shows a small shift toward shorter wavelengths with increasing acidity.

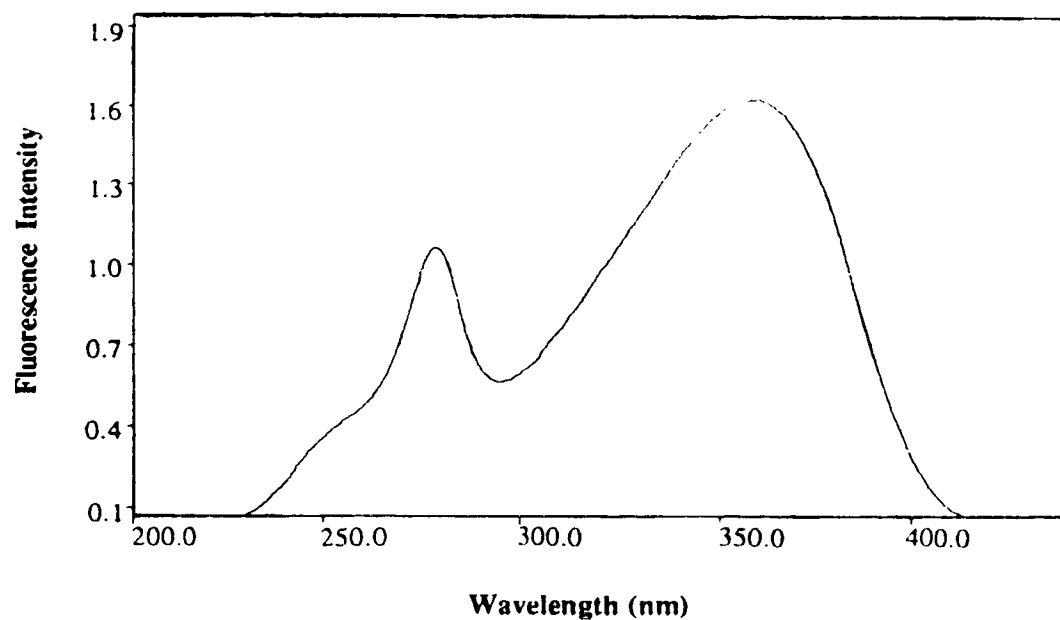


**Figure 2-1a** Excitation spectrum of quin-2

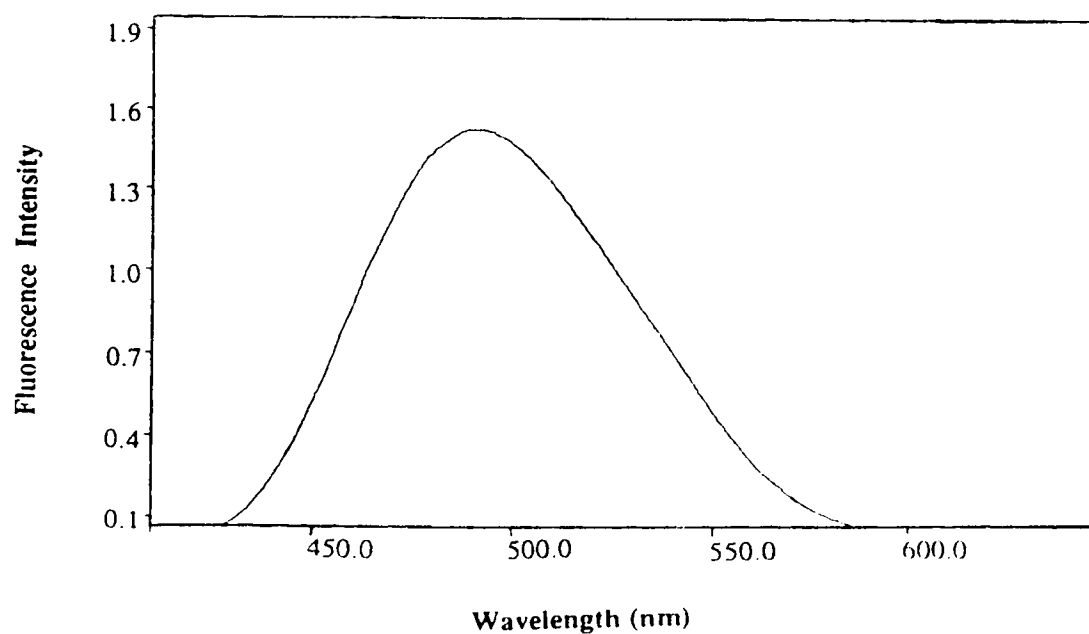


**Figure 2-1b** Emission spectrum of quin-2

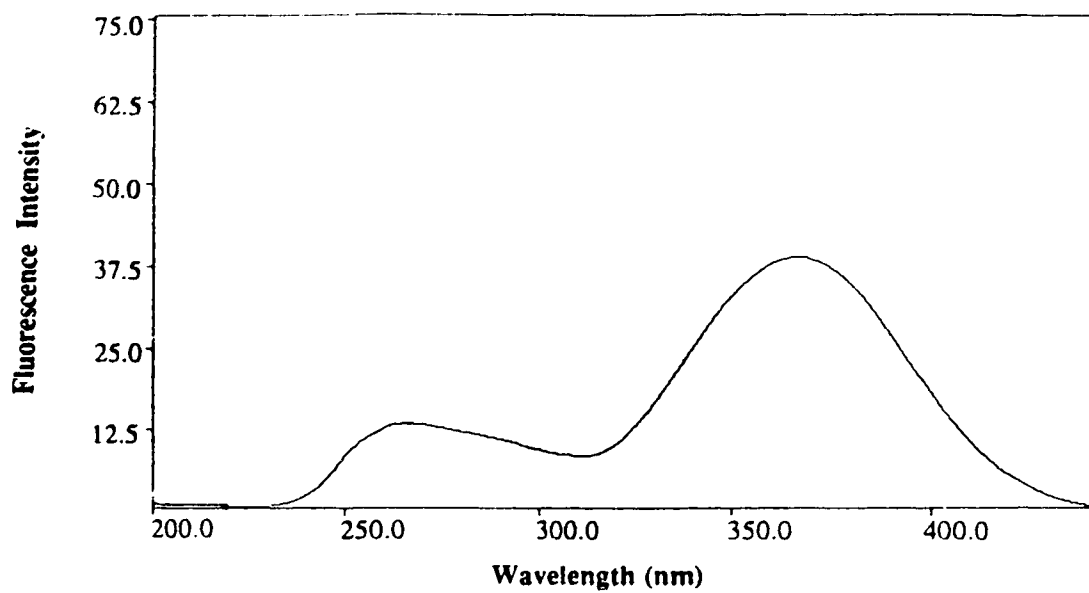


**Figure 2-2a** Excitation spectrum of fura-2

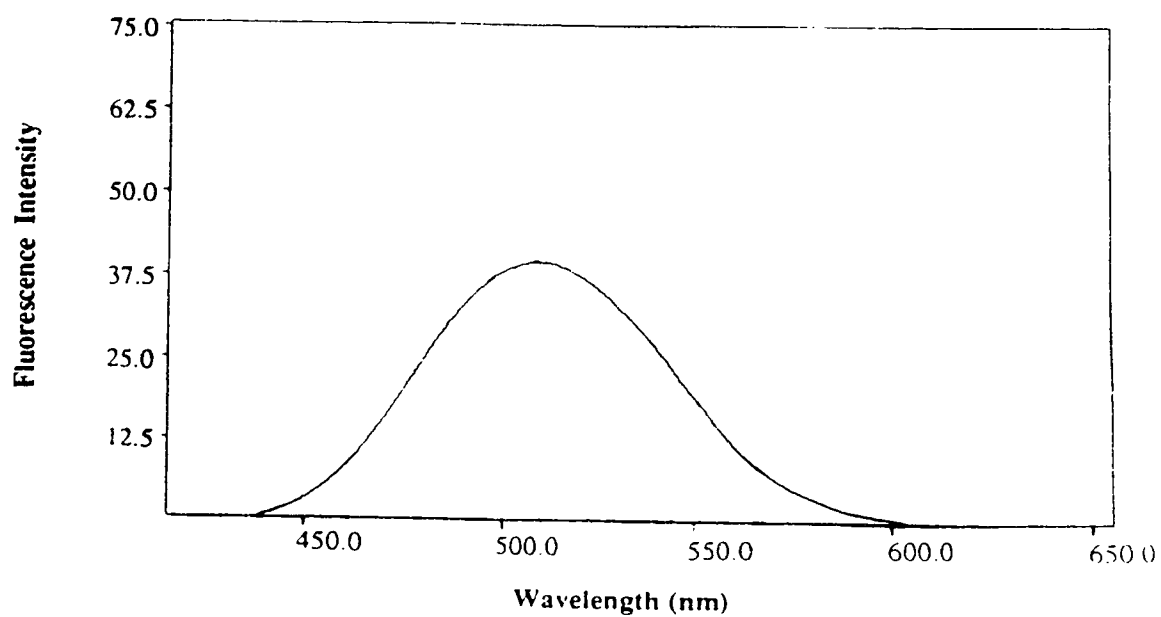


**Figure 2-2b** Emission spectrum of fura-2

**Table 2-1** Calculated quantum yields of quin-2 and fura-2 based on tabulated quantum yield of quinine sulfate at room temperature

<u>Dye Samples</u>	<u>F</u> <sup>a</sup>	<u>RSD</u> <sup>b</sup>	<u>A</u>	<u>RSD</u> <sup>c</sup>	<u><math>\Phi_f</math></u>	<u>RSD</u> <sup>d</sup>
5 micromolar Fura-2	3003	0.6	0.104	0.7	0.242	1.3
5 micromolar Quinine	7690	0.4	0.118	0.8	0.546	-
5 micromolar Quin-2	109.6	0.9	0.028	0.2	0.033	1.3

<sup>a</sup> Integrated fluorescence area.

<sup>b</sup> The error of the integrated fluorescence area is expressed as relative standard deviation in percent.

<sup>c</sup> Relative standard deviation of absorbance in percent.

<sup>d</sup> Relative standard deviation of quantum efficiency in percent, obtained by taking the square root of sum of the squares of uncertainties of all the known components in equation 2.4 (e.g., for fura-2,  $RSD = [ (0.6)^2 + (0.7)^2 + (0.4)^2 + (0.8)^2 ]^{1/2}$  ).

**Table 2-2** Effect of self absorption and concentration quenching on quantum yield of quin-2.

<u>Conc.</u> <u>(millimolar)</u>	<u>Intensity</u>	<u>RSD</u>	<u>A</u>	<u>RSD</u>	<u>F</u> <sup>a</sup>	<u>RSD</u>	<u><math>\phi_f</math></u>	<u>RSD</u> <sup>b</sup>
0.000	0.00	0.0	0.000	0.0	0.0	0.0	0.0000	0.0
0.005	1.56	2.5	0.027	0.9	112.3	1.0	0.0326	2.0
0.010	2.99	0.6	0.052	0.7	213	0.6	0.0318	1.8
0.020	5.95	0.6	0.103	1.1	427	0.7	0.0320	2.0
0.050	14.9	1.3	0.255	0.5	1066	0.6	0.0323	1.7
0.100	18.9	2.1	0.477	1.0	1356	0.4	0.0220	2.0
0.250	21.8	0.8	1.108	0.6	1554	1.3	0.0206	2.1
0.500	19.3	1.1	1.905	0.8	1368	0.9	0.0106	1.9
0.750	15.0	0.7	2.581	0.7	1072	0.2	0.0062	1.7
1.000	7.64	0.9	3.150	1.3	543.4	0.7	0.0025	2.1

<sup>a</sup> Integrated fluorescence area.

<sup>b</sup> See the footnote for table 2-1.

**Table 2-3** Effect of self absorption and concentration quenching on quantum yield of fura-2.

<u>Conc.</u> (micromolar)	<u>Intensity</u>	<u>RSD</u>	<u>A</u>	<u>RSD</u>	<u>F</u> <sup>a</sup>	<u>RSD</u>	<u><math>\phi_f</math></u>	<u>RSD</u> <sup>b</sup>
0.0	0.00	0.0	0.000	0.0	0	0.0	0.0000	0.0
1.0	8.01	0.9	0.021	1.0	614	0.9	0.2460	2.1
2.0	16.0	1.9	0.043	0.4	1230	1.8	0.2407	2.4
5.0	39.5	0.6	0.105	1.0	3029	0.5	0.2428	2.0
7.0	55.4	1.4	0.147	0.6	4253	1.3	0.2434	2.1
10.0	77.5	1.5	0.210	1.4	5956	1.6	0.2385	2.7
12.5	90.0	1.2	0.262	0.9	6907	0.9	0.2213	2.0
25.0	135	2.2	0.492	0.4	10378	2.1	0.1771	2.7
50.0	170	0.6	0.809	1.1	13058	0.7	0.1354	2.1

<sup>a</sup> Integrated fluorescence area.

<sup>b</sup> See the footnote for table 2-1.

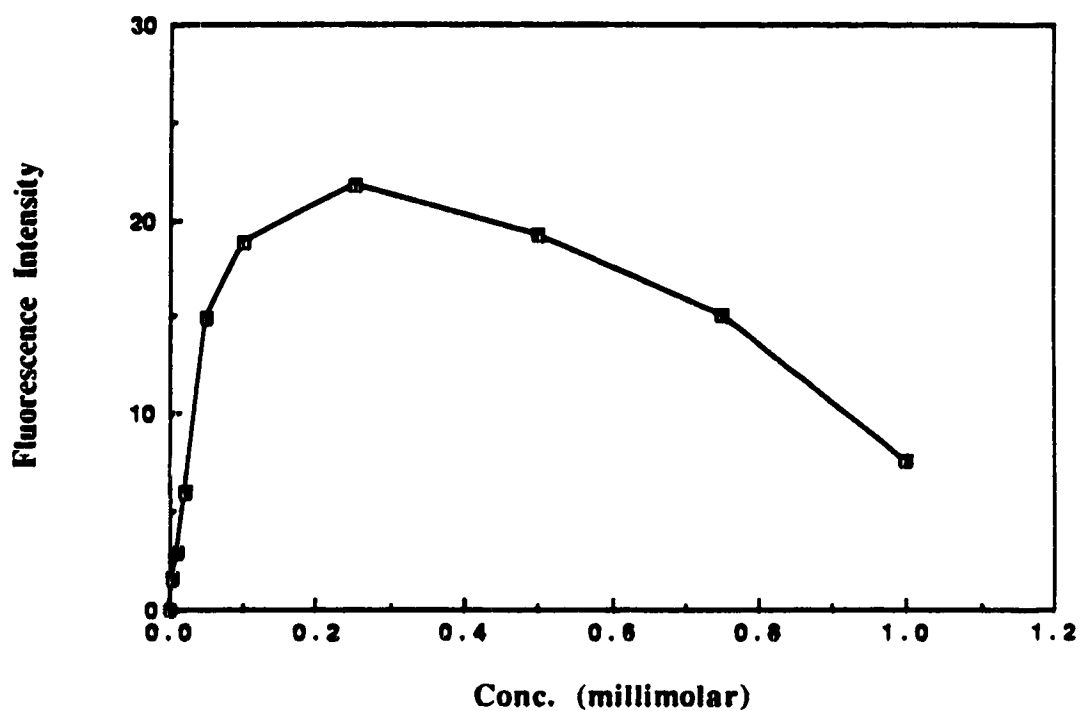


**Figure 2-3a** Effect of concentration on fluorescence intensity of quin-2. The linear region covers a concentration range of 0 to 0.05 millimolar; at higher concentrations the plot starts to deviate from linearity and above 0.25 millimolar the intensity starts to decrease.



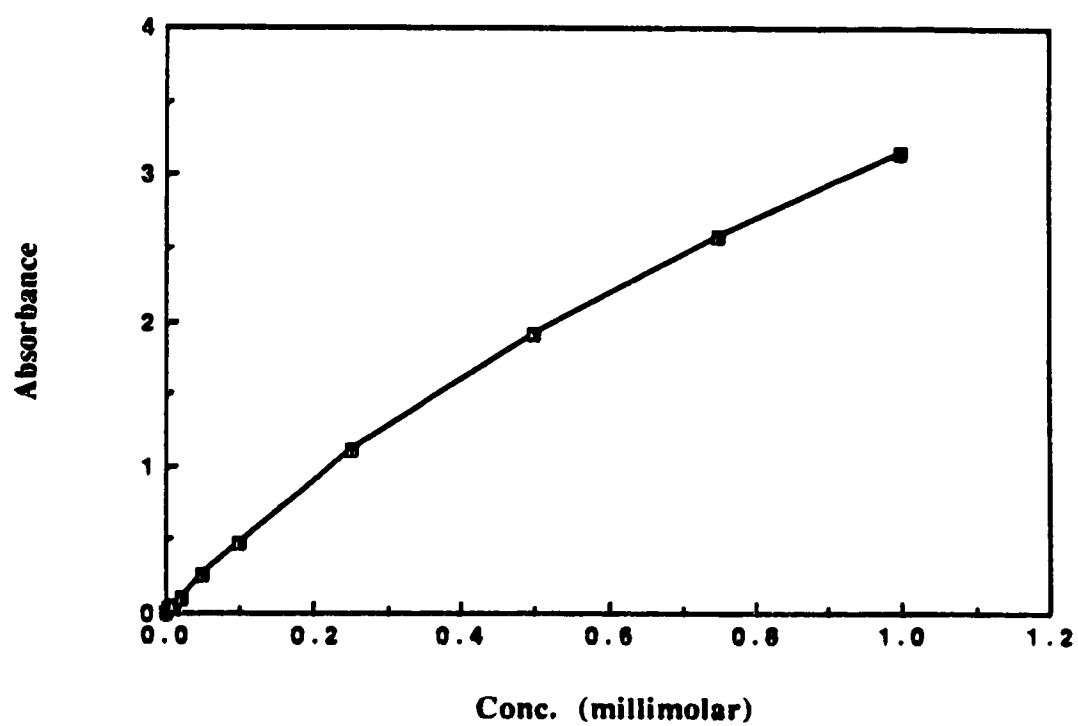


**Figure 2-3b** Absorbance versus concentration plot for quin-2. The curve starts to deviate from linearity at about 0.25 millimolar.

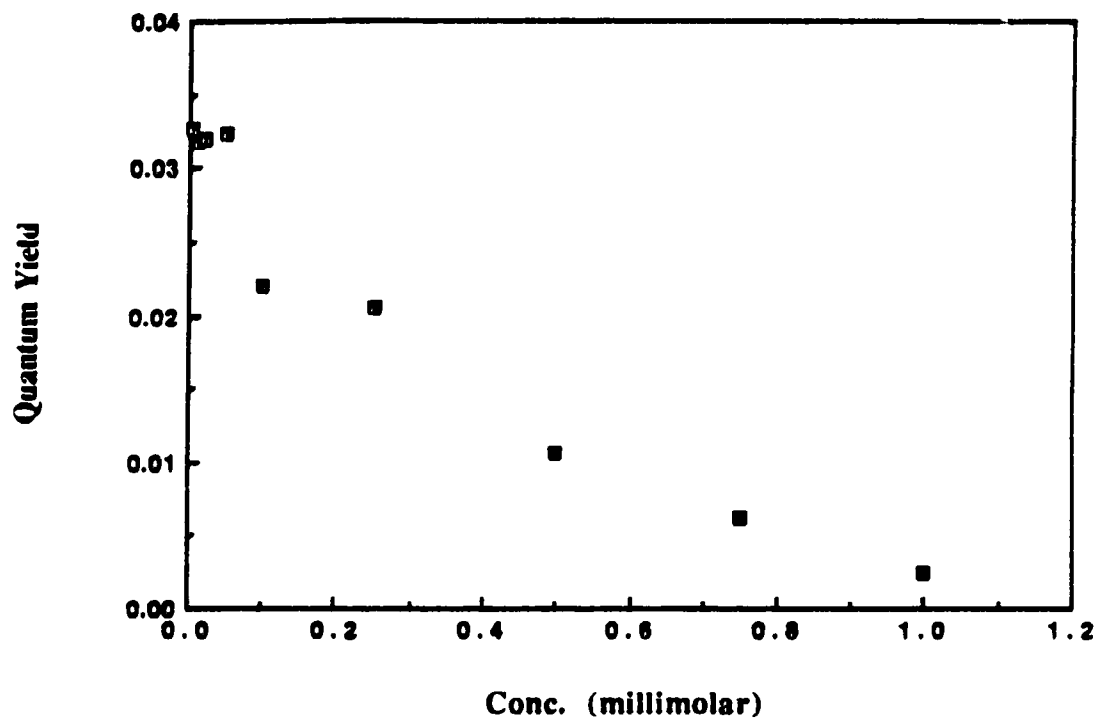


**Figure 2-3c** Effect of concentration on quantum efficiency of quin-2. No variation of quantum yield is observed over a concentration range of 0.005 to 0.05 millimolar ( $\phi_f \sim 0.032$ ). The value drops to 0.0025 at 1 millimolar.

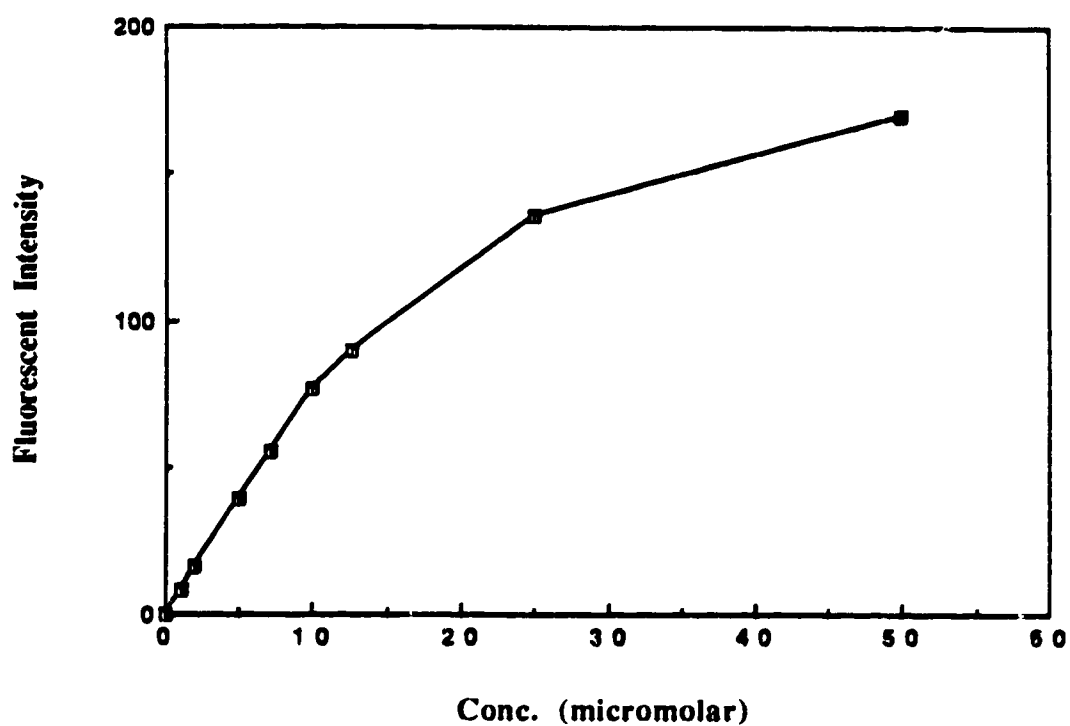


**Figure 2-4a** Effect of concentration on fluorescence intensity of fura-2; the plot starts to deviate from linearity at about 10 micromolar.

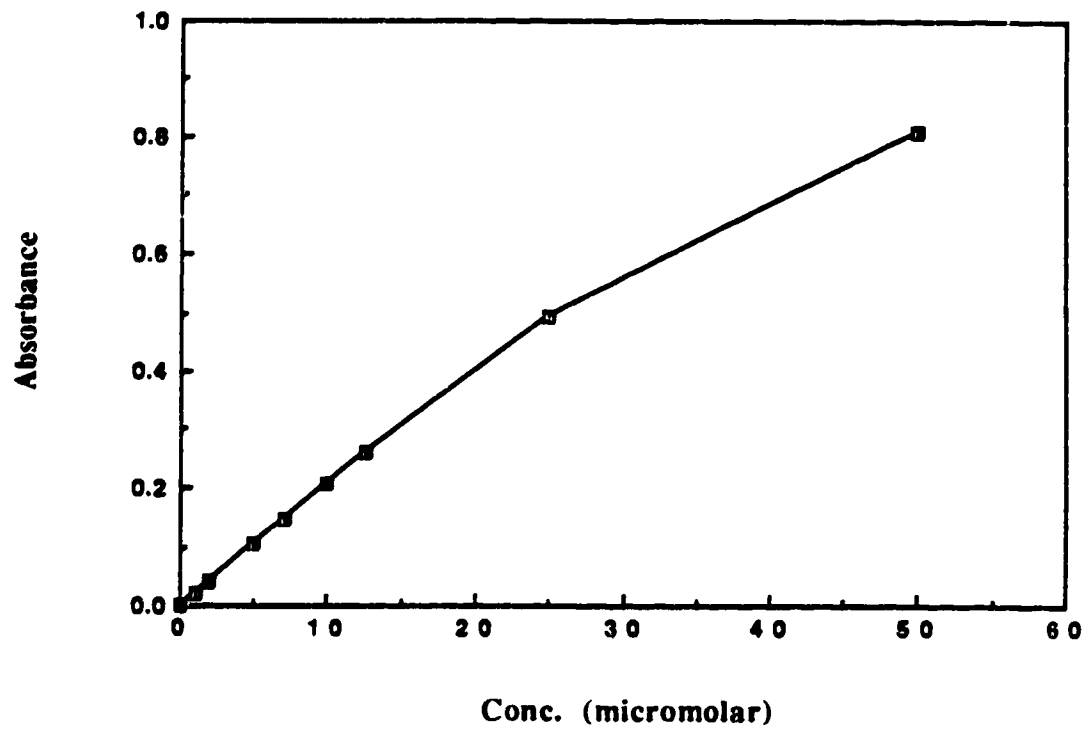


**Figure 2-4b** Absorbance versus concentration plot for fura-2. It begins to deviate from linearity at about 25 micromolar.

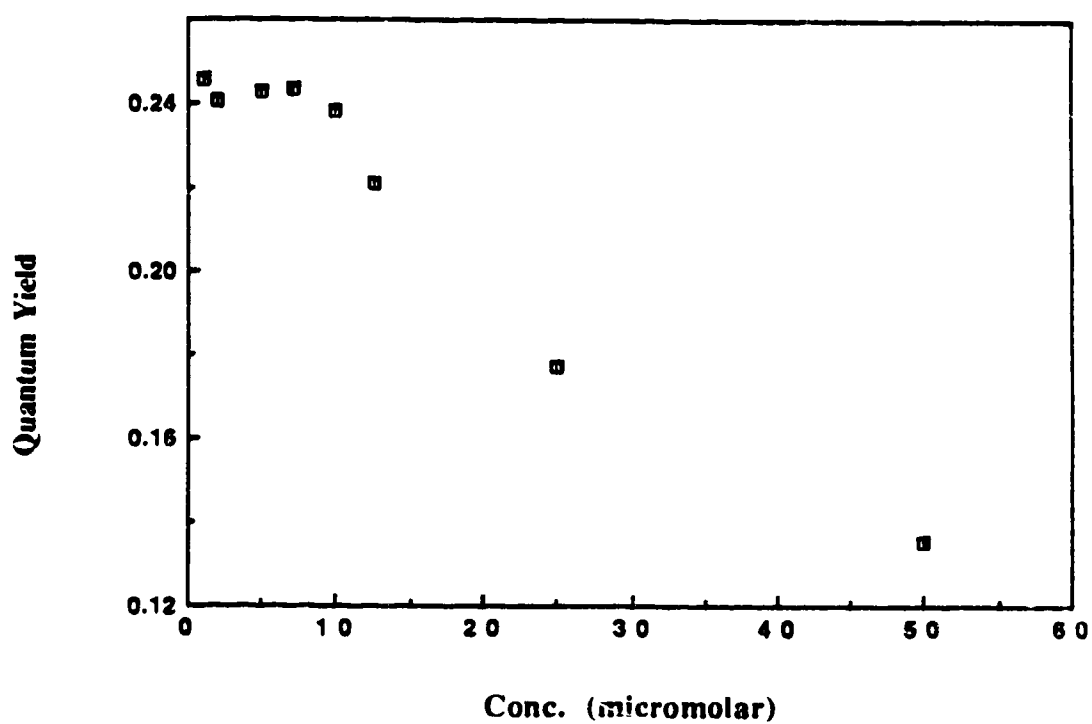


**Figure 2-4c** Effect of concentration on quantum efficiency of fura-2. There is no considerable variation in quantum yield over a concentration range of 0.001 to 0.01 millimolar ( $\phi_f \sim 0.24$ ). The value drops to 0.135 at 50 micromolar.

**Table 2-4** Effect of temperature on quantum efficiency of quin-2.

<u>T (°C)</u>	<u>n<sup>67</sup></u>	<u>F(<math>\bar{\nu}</math>, T)</u> <sup>a</sup>	<u>RSD</u>	<u><math>\Delta</math></u>	<u>RSD</u>	<u><math>\phi_f</math></u>	<u>RSD</u> <sup>b</sup>
14	1.3335	142	1.1	0.0282	2.7	0.0403	3.2
16	1.3333	134	0.8	0.0277	3.2	0.0388	3.6
20	1.3330	124	0.6	0.0274	2.8	0.0363	3.2
24	1.3326	111	0.9	0.0271	0.2	0.0328	1.2
26	1.3324	105	0.9	0.0274	1.9	0.0308	2.6
28	1.3322	97.9	0.5	0.0268	3.7	0.0293	4.1
32	1.3316	92.4	0.8	0.0269	0.9	0.0275	1.9
36	1.3311	81.9	0.6	0.0264	3.1	0.0249	3.5
38	1.3308	76.0	1.2	0.0261	2.2	0.0232	2.9
40	1.3305	71.7	0.7	0.0258	1.8	0.0219	2.7
44	1.3299	66.3	1.1	0.0253	1.7	0.0209	2.5
48	1.3293	56.9	0.3	0.0252	2.7	0.0179	3.2
50	1.3289	50.0	1.0	0.0252	2.8	0.0158	3.3

<sup>a</sup> Integrated fluorescence area as a function of wavelength and temperature.

<sup>b</sup> See the footnote for table 2-1.

**Table 2-5** Effect of temperature on quantum efficiency of fura-2.

<u>T (°C)</u>	<u>n</u>	<u>F(<math>\bar{\nu}</math>, T)</u> <sup>a</sup>	<u>RSD</u>	<u>A</u>	<u>RSD</u>	<u><math>\phi_f</math></u>	<u>RSD</u> <sup>b</sup>
14	1.3335	3179	0.4	0.109	0.3	0.2451	1.7
16	1.3333	3143	0.1	0.108	0.2	0.2452	1.6
20	1.3330	3064	1.3	0.107	0.6	0.2439	2.1
24	1.3326	3003	1.6	0.104	1.1	0.2421	2.5
26	1.3324	2893	1.3	0.104	1.3	0.2332	2.4
28	1.3322	2781	0.1	0.104	0.1	0.2269	1.6
32	1.3316	2728	0.6	0.103	1.8	0.2210	2.5
36	1.3311	2571	0.4	0.103	0.4	0.2094	1.7
38	1.3308	2482	0.5	0.103	0.6	0.2000	1.8
40	1.3305	2389	0.8	0.102	0.9	0.1955	2.0
44	1.3299	2279	1.4	0.102	2.1	0.1867	3.0
48	1.3293	2144	1.4	0.102	0.2	0.1751	2.1
50	1.3289	2011	0.3	0.102	0.1	0.1647	1.6

<sup>a</sup> Integrated fluorescence area as a function of wavelength and temperature.

<sup>b</sup> See the footnote for table 2-1.

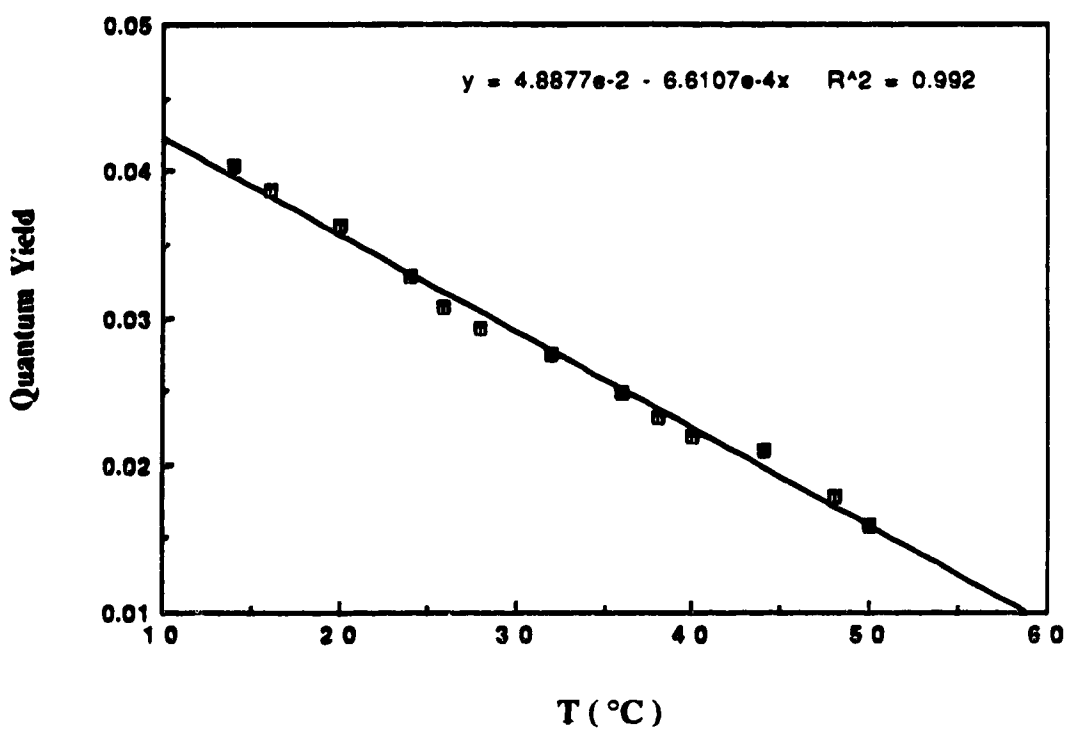


**Figure 2-5** Effect of temperature on the quantum efficiency of quin-2; The results show a drop of 61% in quantum yield over a temperature range of 14 to 50 °C



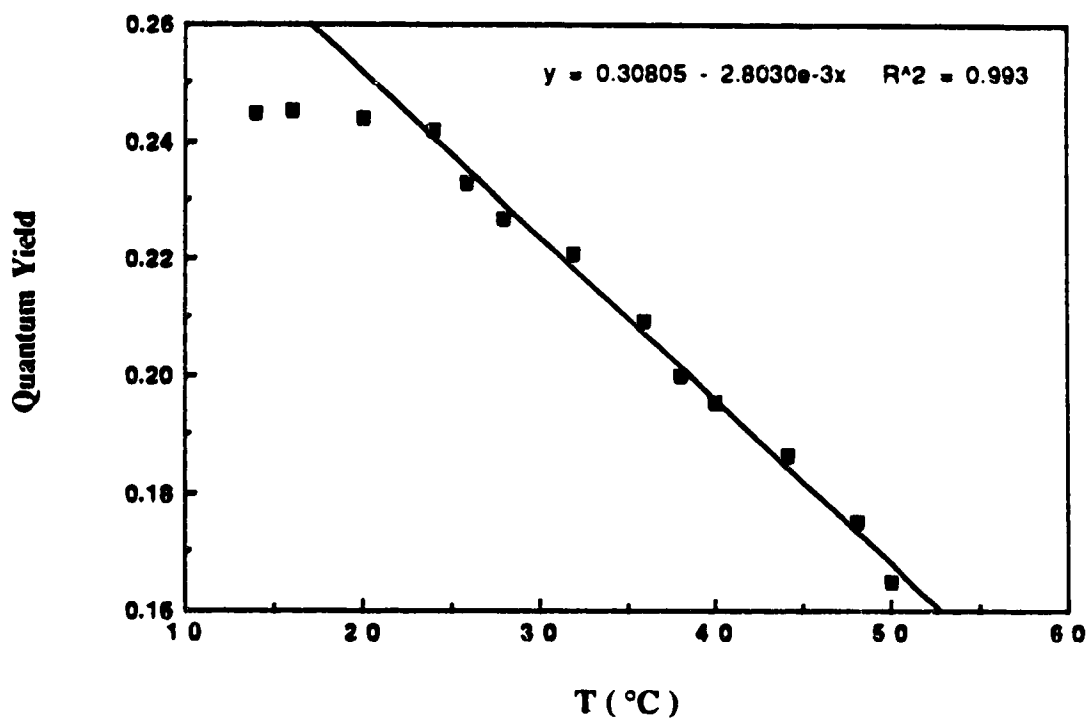


**Figure 2-6** Effect of temperature on the quantum efficiency of fura-2; little variation in quantum yield is observed over a temperature range of 14 to 24°C. Over the temperature range of 24 to 50°C the drop in quantum yield is about 33%.

**Table 2-6** Photochemical decomposition of quin-2 at excitation and emission slit widths of 5 and 10 nm respectively.

<u>Time (min)</u>	<u>E<sup>a</sup></u>	<u>RSD</u>	<u><math>\Phi_f</math></u>	<u>RSD<sup>b</sup></u>
0	111.4	0.3	0.0329	1.5
3	111.5	0.4	0.0329	1.6
6	108.8	0.1	0.0320	1.5
9	108.4	1.0	0.0319	1.8
12	107.4	0.2	0.0317	1.5
15	106.5	2.6	0.0313	3.0
18	105.1	1.9	0.0309	2.4
21	106.4	1.0	0.0313	1.8
24	106.3	0.4	0.0312	1.5
27	105.6	1.2	0.0311	1.9
30	105.3	0.8	0.0310	1.7
33	105.7	0.6	0.0311	1.6
36	104.7	0.4	0.0308	1.6
39	104.9	0.7	0.0309	1.7
42	104.1	1.6	0.0306	2.2
45	105.0	0.7	0.0309	1.7
48	103.6	1.0	0.0305	1.8
51	103.5	0.5	0.0305	1.8
54	103.1	1.3	0.0304	2.0
57	103.0	0.4	0.0304	1.6
60	102.3	1.3	0.0301	2.0
63	103.2	0.6	0.0304	1.6
66	102.6	0.6	0.0301	1.6
69	102.2	0.7	0.0300	1.7
72	102.5	0.7	0.0301	1.7
75	101.4	1.6	0.0298	2.2

<sup>a</sup> Integrated fluorescence area.

<sup>b</sup> See the footnote for table 2-1.

**Table 2-7** Photochemical decomposition of quin-2 at excitation and emission slit widths of 10 and 10 nm respectively.

<u>Time (min)</u>	<u>E<sup>a</sup></u>	<u>RSD</u>	<u><math>\phi_f</math></u>	<u>RSD<sup>b</sup></u>
0	245.2	0.6	0.0328	1.2
3	236.7	1.3	0.0317	1.9
6	228.4	1.4	0.0306	2.0
9	222.2	1.3	0.0297	1.9
12	221.0	1.2	0.0296	1.8
15	216.8	2.3	0.0289	2.7
18	214.3	0.8	0.0286	1.6
21	212.7	0.4	0.0284	1.4
24	105.2	2.1	0.0274	2.5
27	205.0	0.1	0.0274	1.4
30	202.9	0.6	0.0272	1.5
33	198.1	0.6	0.0265	1.5
36	196.4	0.3	0.0263	1.4
39	192.9	1.2	0.0257	1.8
42	190.5	0.7	0.0254	1.5
45	187.4	0.7	0.0251	1.5
48	187.4	0.5	0.0251	1.4
51	182.8	0.4	0.0244	1.4
54	184.0	0.9	0.0246	1.6
57	179.7	1.3	0.0242	1.9
60	180.7	1.7	0.0242	2.2
63	180.2	0.2	0.0241	1.4
66	180.2	0.1	0.0241	1.4
69	179.2	0.8	0.0240	1.6
72	178.1	0.3	0.0238	1.4
75	175.0	1.1	0.0234	1.7

<sup>a</sup> Integrated fluorescence area.

<sup>b</sup> See the footnote for table 2-1.

**Table 2-8** Photochemical decomposition of quin-2 at excitation and emission slit widths of 15 and 15 nm.

<u>Time (min)</u>	<u>F<sup>a</sup></u>	<u>RSD</u>	<u><math>\Phi_f</math></u>	<u>RSD<sup>b</sup></u>
0	992.5	1.1	0.0328	1.2
3	961.0	0.9	0.0318	1.9
6	918.8	0.1	0.0287	1.6
9	892.5	2.2	0.0295	2.7
12	858.5	1.1	0.0284	2.0
15	848.0	0.5	0.0280	1.7
18	834.5	1.9	0.0276	2.5
21	818.7	0.8	0.0271	1.8
24	792.3	0.3	0.0262	1.7
27	776.4	0.9	0.0256	1.9
30	760.7	1.4	0.0251	2.2
33	750.1	1.7	0.0248	2.4
36	739.6	0.2	0.0244	1.7
39	723.8	2.2	0.0239	2.7
42	718.5	0.3	0.0238	1.7
45	702.7	1.0	0.0232	1.9
48	697.6	0.8	0.0230	1.8
51	692.3	0.1	0.0229	1.6
54	681.8	0.1	0.0226	1.6
57	681.7	0.8	0.0226	1.8
60	671.1	0.4	0.0222	1.7
63	660.6	0.5	0.0218	1.7
66	655.4	0.4	0.0217	1.7
69	655.4	0.1	0.0217	1.6
72	654.3	0.3	0.0217	1.7
75	654.7	0.5	0.0217	1.7

<sup>a</sup> Integrated fluorescence area.

<sup>b</sup> See the footnote for table 2-1.

**Table 2-9** Effect of photodecomposition on fura-2 at excitation and emission slit widths of 5 and 10 nm.

<u>Time (min)</u>	<u>F<sup>a</sup></u>	<u>RSD</u>	<u><math>\Phi_f</math></u>	<u>RSD<sup>b</sup></u>
0	3005	0.3	0.2421	1.3
3	2895	1.5	0.2332	2.1
6	2992	0.8	0.2411	1.6
9	3019	0.1	0.2432	1.4
12	2924	2.0	0.2356	2.5
15	2947	1.5	0.2375	2.1
18	2974	0.7	0.2396	1.6
21	2788	0.6	0.2247	1.6
24	2819	1.6	0.2272	2.1
27	2782	1.6	0.2242	1.8
30	3037	1.2	0.2448	1.9
33	3033	1.1	0.2444	1.8
36	2863	1.3	0.2307	1.9
39	2871	1.1	0.2313	1.8
42	2871	0.7	0.2313	1.6
45	2842	0.2	0.2290	1.4
48	2878	0.6	0.2319	1.6
51	2926	0.2	0.2357	1.4
54	2833	0.2	0.2283	1.4
57	2809	0.4	0.2265	1.5
60	2882	0.3	0.2322	1.5
63	2831	0.5	0.2281	1.5
66	2795	1.1	0.2253	1.8
69	2911	1.0	0.2345	1.7
72	2853	0.6	0.2299	1.6
75	2847	1.5	0.2295	2.1

<sup>a</sup> Integrated fluorescence area.

<sup>b</sup> See the footnote for table 2-1.

**Table 2-10** Photochemical decomposition of fura-2 at excitation and emission slit widths of 10 and 10 nm.

<u>Time (min)</u>	<u>F<sup>a</sup></u>	<u>RSD</u>	<u><math>\Phi_f</math></u>	<u>RSD<sup>b</sup></u>
0	6746	0.8	0.2421	1.3
3	6507	0.9	0.2335	1.7
6	6396	1.1	0.2296	1.8
9	5963	0.4	0.2141	1.5
12	6156	2.1	0.2209	2.5
15	6156	0.2	0.2209	1.4
18	6001	0.8	0.2154	1.6
21	5730	1.4	0.2056	2.0
24	5807	3.6	0.2085	3.8
27	6105	0.5	0.2191	1.5
30	6069	2.0	0.2178	2.5
33	5805	2.5	0.2083	2.9
36	5818	2.1	0.2088	2.5
39	5925	0.8	0.2126	1.6
42	5707	1.8	0.2048	2.3
45	5728	2.4	0.2127	2.8
48	5732	1.5	0.2057	2.1
51	5608	1.0	0.2002	1.7
54	5462	1.1	0.1960	1.8
57	5394	2.1	0.1935	2.5
60	5311	1.4	0.1906	2.0
63	5213	1.0	0.1907	1.7
66	5244	1.7	0.1882	2.2
69	5288	0.8	0.1898	1.6
72	5176	0.8	0.1858	1.6
75	5181	0.2	0.1859	1.4

<sup>a</sup> Integrated fluorescence area.

<sup>b</sup> See the footnote for table 2-1.

**Table 2-11** Photochemical decomposition of fura-2 at excitation and emission slit width of 15 and 15 nm.

<u>Time (min)</u>	<u>F<sup>a</sup></u>	<u>RSD</u>	<u><math>\Phi_f</math></u>	<u>RSD<sup>b</sup></u>
0	25740	1.12	0.2421	1.8
3	24795	2.13	0.2332	2.6
6	23776	0.71	0.2236	1.6
9	22812	2.14	0.2146	2.6
12	21958	1.79	0.2066	2.3
15	23061	1.76	0.2169	2.3
18	22430	1.85	0.2110	2.3
21	23006	1.63	0.2164	2.2
24	21938	1.31	0.2064	1.9
27	21800	0.86	0.2050	1.7
30	21958	0.72	0.2066	1.6
33	22160	0.46	0.2085	1.5
36	22468	0.34	0.2113	1.5
39	22506	1.10	0.2116	1.8
42	22419	0.79	0.2109	1.6
45	22273	0.55	0.2096	1.5
48	20544	1.13	0.1933	1.8
51	21169	0.67	0.1991	1.6
54	21169	0.83	0.1991	1.7
57	20390	0.93	0.1881	1.7
60	19909	0.36	0.1872	1.5
63	19798	0.18	0.1862	1.4
66	19594	0.08	0.1844	1.4
69	19594	0.31	0.1844	1.4
72	19698	0.59	0.1852	1.5
75	19643	0.28	0.1848	1.4

<sup>a</sup> Integrated fluorescence area.

<sup>b</sup> See the footnote for table 2-1.

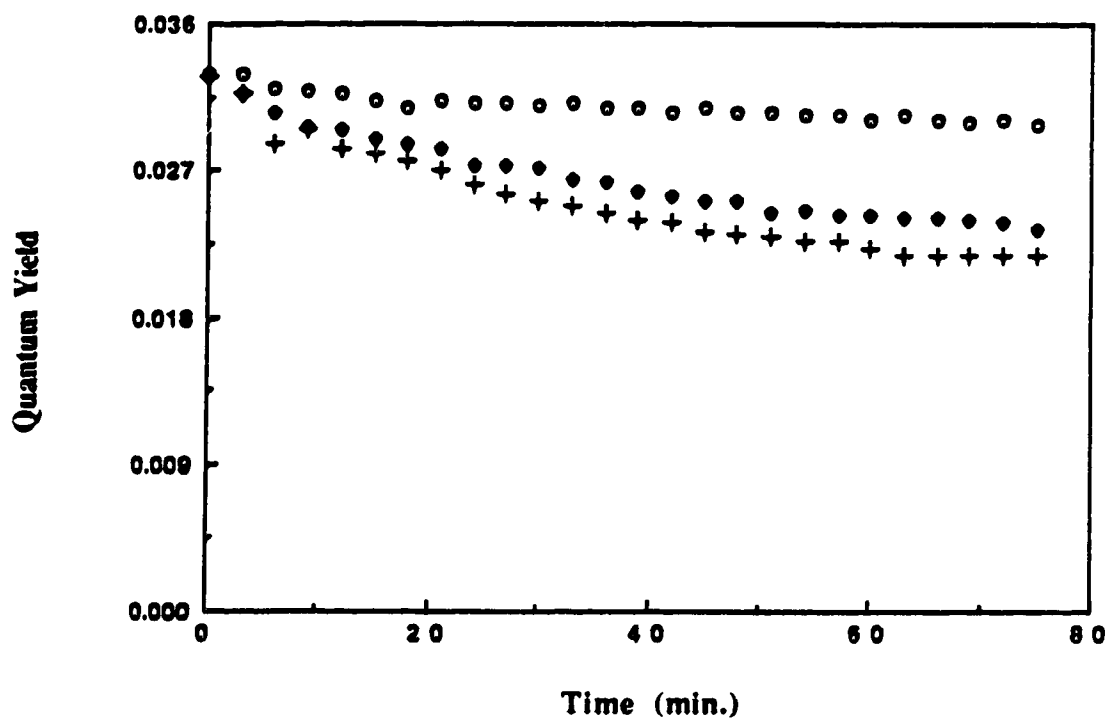


**Figure 2-7** Effect on quantum yield of exposure of a 5 micromolar solution of quin-2 to radiation at  $\lambda_{\text{ex}}$ , 360 nm, from the 150 W xenon source lamp of the Shimadzu fluorometer over a period of 75 minutes at three sets of excitation and emission slit widths: 5 & 10 nm ( o ), 10 & 10 nm ( • ), and 15 & 15 nm ( + ).



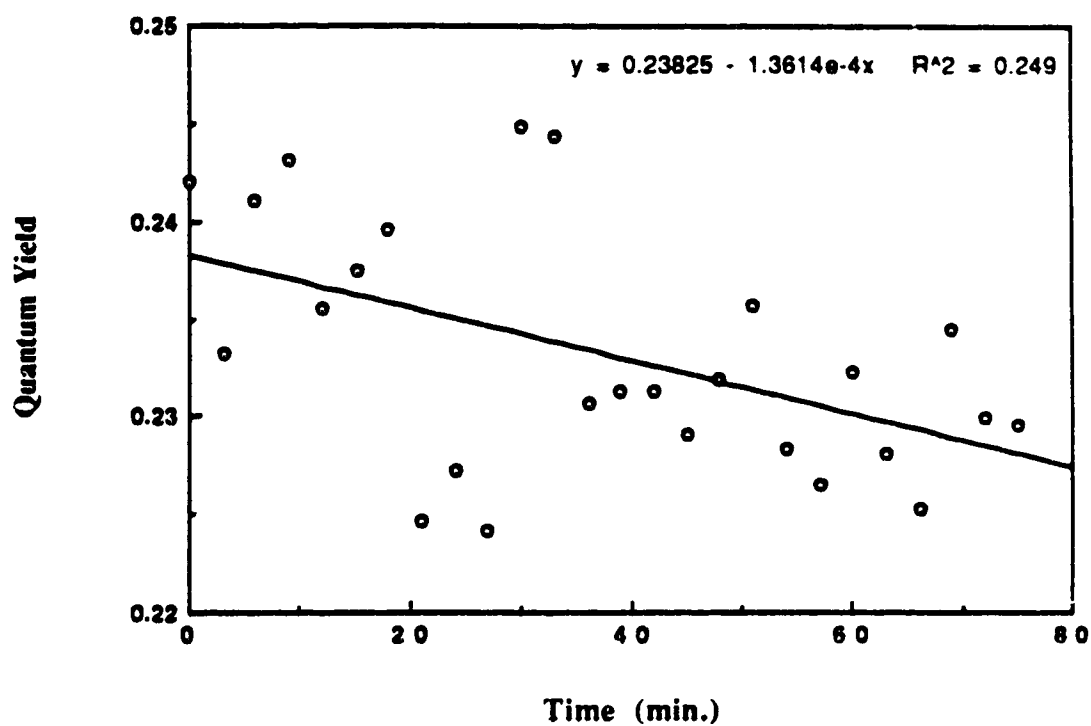


**Figure 2-8a** Variation in quantum yield of 5 micromolar fura-2 as a result of exposure of the dye to radiation from the 150 W xenon source lamp of the Shimadzu fluorometer for 75 minutes at excitation and emission slit widths of 5 and 10 nm.

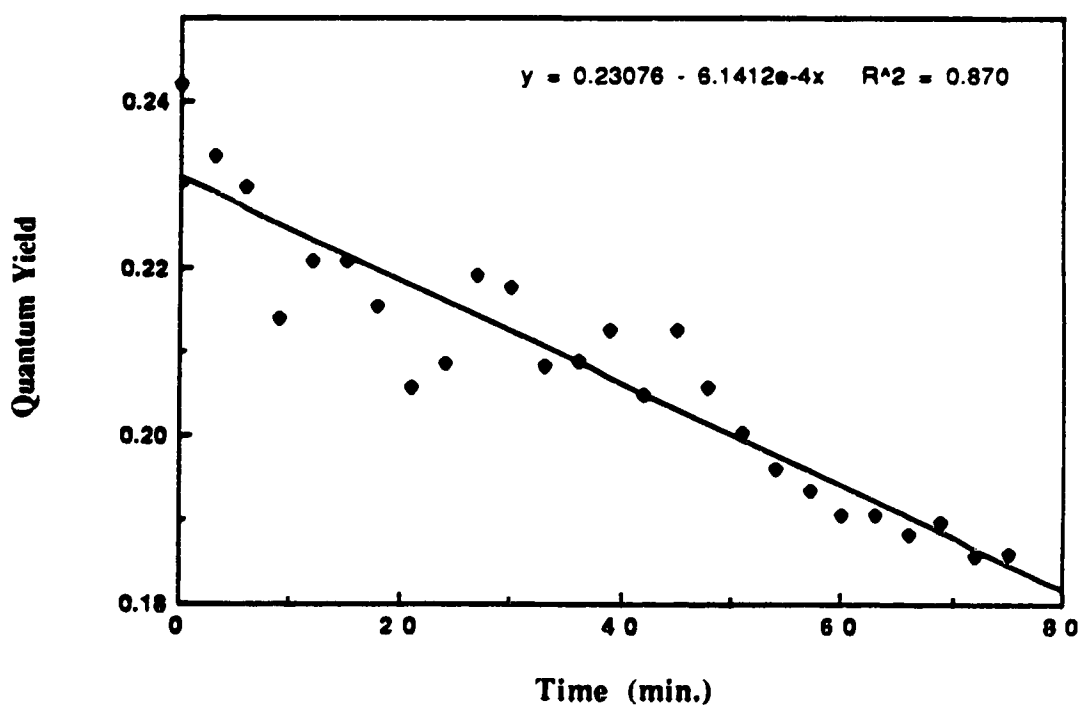


**Figure 2-8b** Variation in quantum yield of 5 micromolar fura-2 as a result of exposure of the dye to radiation from the 150 W xenon source lamp of the Shimadzu fluorometer for 75 minutes at excitation and emission slit widths of 10 and 10 nm.

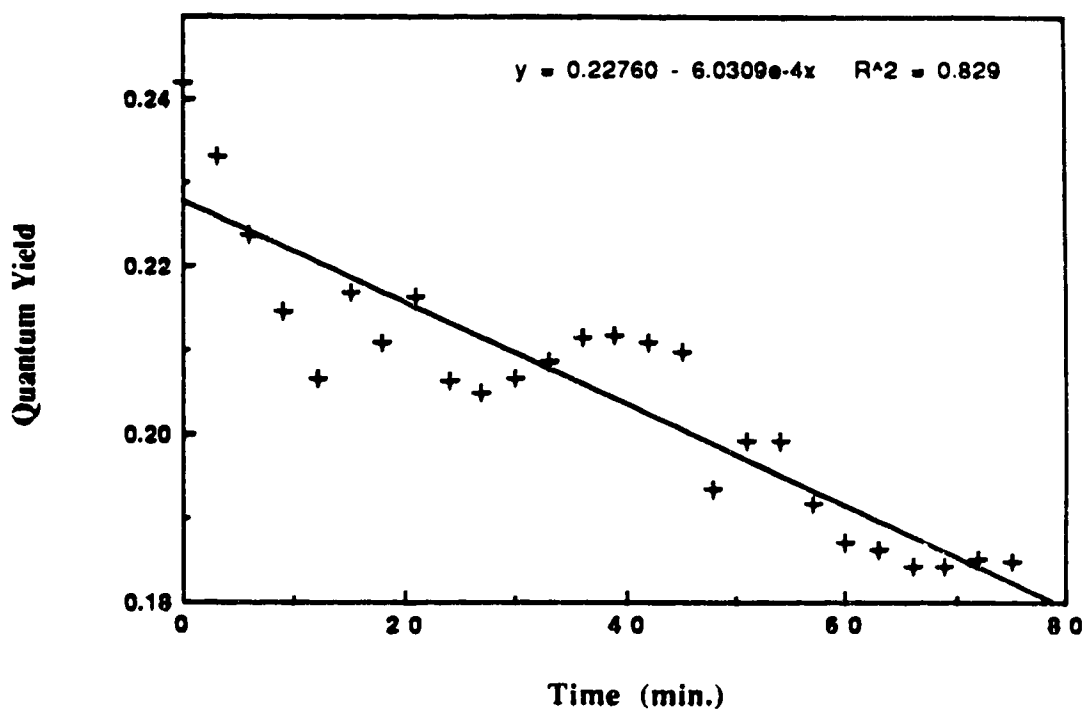


**Figure 2-8c** Variation in quantum yield of 5 micromolar fura-2 as a result of exposure of the dye to radiation from the 150 W xenon source lamp of the Shimadzu fluorometer for 75 minutes at excitation and emission slit widths of 15 and 15 nm.

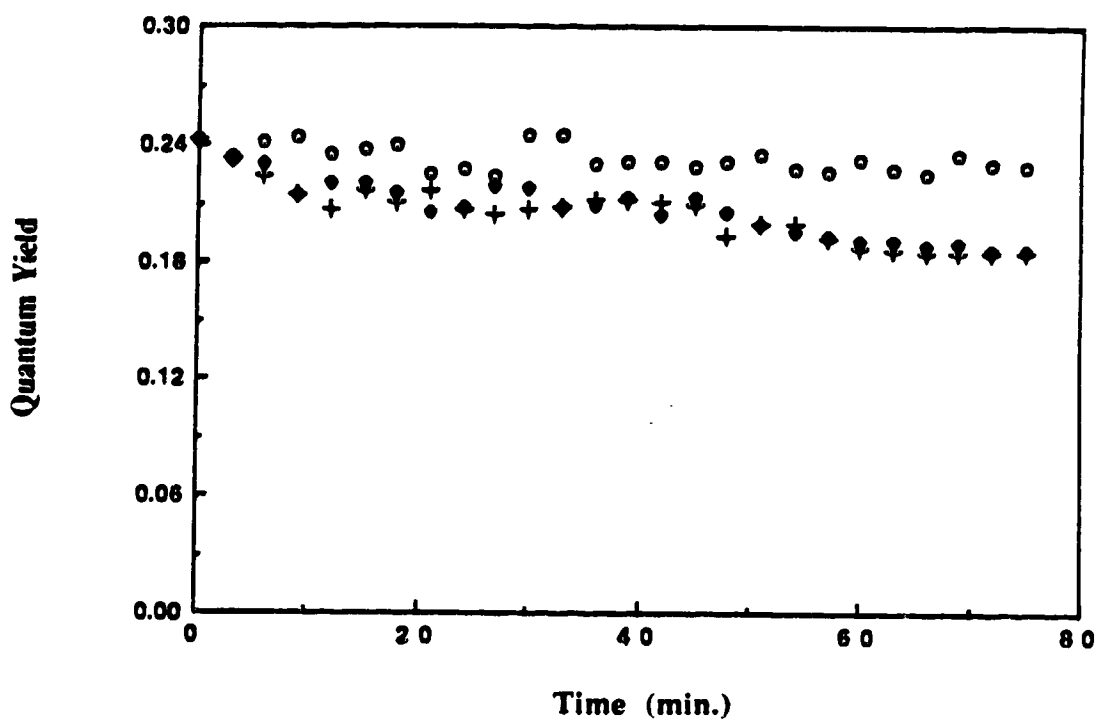


**Figure 2-8d** Effect on quantum yield of exposure of a 5 micromolar solution of fura-2 to radiation at  $\lambda_{\text{ex}}$ , 365 nm, from the 150 W xenon lamp over a period of 75 minutes at three sets of excitation and emission slit widths: 5 & 10 nm ( $\circ$ ), 10 & 10 nm ( $\bullet$ ), and 15 & 15 nm ( $+$ ).

**Table 2-12 Photochemical decomposition of quin-2 as a result of exposure to the conventional laboratory lights.**

<b>Time (hr)</b>	<b>F <sup>a</sup></b>	<b>RSD</b>	<b><math>\Phi_f</math></b>	<b>RSD <sup>b</sup></b>
0	1089	0.7	0.0338	1.7
1/2	1032	0.9	0.0320	1.8
1	1021	2.7	0.0318	3.1
1 1/2	983	1.6	0.0305	2.2
2	970	0.8	0.0300	1.7
2 1/2	932	2.1	0.0289	2.6
3	926	1.3	0.0287	2.0
3 1/2	910	1.1	0.0283	1.9
4	894	0.5	0.0277	1.6
4 1/2	887	0.3	0.0275	1.5
5	883	1.5	0.0274	2.1
5 1/2	881	0.8	0.0273	1.7
6	878	0.6	0.0272	1.6
20	819	0.4	0.0254	1.6
24	795	0.7	0.0246	1.7
30	770	1.2	0.0239	1.9
44	692	0.5	0.0215	1.6
48	685	0.3	0.0212	1.5
54	660	0.8	0.0205	1.7
68	589	0.8	0.0183	1.7
72	582	0.8	0.0180	1.7
78	553	1.3	0.0172	2.0
92	514	0.6	0.0160	1.6
96	500	2.1	0.0155	2.6

<sup>a</sup> Integrated fluorescence area.

<sup>b</sup> See the footnote for table 2-1.

**Table 2-13** Photochemical decomposition of fura-2 as a result of exposure to the conventional laboratory lights.

<u>Time (hr)</u>	<u>F</u> <sup>a</sup>	<u>RSD</u>	<u><math>\Phi_f</math></u>	<u>RSD</u> <sup>b</sup>
0	3018	0.5	0.2432	1.5
1/2	3002	1.5	0.2419	2.1
1	2996	0.4	0.2395	1.6
1 1/2	2972	1.9	0.2395	2.4
2	2955	1.2	0.2382	1.9
2 1/2	2875	2.0	0.2317	2.5
3	2935	1.3	0.2365	2.0
3 1/2	2955	1.9	0.2382	2.4
4	2913	1.7	0.2347	2.3
4 1/2	2903	0.6	0.2339	1.6
5	2875	0.4	0.2317	1.6
5 1/2	2867	1.1	0.2310	1.9
6	2860	0.4	0.2305	1.6
20	2709	1.2	0.2184	1.9
24	2720	0.9	0.2192	1.8
30	2726	2.0	0.2197	2.5
44	2647	1.1	0.2133	1.9
48	2663	0.4	0.2135	1.6
54	2553	0.9	0.2057	1.8
68	2469	1.0	0.1990	1.8
72	2437	0.2	0.1964	1.5
78	2349	1.7	0.1893	2.3
92	2202	0.5	0.1774	1.6
96	2191	2.1	0.1750	2.5

<sup>a</sup> Integrated fluorescence area.

<sup>b</sup> See the footnote for table 2-1.

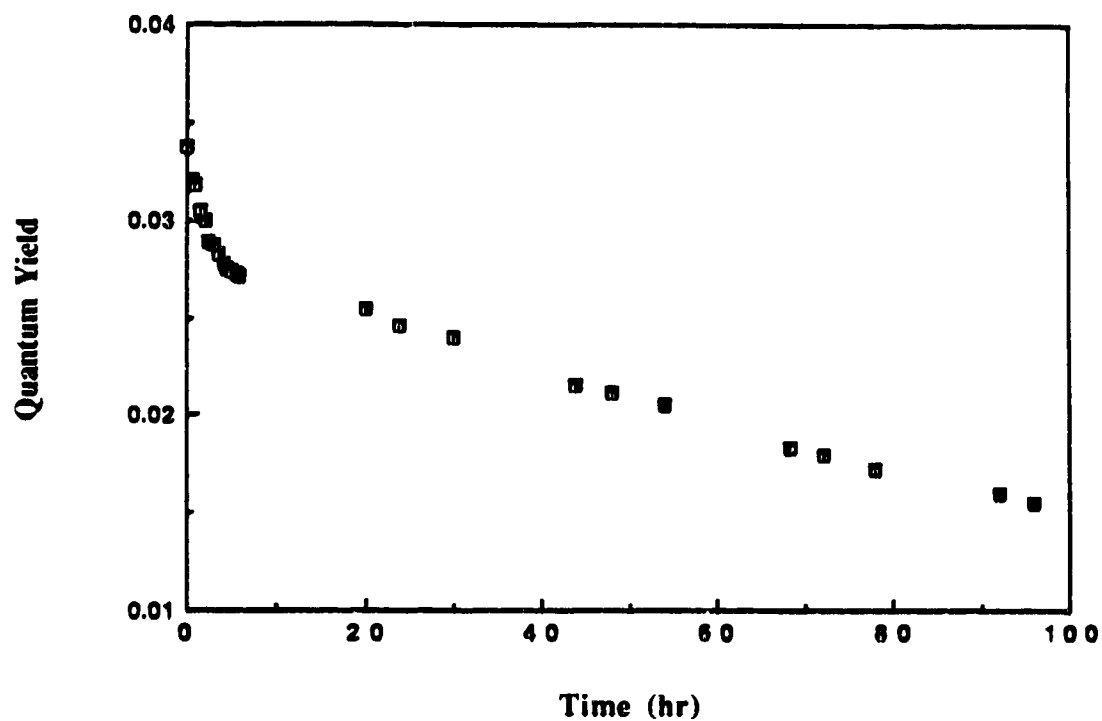


**Figure 2-9** Effect of conventional fluorescent laboratory illumination on quantum yield of quin-2 over a period of 96 hours; the data show a sharp drop in the first 6 hours followed by a more gradual constant decrease over the rest of the period.

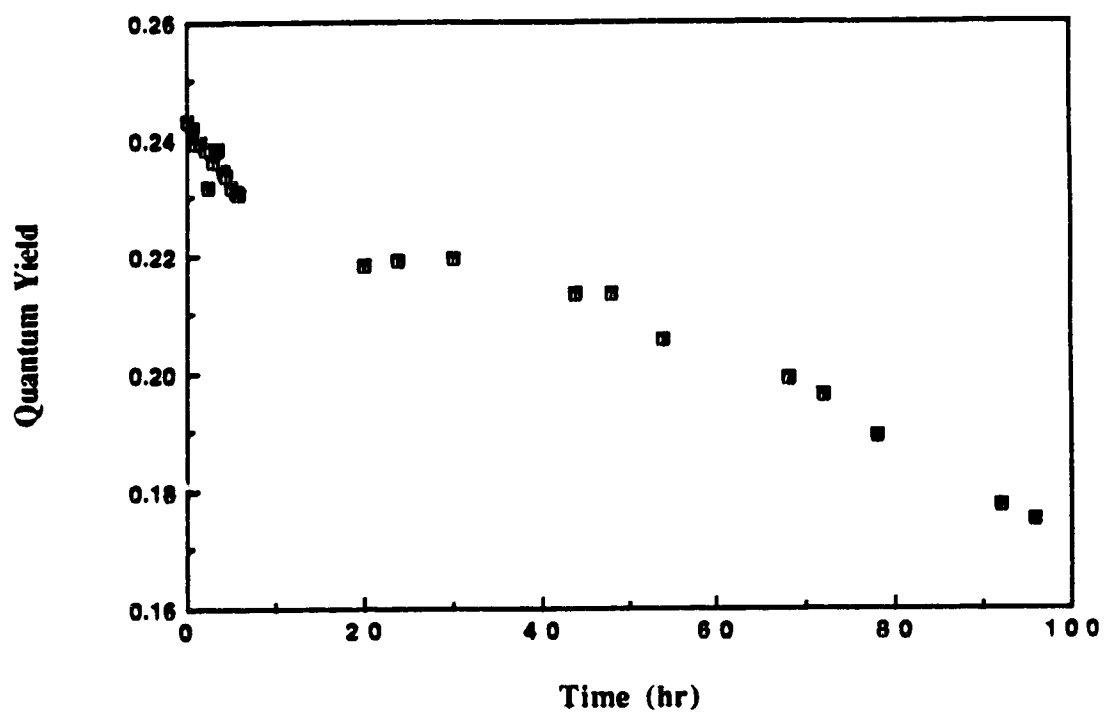


**Figure 2-10** Effect of conventional fluorescent laboratory illumination on quantum yield of fura-2 over a period of 96 hours; the data show an overall drop of 28%.



**Table 2-14** Variation of quantum yield of quin-2 with pH.

<b>pH</b>	<b>F<sup>a</sup></b>	<b>RSD</b>	<b><math>\lambda_{em}</math></b>	<b><math>\lambda_{ex}</math></b>	<b>A</b>	<b>RSD</b>	<b><math>\lambda_{abs}</math></b>	<b><math>\phi_f</math></b>	<b>RSD<sup>b</sup></b>
4.2	85.7	0.6	476	349	0.0501	1.4	340	0.0132	2.0
5.0	111.6	0.9	490	352	0.0500	1.9	340	0.0172	2.1
5.9	149.8	1.7	492	356	0.0506	2.8	342	0.0231	2.5
6.2	162.0	1.2	491	355	0.0510	0.8	344	0.0250	2.2
6.8	177.1	2.0	492	355	0.0504	2.0	348	0.0273	2.8
7.0	214.6	0.5	492	358	0.0508	1.4	350	0.0331	2.1
7.2	215.1	0.4	492	360	0.0513	2.4	350	0.0332	1.9
7.6	217.4	1.4	492	358	0.0518	0.8	354	0.0334	2.4
8.0	211.6	1.9	492	359	0.0509	2.0	354	0.0327	2.7
10.0	144.7	2.1	492	358	0.0505	2.2	356	0.0222	2.8

<sup>a</sup> Integrated fluorescence area.<sup>b</sup> See the footnote for table 2-1.

**Table 2-15** Variation of quantum yield of fura-2 with pH.

<b>pH</b>	<b>F<sup>a</sup></b>	<b>RSD</b>	<b><math>\lambda_{em}</math></b>	<b><math>\lambda_{ex}</math></b>	<b><math>\Delta</math></b>	<b>RSD</b>	<b><math>\lambda_{abs}</math></b>	<b><math>\Phi_f</math></b>	<b>RSD<sup>b</sup></b>
4.2	13273	1.2	500	362	0.202	2.8	364	0.5317	2.9
5.0	12448	0.8	500	362	0.199	0.8	364	0.4987	3.2
5.9	9440	0.9	500	363	0.206	3.1	364	0.3782	3.3
6.2	8124	1.7	504	364	0.198	0.7	364	0.3255	3.6
6.8	6602	2.0	509	367	0.207	2.5	364	0.2646	3.7
7.0	5936	0.6	509	366	0.208	2.1	364	0.2378	3.2
7.2	5929	1.7	510	368	0.211	0.5	364	0.2375	3.6
7.6	5959	0.6	510	367	0.209	1.3	364	0.2387	3.2
8.0	5990	0.8	510	367	0.208	0.9	364	0.2400	3.2
10.0	6151	1.1	509	367	0.201	2.4	364	0.2464	3.3

<sup>a</sup> Integrated fluorescence area.

<sup>b</sup> See the footnote for table 2-1.

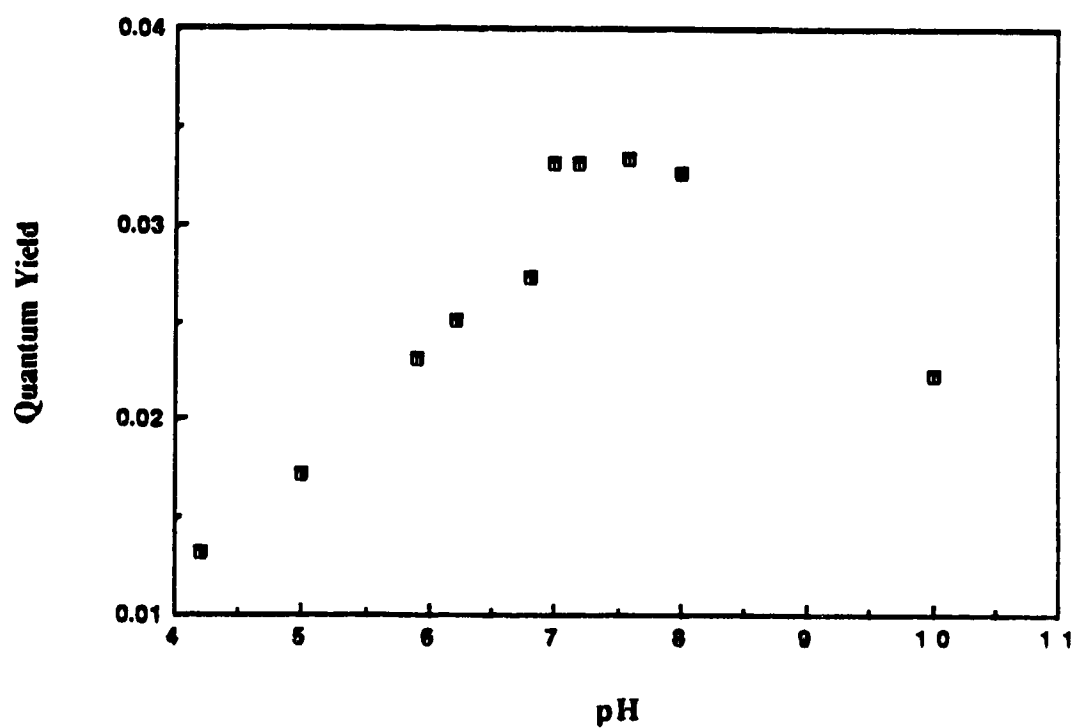


**Figure 2-11** Variation in quantum yield of quin-2 as a function of pH; the yield shows a rise as it moves from acidic pH values toward neutrality, and then drops again under more alkaline conditions.

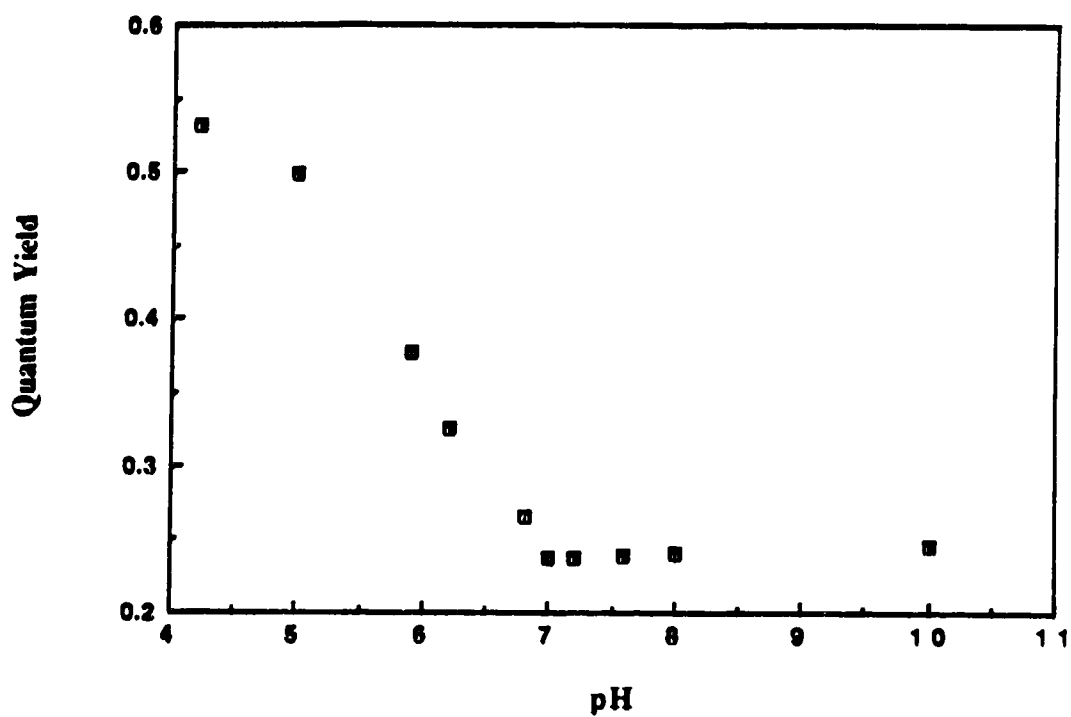


**Figure 2-12** Variation in quantum yield of fura-2 as a function of pH; the yield shows a decrease with decreasing acidity upto pH 7. A slight increase is seen on moving from pH 7 to pH 10.

## **Chapter 3**

### **Complexation of Free Calcium(II) in Solution with Quin-2 and Fura-2 under Physiological Conditions**

#### **1. Background**

In this chapter the effect of physiological environmental conditions, including pH, temperature, ionic strength and presence of magnesium as a competing metal ion, on the chelating properties of quin-2 and fura-2 toward  $\text{Ca}^{2+}$  is reported. To avoid potential problems with shifting of free calcium concentrations for calibration curves at low calcium ion levels, Ca-EGTA buffers were used.<sup>65, 68</sup>

The four carboxyl groups on EGTA are highly acidic, with pKa's below 3.0. For our purposes EGTA may be considered always to be negatively charged. The two amino nitrogens of EGTA bind protons with pKa's above the physiological pH range, so they will tend to be mainly in the protonated form under the conditions of interest in this work. Protonation of these nitrogens greatly reduces the affinity of EGTA for calcium and other metal ions; the doubly protonated species, which is the most abundant one in the physiological pH range, has a negligible affinity for metal ions. The singly protonated species, on the other hand, has a much lower affinity than the unprotonated species, but still enough that it cannot always be neglected. Hence metal-ion binding of EGTA may be regarded as being accomplished entirely by the unprotonated and the monoprotonated forms of the molecule, even though the fraction of the total ligand present in these forms is much lower than that of the doubly protonated species.

Protonation has a much more pronounced effect in the case of Ca-EGTA binding than in that of Mg-EGTA. The association constant for  $\text{Ca}^{2+}(\text{EGTA})$  is reduced more than five log units by the addition of one proton to EGTA while that for  $\text{Mg}^{2+}(\text{EGTA})$  is reduced by less than two log units.

The conditional association constant,  $K'$ , for the binding of a metal ion to a chelator is defined as if the chelator existed as a single unprotonated species capable of binding metal ions and is written as:

$$K' = \frac{[\text{metal-chelator complex}]}{[\text{metal ion}][\text{free chelator}]}$$

To calculate a conditional, association constant corresponding to a particular pH, one must determine the fraction of the chelator (ligand) in the unprotonated (L) and monoprotonated (HL) states, multiply the corresponding absolute metal ion association constants by those fractions, and sum the contributions of all the species. To make these calculations one needs to know the absolute metal ion association constants for the unprotonated species ( $K_{\text{ML}}^{\text{M}}$ ) and the monoprotonated species ( $K_{\text{MHL}}^{\text{M}}$ ), as well as the proton association constants for any proton binding sites on the ligand that may be occupied to a significant extent at the pH under consideration.

The association, or stability, constants reported in standard tables (e.g. Martell and Smith, 1974) are obtained at specified particular temperatures and ionic strengths. For them to be used for calculation of conditional constants  $K'$  at the conditions of interest, corrections of temperature and ionic strength to as similar a condition as possible are required.

To calculate an association constant at a temperature of interest differing from a reported table value, one can use the Clausius-Clapyeron equation<sup>69</sup>:

$$\log K_2 = \log K_1 + \frac{\Delta H}{2.303R} \left( \frac{1}{T_1} - \frac{1}{T_2} \right) \quad (3.1)$$

Here  $K_2$  is the association constant at the temperature of interest  $T_2$ ,  $K_1$  is the tabulated association constant at temperature  $T_1$ ,  $R$  is the ideal gas constant, and  $\Delta H$  is the enthalpy of complexation.

Corrections for ionic strength can be made if the activity coefficients for the ionic strength of interest and the ionic strengths of the tabulated association constants are known. The thermodynamic association constant  $K^\circ$  for the formation of the metal-ligand complex (ML) can be written as follows:

$$K^\circ = \frac{[ML]}{[M][L]} \frac{\gamma_{ML}}{\gamma_M \gamma_L} \quad (3.2)$$

where  $\gamma_M$ ,  $\gamma_L$  and  $\gamma_{ML}$  are the activity coefficients of metal, ligand and metal-ligand complex respectively. If the conditional stability constant for a particular ionic strength, e.g., 0.1, is denoted as  $K_{0.1}$ , the following equation can be written:

$$K^\circ = K_{0.1} \left( \frac{\gamma_{ML}}{\gamma_M \gamma_L} \right)_{0.1} \quad (3.3)$$

A similar equation can be written for a different ionic strength, e.g., 0.2, and since  $K^\circ$  is a constant, the following relationship can be written:

$$K_{0.1} \left( \frac{\gamma_{ML}}{\gamma_M \gamma_L} \right)_{0.1} = K_{0.2} \left( \frac{\gamma_{ML}}{\gamma_M \gamma_L} \right)_{0.2} \quad (3.4)$$

Hence in order to calculate  $K_{0.2}$ ,  $K_{0.1}$  can be obtained from standard tables and activity coefficients can be calculated using the Davies equation. The form of the Davies equation used in this work is<sup>22</sup>:

$$-\log \gamma = AZ^2 \left[ \frac{\sqrt{\mu}}{1 + \sqrt{\mu}} - 0.3\mu \right] \quad (3.5)$$

Here  $A$  is a constant at a particular temperature,  $Z$  is the charge on the ion and  $\mu$  is the ionic strength.

As was mentioned earlier, the apparent association constant at any given pH reflects the binding of metal ions to both the unprotonated and monoprotonated forms of the chelator. In the case of  $\text{Ca}^{2+}$ , the affinity of the unprotonated form of EGTA is so high relative to that of the monoprotonated one (more than five orders of magnitude greater) that the contribution of the latter can be neglected, even though it is usually present in higher concentration than the unprotonated form. This situation is quite different for  $\text{Mg}^{2+}$ , where the metal-ion association constants of the unprotonated and monoprotonated forms of EGTA are separated by less than two orders of magnitude. In this case the binding of  $\text{Mg}^{2+}$  to the monoprotonated species contributes substantially to the apparent association constant.

For the general case, an expression for the apparent dissociation constant must be derived that takes into consideration the contributions of both the unprotonated and the monoprotonated forms of the ligand to the metal binding. To do this the conditional association constants ( $K'_{\text{ML}}^{\text{M}}$  and  $K'_{\text{MHL}}^{\text{M}}$ ) for each individual species are derived and then added together to obtain  $K'$ .

$$K'_{\text{ML}}^{\text{M}} = \frac{[\text{ML}]}{[\text{M}][\text{L}_\text{T} - \text{ML}_\text{T}]} \quad (3.6)$$



$$K'_{MHL}^M = \frac{[MHL]}{[M][L_T - ML_T]} \quad (3.7)$$

Here  $L_T$  refers to the total concentration of the ligand and  $ML_T$  to the concentration of the ligand bound to the metal ion, i.e.,  $[L_T - ML_T]$  refers to the concentration of the free ligand in the protonated and unprotonated forms.

$$K' = K'_{ML}^M + K'_{MHL}^M = \frac{[ML] + [MHL]}{[M][L_T - ML_T]} = \frac{[ML_T]}{[M][L_T - ML_T]} \quad (3.8)$$

The expressions for  $K_{ML}^M$  and  $K'_{ML}^M$  differ only in one term in the denominator

$$K_{ML}^M = \frac{[ML]}{[M][L]} ; K'_{ML}^M = \frac{[ML]}{[M][L_T - ML_T]}$$

To convert  $K_{ML}^M$  to  $K'_{ML}^M$  it should be multiplied by  $[L] / [L_T - ML_T]$ , which is the non-bound fraction of the ligand in the unprotonated form. Similarly, conversion of  $K_{MHL}^M$  to  $K'_{MHL}^M$  involves multiplication by  $[HL] / [L_T - ML_T]$ . The denominator can be expressed in terms of protonated and unprotonated forms of the ligand (the positive charge on the hydrogen is not shown for simplicity):

$$[L_T - ML_T] = [L] + [HL] + [H_2L] \quad (3.9)$$

Here the  $H_3L$  and  $H_4L$  species are ignored because at physiological pH levels their concentrations are negligibly small. All the terms on the right hand side of the equation can be expressed in terms of  $[L]$ .

$$[HL] = K_{HL}^H [H][L] \quad (3.10)$$

$$[H_2L] = K_{H_2L}^H [H][HL] = K_{H_2L}^H [H] K_{HL}^H [H][L] \quad (3.11)$$

Thus

$$[L_T - ML_T] = [L] + K_{HL}^H [H][L] + K_{H_2L}^H [H] K_{HL}^H [H][L] \quad (3.12)$$

and

$$\frac{[L]}{[L_T - ML_T]} = \frac{1}{1 + K_{HL}^H [H] + K_{HL}^H K_{H_2L}^H [H]^2} \quad (3.13)$$

and

$$\frac{[HL]}{[L_T - ML_T]} = \frac{K_{HL}^H [H]}{1 + K_{HL}^H [H] + K_{HL}^H K_{H_2L}^H [H]^2} \quad (3.14)$$

To obtain the apparent association constant  $K'$  at a particular pH, therefore, one should calculate the factors defined by equations 3.13 and 3.14 using the tabulated  $K_{HL}^H$  and  $K_{H_2L}^H$  values, then multiply by the absolute association constants  $K_{ML}^M$  and  $K_{MHL}^M$ , respectively, and add the products.

$$K' = K_{ML}^M \frac{[L]}{[L_T - ML_T]} + K_{MHL}^M \frac{[HL]}{[L_T - ML_T]} \quad (3.15)$$

It should be noted that if the temperature and ionic strength are different for tabulated  $K$  values, corrections to the experimental conditions must be made as described earlier prior to calculating  $K'$ .

## **2. Experimental**

### **2.1 Reagents, solutions and Apparatus**

All chemicals were reagent grade and used as supplied. Distilled, deionized water (DDW) was used for the preparation of all solutions.

12.4 M hydrochloric acid. 12.4 M solution of HCl (BDH) was used as supplied.

Potassium Chloride salt. The salt (BDH) was dried at 80°C overnight to remove absorbed moisture.

Sodium Chloride salt. The salt (BDH) was dried at 80°C overnight to remove the absorbed moisture.

2.50 M potassium chloride solution. 9.325 g of dried KCl (BDH) was dissolved and diluted to 50 ml with DDW to produce a 2.50 M solution.

0.0439 M calcium chloride solution. 2.775 g of anhydrous  $\text{CaCl}_2$  (Anachemia) was dissolved in 500 ml of DDW and standardized by titration with 0.0298 M standard EDTA solution using calmagite as indicator.

0.0250 M magnesium chloride solution. 2.531 g of  $\text{MgCl}_2 \cdot 6\text{H}_2\text{O}$  (Anachemia) was dissolved in 500 ml of DDW and standardized by titration with 0.0298 M standard EDTA solution using calmagite as indicator.

0.0298 M standard EDTA solution. 22.4 g of disodium ethylenediamine tetraacetate (Fisher Scientific Company) was dissolved in DDW, 10 ml of 0.1007 M  $\text{Mg}(\text{NO}_3)_2$  was added and the solution diluted to 2 liters. Then it was standardized by titration with 0.1027 M standard  $\text{Ca}(\text{NO}_3)_2$  solution using calmagite as indicator.

0.1 M magnesium nitrate solution. 6.410 g of  $\text{Mg}(\text{NO}_3)_2 \cdot 6\text{H}_2\text{O}$  (Baker Chemical Co.) was dissolved and diluted to 250 ml with DDW, then standardized by titration with 0.0298 M EDTA solution using calmagite as indicator.

Solutions of quin-2, fura-2, EGTA, MOPS, potassium hydroxide and calcium nitrate were the same as described in the previous chapter.

Fisher-Accumet (model 520 digital) pH/Ion meter equipped with an Accu-pHast combination electrode, Shimadzu RF-5000 spectrofluorophotometer and

K-4/RD Lauda/Brinkmann circulating water bath were used for the experiments in this chapter the same way as the previous one

## **2.2 Procedure**

Solutions of quin-2/ $\text{Ca}^{2+}$  were prepared by mixing of measured amounts of 25 micromolar quin-2, 10 millimolar MOPS buffer, 130 millimolar KCl, 20 millimolar NaCl, and enough 0.0477 M  $\text{K}_2\text{H}_2\text{EGTA}$  and 0.0439 M  $\text{CaCl}_2$  to provide 2 mM free EGTA and free calcium concentrations in the range of 0 to 1 millimolar. Because of the great sensitivity of the Ca-EGTA system to pH, the pH values of all solutions were carefully adjusted to  $7.200 \pm 0.005$  with concentrated KOH or HCl. The ionic strength of each solution was adjusted to 0.2 M by addition of the required amount of 2.5 M KCl. A similar set of solutions were prepared for fura-2 using 1 micromolar of the dye instead of 25 micromolar. Since at the same concentration the fluorescence intensity of fura-2 is about 25 fold higher than that of quin-2, a 1 micromolar solution of fura-2 produces almost the same sensitivity as 25 micromolar quin-2. (Because their preparation is relatively complex, an example of a detailed calculation of the various concentrations of species for the preparation of these solutions is provided in appendix A.) All solutions were passed through a 0.2 micron filter, deoxygenated, and brought to  $25^\circ\text{C}$  prior to fluorescence measurements.

Excitation spectra of the quin-2 solutions were collected by setting the emission monochromator at 490 nm and scanning from 300 to 450 nm. The emission spectra were obtained at an excitation wavelength  $\lambda_{\text{ex}}$  of 337 nm. The excitation spectra of the fura-2 solutions were obtained by setting the emission monochromator at a wavelength  $\lambda_{\text{em}}$  of 510 nm. The emission spectra were collected at several  $\lambda_{\text{ex}}$ 's values because the maximum excitation wavelength for

fura-2 varies according to the concentration of calcium  $[Ca^{2+}]$  present. The excitation and emission slit widths were set at 5 and 10 nm respectively for all measurements.

### **2.2.1 Stoichiometry of quin-2 and fura-2 with calcium**

To determine the stoichiometry of the quin-2/ $Ca^{2+}$  system, fluorescence spectra of solutions of the dye-metal system were analyzed by a plot of  $\log [(I_f - I_{f(min)}) / (I_{f(max)} - I_f)] \equiv y$  vs.  $\log [Ca^{2+}] \equiv x$ . In these expressions  $I_{f(min)}$  is the fluorescence intensity of the free dye,  $I_{f(max)}$  the fluorescence intensity of the dye when it is saturated with calcium, and  $I_f$  the fluorescence intensity of the dye at an intermediate  $Ca^{2+}$  level, all measured at the same wavelength under the same conditions. The slope of the line indicates the metal to ligand stoichiometry of the  $Ca^{2+}$ /quin-2 complex.

For the fura-2/ $Ca^{2+}$  system the ratio of the fluorescence intensities at two different wavelengths (340 and 380 nm) were taken and  $\log [(R - R_{(min)}) / (R_{(max)} - R)]B$  plotted against  $\log [Ca^{2+}]$ . Here  $R_{(min)}$  is the ratio of the fluorescence intensity of the free dye at 340 nm to that at 380 nm,  $R_{max}$  is the ratio of the intensity of the saturated dye at 340 nm to that at 380 nm, and  $R$  is the ratio of the intensity of the solution for an intermediate calcium concentration at 340 nm to that of the same solution at 380 nm.  $B$  is a constant that represents the ratio of the intensity of the calcium-free fura-2 to that of calcium-saturated fura-2 at 380 nm.

### **2.2.2 Effect of environmental conditions on the binding affinity of quin-2 and fura-2 for calcium(II)**

The conditional association constants of the  $\text{Ca}^{2+}$ (quin-2) and  $\text{Ca}^{2+}$ (fura-2) complexes vary with temperature, pH and ionic strength. In order to study the effect of temperature on the affinity of quin-2 and fura-2 for calcium, a series of fluorescence spectra were obtained for solutions of 25 micromolar quin-2 and 1 micromolar fura-2. Each solution contained 130 millimolar KCl, 20 millimolar NaCl, 10 millimolar MOPS, and amounts of  $\text{K}_2\text{H}_2\text{EGTA}$  and  $\text{CaCl}_2$  sufficient to yield 2 millimolar free EGTA and free calcium concentrations ranging from 0 to 1 millimolar. These solutions were prepared based on the calculated  $K'$  of Ca-EGTA at temperatures of 18, 25 and 37°C. The pH of each solution was adjusted to  $7.200 \pm 0.005$  at each temperature by dropwise addition of concentrated KOH or HCl prior to measurement. The ionic strengths of all solutions were adjusted to 0.2 with 2.5 M KCl. The excitation spectra of the quin-2 and fura-2 solutions were collected at 490 and 510 nm respectively on a Shimadzu RF 5000 spectrofluorophotometer, using excitation and emission slit widths of 5 and 10 nm.

To test the effect of pH, the same spectra as above were recorded with the difference that the temperature was set at 25°C and solutions of each concentration were prepared at pH values of 6.7, 7.2 and 7.6. These values were selected because they cover the physiological pH range for most biological systems. The pH adjustments were made using MOPS buffer and concentrated KOH and HCl as before.

To evaluate the effect of ionic strength, solutions of 25 micromolar quin-2 and 1 micromolar fura-2 in a series of Ca-EGTA buffers were prepared at 25°C,

pH 7.2 and ionic strengths of 0.1, 0.2, and 0.4 and the excitation spectra were collected as previously described.

### **2.2.3 Effect of magnesium(II) on the complexation of quin-2 and fura-2 by calcium(II)**

The presence of  $Mg^{2+}$  in cytoplasm and biological fluids influences the effective affinity of quin-2 and fura-2 for  $Ca^{2+}$  by direct competition for these ligands. According to a study by Grynkiewicz, Poenie and Tsien, quin-2 and fura-2 bind  $Mg^{2+}$  with association constants of  $5 \times 10^2$  to  $1 \times 10^3$  and  $1 \times 10^2$  respectively.<sup>53</sup> To examine the effect of free  $Mg^{2+}$  on the affinity of these dyes for calcium, excitation spectra of Ca-quin-2 and Ca-fura-2 were obtained under conditions of 25°C, pH 7.2 and ionic strength of 0.2 M in the presence of 1 millimolar free magnesium. The calibration solutions were prepared using Ca-Mg-EGTA buffers whose concentrations were calculated on the basis of apparent association constants of Ca-EGTA and Mg-EGTA determined for the above conditions. (See appendix A for sample calculations.)

## **3. Results and Discussion**

The excitation and emission spectra of quin-2/ $Ca^{2+}$  and fura-2/ $Ca^{2+}$  are presented in figures 3-1 and 3-2. From figure 3-1 it can be seen that the peak maximum in the excitation spectrum for quin-2 shifts as much as 23 nm toward shorter wavelengths upon binding to calcium. The maximum in the excitation peak for fura-2 also shifts toward shorter wavelengths upon binding of the dye to calcium, but the magnitude of this shift varies with the free calcium concentration. At saturation with calcium ion the value for  $\lambda_{ex}$  is about 25 nm smaller than when

no calcium is present. No major shift of wavelength is observed in the emission spectra of either quin-2 or fura-2 upon binding to calcium. A possible explanation for the shift in the excitation spectra may be that calcium chelation reduces delocalization of the lone pair of electrons on the amino nitrogen, possibly by twisting the bond between the nitrogen and the ring. This would disrupt conjugation between the lone pair and the remainder of the chromophore. The stokes shifts for quin-2 and fura-2 were calculated at different calcium concentrations and are shown in table 3-1.

Since fluorescence intensity is dependent on many variable factors such as emission efficiency, dye concentration, and thickness of the cell in the optical path, it is quite advantageous to use an indicator dye that shifts in wavelength as well as changes in intensity upon binding to calcium.<sup>53,70,71</sup> Under these conditions it becomes possible to use the ratio of fluorescence intensities at two suitably chosen wavelengths ( $\lambda_1$  and  $\lambda_2$ ) to determine the calcium signal, thereby canceling out many of the other variables. Even though the excitation spectrum of quin-2 shifts upon binding of the dye to calcium, the intensity of the calcium-free peak amplitude is low. For this reason only fluorescence intensities at 337 nm are used to determine free calcium in an unknown sample or to calculate the dissociation constant of the calcium-quin-2 complex, . On the other hand, when carrying out the same calculations for fura-2 it is advantageous to use the ratio of the fluorescence intensities at 340 nm and 380 nm.



### **3.1 Derivation of expressions for calculation of free calcium(II) concentrations from fluorescence measurements**

For a mixture of free and  $\text{Ca}^{2+}$ -bound dye at respective concentrations of  $c_f$  and  $c_b$ , the total fluorescence intensities ( $I_{F1}$  and  $I_{F2}$ ) at  $\lambda_1$  and  $\lambda_2$  are expressed as follows:<sup>53</sup>

$$I_{F1} = S_{f1}c_f + S_{b1}c_b \quad (3.21a)$$

$$I_{F2} = S_{f2}c_f + S_{b2}c_b \quad (3.21b)$$

Each S factor may be called a proportionality coefficient, which is the product of excitation intensity,  $\ln 10$ , extinction coefficient, path length of light in the cuvette, and fluorescence quantum efficiency of the molecule. Factors  $S_{f1}$  and  $S_{f2}$  are the proportionality coefficients for the free-calcium dye at  $\lambda_1$  and  $\lambda_2$ , and  $S_{b1}$  and  $S_{b2}$  are the proportionality coefficients for the calcium-bound dye at  $\lambda_1$  and  $\lambda_2$ . The concentrations  $c_f$  and  $c_b$  are related to the free calcium concentration  $[\text{Ca}^{2+}]$  by the association constant expression

$$K' = \frac{c_b}{[\text{Ca}^{2+}]^m c_f} \quad (3.22)$$

where  $K'$  is the conditional association constant, and  $m$  represents the stoichiometry coefficient of  $\text{Ca}^{2+}$  for each dye molecule. The fluorescence ratio  $R$  is expressed as follows:

$$R = \frac{I_{F1}}{I_{F2}} = \frac{S_{f1}c_f + S_{b1}c_b}{S_{f2}c_f + S_{b2}c_b} = \frac{S_{f1} + (S_{b1} K' [\text{Ca}^{2+}]^m)}{S_{f2} + (S_{b2} K' [\text{Ca}^{2+}]^m)} \quad (3.23)$$

Solving for  $R$  yields the following calibration equation:

$$\left( \frac{R - \left( \frac{S_{f1}}{S_{f2}} \right)}{\left( \frac{S_{b1}}{S_{b2}} \right) - R} \right) \left( \frac{S_{f2}}{S_{b2}} \right) = K' [Ca^{2+}]^m \quad (3.24)$$

At zero  $[Ca^{2+}]$ , all the dye exists in the  $c_f$  form, hence the terms  $S_{b1}c_b$  and  $S_{b2}c_b$  from equations 3.21a and 3.21b will be eliminated; then  $R$  will be simply equal to  $S_{f1}/S_{f2}$  and may be expressed as  $R_{min}$ . At maximum  $[Ca^{2+}]$  the terms  $S_{f1}c_f$  and  $S_{f2}c_f$  from equations 3.21a and 3.21b will be eliminated and  $R$  will be equal to  $S_{b1}/S_{b2}$ , which can be expressed as  $R_{max}$ . Since  $c_f$  at zero  $[Ca^{2+}]$  is equal to  $c_b$  at saturating concentrations of  $[Ca^{2+}]$ , the term  $S_{f2}/S_{b2}$  would be the ratio of the fluorescence intensity of the calcium-free dye to the calcium-saturated dye at  $\lambda_2$  and may be shown as  $B$ . Equation 3.24 may therefore be written as:

$$\left( \frac{R - R_{min}}{R_{max} - R} \right) B = K' [Ca^{2+}]^m \quad (3.25)$$

Of course the term  $B$  is eliminated if the measurements are taken at only one wavelength, as is the case for quin-2, and in this situation equation (3.25) can be written as:

$$\left( \frac{I_f - I_{f(min)}}{I_{f(max)} - I_f} \right) = K' [Ca^{2+}]^m \quad (3.26)$$

### **3.2 Stoichiometry of calcium to quin-2 and fura-2 in the calcium-dye complexes**

The values of  $m$  which determine the stoichiometries of the  $Ca^{2+}$ /dye systems were obtained for quin-2 and fura-2 by plotting  $\log [(I_f - I_{f(min)}) / (I_{f(max)} - I_f)]$  and  $\log [(R - R_{min}) / (R_{max} - R)]B$  versus  $\log [Ca^{2+}]$ . The plots are shown

in figures 3-3 and 3-4. In these plots the slope of the line yields  $m$  and the intercept yields  $\log K'$ . For the  $\text{Ca}^{2+}/\text{quin-2}$  system a value of 1.08 was obtained for  $m$ ; for the  $\text{Ca}^{2+}/\text{fura-2}$  a value of 0.96 was obtained. Both values of  $m$  can be considered to be unity within experimental error, which indicates a 1:1 stoichiometry for both  $\text{Ca}^{2+}/\text{quin-2}$  and  $\text{Ca}^{2+}/\text{fura-2}$ .

### **3.3 Conditional association constants of Ca-quin-2 and Ca-fura-2**

Variation in the fluorescence intensity of quin-2 as a function of  $[\text{Ca}^{2+}]$  is presented in figure 3-5. The plot shows a linear relationship between the fluorescence response and  $[\text{Ca}^{2+}]$  up to about 0.5 micromolar calcium. Above about 1 micromolar  $[\text{Ca}^{2+}]$ , however, the response begins to deviate significantly from linearity. From the slope of the line in the range of 0 to 0.5 micromolar calcium the conditional association constant of the complex under the conditions of the experiment is found to be  $1.9 \times 10^7 \text{ M}^{-1}$ . The effective dissociation constant, defined as the reciprocal of the slope, is 0.052 micromolar. This means that at a  $[\text{Ca}^{2+}]$  of 0.052 micromolar the dye is 50 percent bound to calcium(II) ( $c_b = c_f$ ).

For fura-2 a plot of normalized intensity versus free calcium concentration (figure 3-6) covers a wider range of calcium ion concentration. The fluorescence response shows linearity up to a  $[\text{Ca}^{2+}]$  level of 2 micromolar, and yields a value for the conditional association constant of  $6.2 \times 10^6$ . The apparent dissociation constant under the conditions of the experiment is 0.162 micromolar; as described for quin-2, this is the  $[\text{Ca}^{2+}]$  concentration for which 50% of fura-2 is present in the form of a calcium complex. The greater dissociation constant of fura-2 compared to quin-2 indicates the lower affinity of this dye for calcium. This may

be partially related to the slightly stronger electron withdrawing effects of the substituent groups in fura-2 over the methoxy group in quin-2.

### **3.4 Effect of environmental conditions on affinity of quin-2 and fura-2 for calcium**

The conditional association constants of quin-2 and fura-2 with calcium are sensitive to variations in environmental conditions. Figures 3-7 and 3-8 show the effect of temperature on  $K'$  values. The decreases in the slopes of the lines with increasing temperature indicates that the reactions of quin-2 and fura-2 with calcium are exothermic processes (i.e., have negative enthalpies) and hence elevation of temperature decreases the affinity of these dyes for calcium.

The effect of pH on the association constants of  $\text{Ca}^{2+}$ (quin-2) and  $\text{Ca}^{2+}$ (fura-2) is presented in figures 3-9 and 3-10. The quin-2 system shows hardly any variation on going from pH 7.2 to 7.6; there is, however, some drop in the  $K'$  value when conditions are made slightly acidic (pH 6.7). A likely interpretation is that under more acidic conditions proton binding to one of the aromatic amines may compete with  $\text{Ca}^{2+}$  for part of the binding site without directly affecting the chromophore properties of the ligand. For fura-2 the effect of pH on its binding ability with calcium is similar, as indicated by a slight increase in the slope of the plots in figure 3-10 as the pH increases. Presumably a competition between calcium and hydrogen ions for basic sites on the ligand occurs with fura-2 also. An increase in the ionic strength of the solution causes a decrease in the values found for the association constants of  $\text{Ca}^{2+}$ (quin-2) and  $\text{Ca}^{2+}$ (fura-2) ( figures 3-11 and 3-12). The thermodynamic association constant for each dye with calcium may be written as

$$K^{\circ} = K \left( \frac{\gamma^{\pm 2}}{\gamma^{\pm 2} \gamma^{\pm 4}} \right) \quad (3.27)$$

Assuming the pKa values of the carboxylate and aromatic amine groups of both ligands to be less than 7, they can be considered to exist predominately as tetravalent anions at pH 7.2. Hence the conditional association constant can be expressed as

$$K = K^{\circ} \gamma^{\pm 4} \quad (3.28)$$

Table 3-10 and figure 3-13 show the variation in activity coefficient of a tetravalent ion with ionic strength, as calculated by the Davies equation. An increase in ionic strength causes a decrease in the activity coefficient and hence in the value of K. This variation is most pronounced in the 0 to 0.2 ionic strength region.

### **3.5 Binding affinity of quin-2 and fura-2 for calcium in the presence of 1 millimolar magnesium(II)**

Figures 3-14 and 3-15 show the effect of 1 millimolar free magnesium on the  $\text{Ca}^{2+}$ (quin-2) and  $\text{Ca}^{2+}$ (fura-2) systems. The slope of the linear region of the plot for quin-2 decreases from 19.4 to 8.3, and that for fura-2 from 6.2 to 4.1. Even though the structural cavity of these dyes does not have the optimum size and shape for the smaller ionic radius of the magnesium ion as compared to calcium, it is apparent that at the millimolar level magnesium(II) can bind to both of the dyes and compete with calcium for the binding sites. In an early study Tsien examined the binding affinity of the ligand BAPTA for magnesium(II).<sup>54</sup> He

reported an association constant for the magnesium(II)-BAPTA system of 59 for concentrations of free magnesium(II) up to 100 millimolar. The corresponding dissociation constant of 17 millimolar for the magnesium(II)-BAPTA system is larger than that for calcium with this ligand by about five orders of magnitude. The spectral shift observed for magnesium complex formation was only about half that seen for calcium in the linear region; to produce any significant further spectral shifts requires much higher concentrations of magnesium(II). It appears that in this concentration range the smaller  $Mg^{2+}$  binds to just one of the two halves of the BAPTA molecule. This produces some spectral shift, but does not influence the aromatic group in the second half of the ligand. At magnesium concentrations above 100 millimolar a second magnesium ion binds to the other half of the molecule and completes the spectral shift. The dissociation constant for this binding to the second half of the BAPTA molecule is, significantly larger than the first ( $\sim 0.5$  M).<sup>54</sup>

In the present work it was observed that in the presence of 1 millimolar free magnesium and no calcium the excitation maximum of quin-2 shifts to 337 nm. This is the same shift that was observed upon chelation of the dye to calcium for this ligand. On the other hand, the presence of 1 millimolar  $Mg^{2+}$  causes no shift in the excitation spectrum of fura-2. It is possible that under the conditions used magnesium binds to the quinoline portion of the quin-2 molecule, which is the fluorescent chromophore, and hence produces the maximum spectral shift seen for this ligand, whereas for fura-2 it is the non-conjugated, non-chromophore portion of the molecule that is binding magnesium and so does not produce a spectral shift.

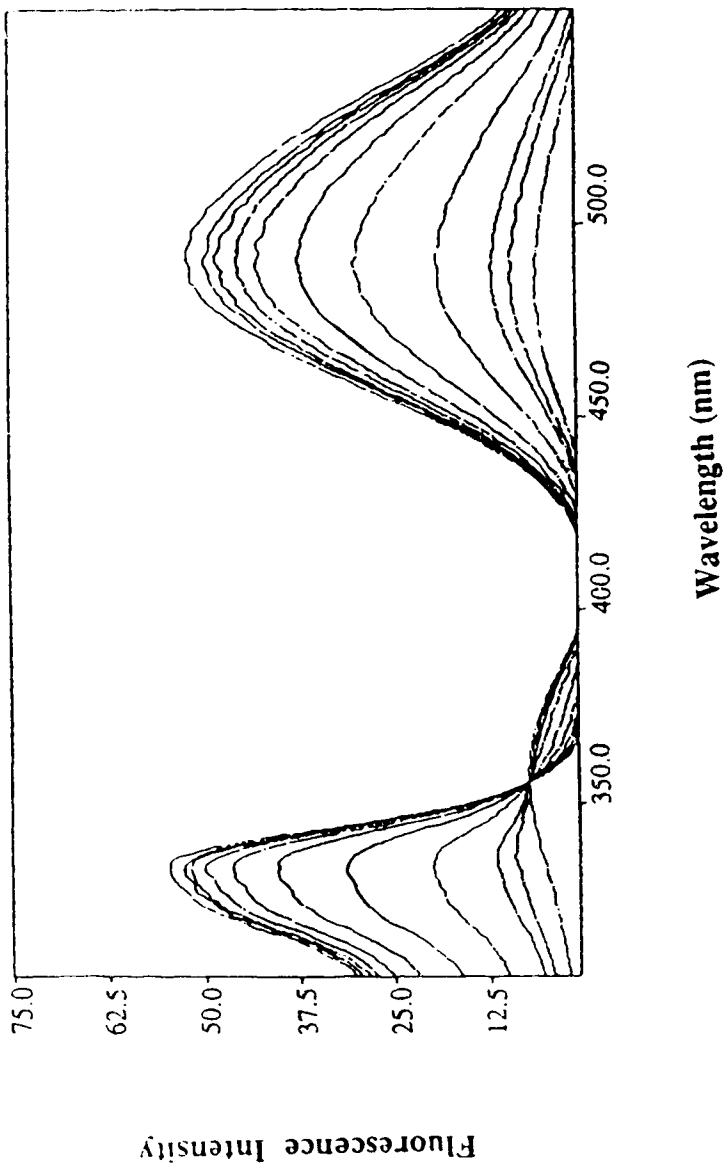


**Figure 3-1** Excitation (below 400 nm) and emission (above 420 nm) spectra of 25 micromolar quin-2 for values of  $[Ca^{2+}]$  ranging from 0 to 1 millimolar at 25°C, pH 7.2 and ionic strength of 0.2. The curves, from lowest to highest intensity, correspond to 0, 0.005, 0.01, 0.02, 0.05, 0.15, 0.25, 0.5, 1, 2 and 1000 micromolar  $[Ca^{2+}]$ .

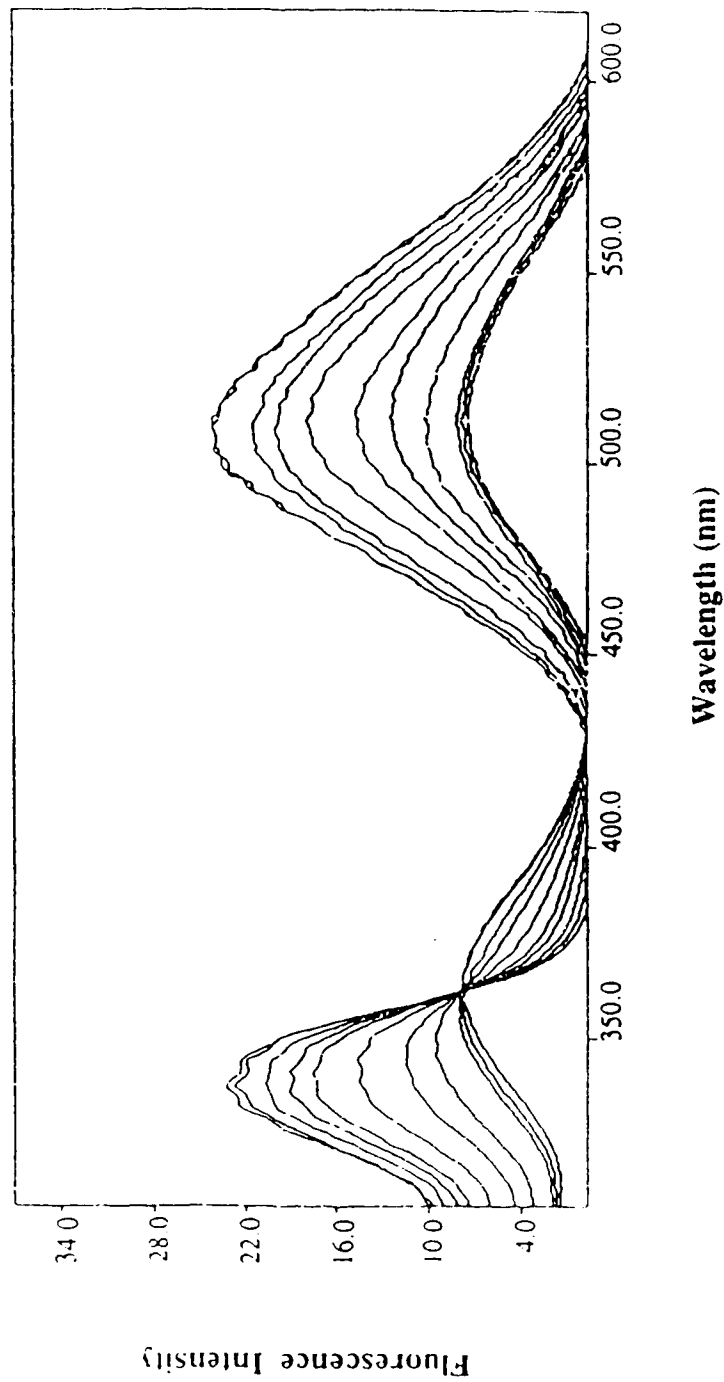


**Figure 3-2** Excitation (below 430 nm) and emission (above 430 nm) spectra of 1 micromolar fura-2 for values of  $[Ca^{2+}]$  ranging from 0 to 1 millimolar at 25°C, pH 7.2 and an ionic strength of 0.2. The curves, from the lowest to the highest intensity, correspond to 0, 0.005, 0.01, 0.02, 0.05, 0.15, 0.25, 0.5, 1, 2 and 1000 micromolar  $[Ca^{2+}]$ .



**Table 3-1** Stokes Shifts for quin-2 and fura-2 at varying  $[\text{Ca}^{2+}]$ 

$[\text{Ca}^{2+}]$ (micromolar)	Stokes Shift for Quin-2 ( $\text{nm}^{-1}$ )	Stokes Shift for Fura-2 ( $\text{nm}^{-1}$ )
0.000	7370	7828
0.005	9090	8055
0.010	9090	8208
0.020	9348	8882
0.050	9348	9295
0.150	9348	9462
0.250	9348	9593
0.500	9348	9727
1.000	9348	9610
2.000	9348	9784
1000	9348	9784

**Table 3-2** Variation in the normalized fluorescence intensity of 25 micromolar quin-2 with  $[Ca^{2+}]$  at 25°C, pH 7.2 and ionic strength of 0.2.

$[Ca^{2+}]$ (micromolar)	$\log [Ca^{2+}]$	Norm. Int. <sup>a</sup>	RSD <sup>b</sup>	$\log$ (Norm. Int.)
0.000	-	0.000	-	-
0.005	-2.301	0.040	1.2	-1.399
0.010	-2.000	0.095	1.7	-1.024
0.020	-1.700	0.357	2.1	0.447
0.050	-1.301	1.042	0.9	0.018
0.150	-0.824	2.313	2.4	0.364
0.250	-0.602	4.740	1.9	0.676
0.500	-0.301	9.717	1.5	0.988
1.000	0.000	16.78	1.5	1.225
2.000	0.301	24.12	1.5	1.382
1000 <sup>c</sup>	3.000	-	-	-

<sup>a</sup> Normalized intensity is the difference between the intensity of each peak and the intensity of the peak at zero  $[Ca^{2+}]$ , divided by the difference between the intensity of that peak and the intensity of the peak at saturating  $[Ca^{2+}]$ ;

$$[(I_f - I_{f(\min)}) / (I_{f(\max)} - I_f)].$$

<sup>b</sup> Relative standard deviation of the normalized intensity in percent, calculated by the procedure of footnote d in table 2-1.

<sup>c</sup> This is the calcium concentration at which the dye becomes saturated and the corresponding fluorescence intensity is  $I_{f(\max)}$ . Under these conditions the formula for normalized intensity is not applicable.

**Table 3-3** Variation in the normalized fluorescence intensity of 1 micromolar fura-2 with  $[Ca^{2+}]$  at 25°C, pH 7.2 and ionic strength of 0.2.

$[Ca^{2+}]$ (micromolar)	$\log [Ca^{2+}]$	Norm. Int. <sup>a</sup>	RSD <sup>b</sup>	$\log$ (Norm. Int.)
0.000	-	0.000	1.9	-
0.005	-2.301	0.034	2.6	-1.466
0.010	-2.000	0.061	3.0	-1.217
0.020	-1.700	0.249	3.2	0.603
0.050	-1.301	0.487	2.7	0.313
0.150	-0.824	1.169	2.9	0.068
0.250	-0.602	2.030	2.6	0.307
0.500	-0.301	3.274	1.9	0.515
1.000	0.000	5.847	3.0	0.767
2.000	0.301	12.61	2.8	1.101
1000	3.000	-	-	-

<sup>a</sup> Normalized intensity;  $[(R - R_{f(\min)}) / (R_{f(\max)} - R)] B$  (see p. 81)

<sup>b</sup> Relative standard deviation of the normalized intensity in percent, calculated by the procedure of footnote d in table 2-1.

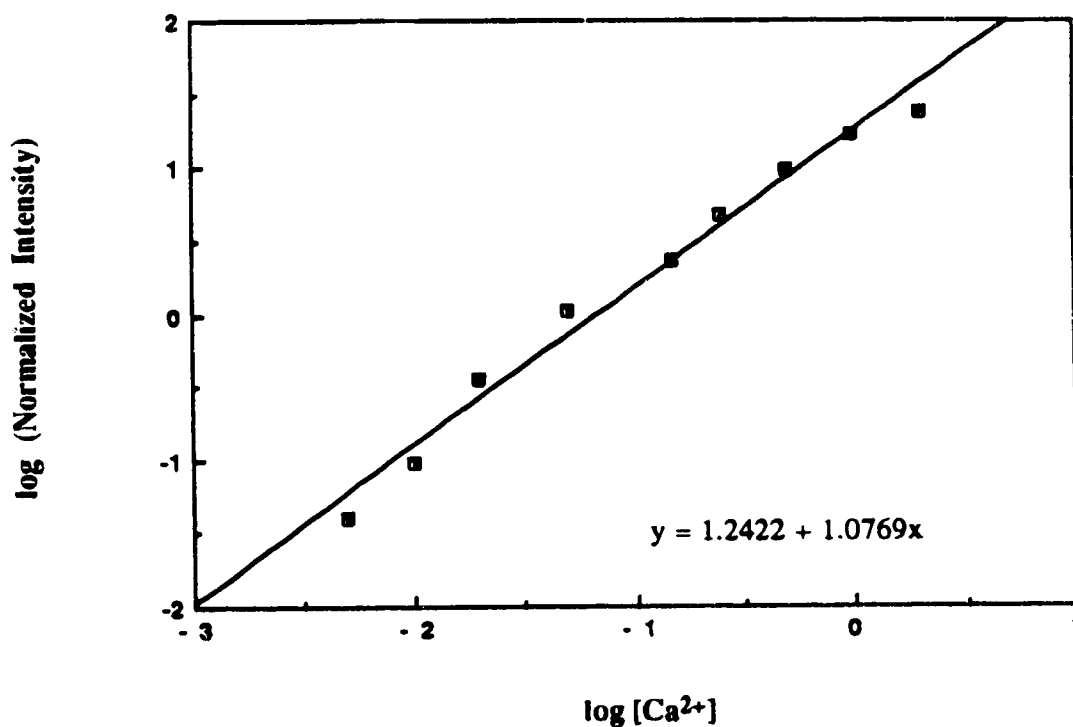


**Figure 3-3** Variation of the normalized fluorescence intensity of quin-2 with  $[Ca^{2+}]$  in logarithmic scale. Slope of the line gives the stoichiometry coefficient ( $m$ ) of  $Ca^{2+}$  to quin-2 in the  $Ca^{2+}(\text{quin-2})$  complex.

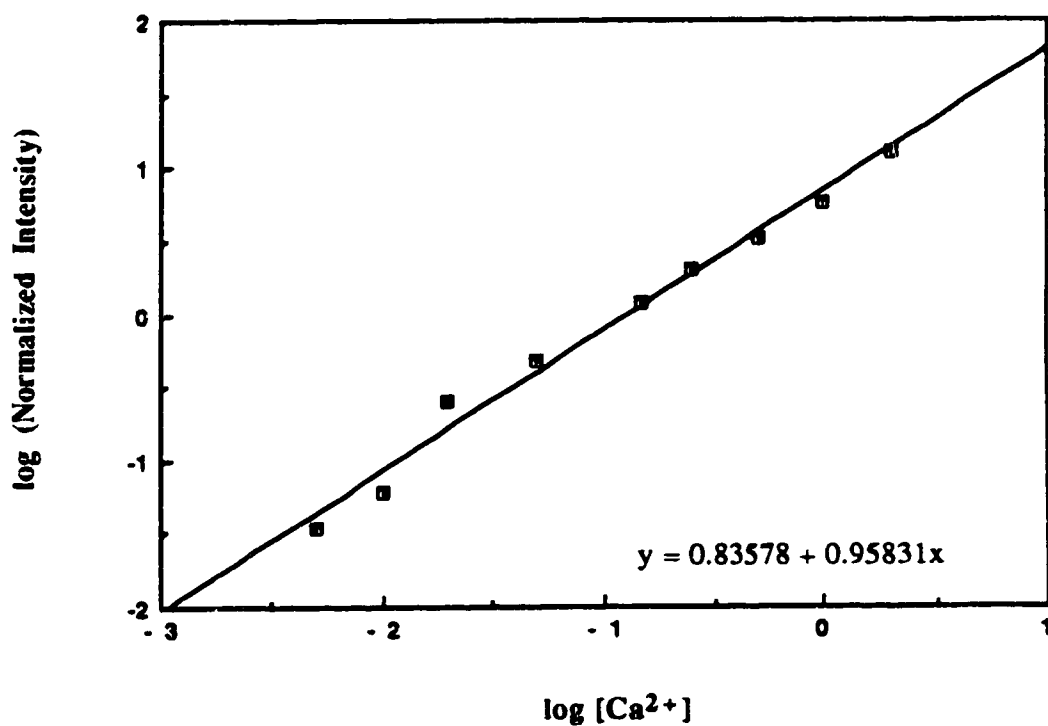


**Figure 3-4** Variation in the normalized fluorescence intensity of fura-2 with [Ca<sup>2+</sup>] in logarithmic scale. Slope of the line gives the stoichiometry coefficient (m) of Ca<sup>2+</sup> to fura-2 in the Ca<sup>2+</sup>-(fura-2) complex.

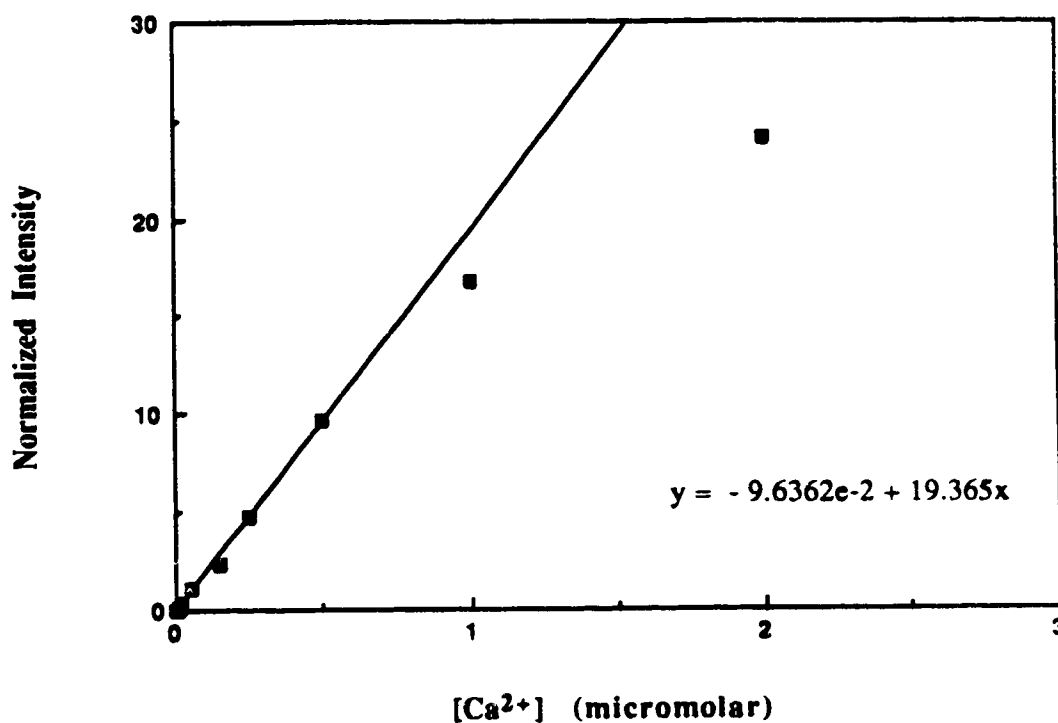


**Figure 3-5** Variation in the normalized fluorescence intensity of 25 micromolar quin-2 over a  $[Ca^{2+}]$  range of 0 to 2 micromolar at 25°C, pH 7.2 and ionic strength of 0.2. The plot starts to deviate from linearity at about 0.5 to 1 micromolar  $Ca^{2+}$ . The slope of the line in the linear region represents the conditional association constant of the  $Ca^{2+}$ (quin-2) complex.

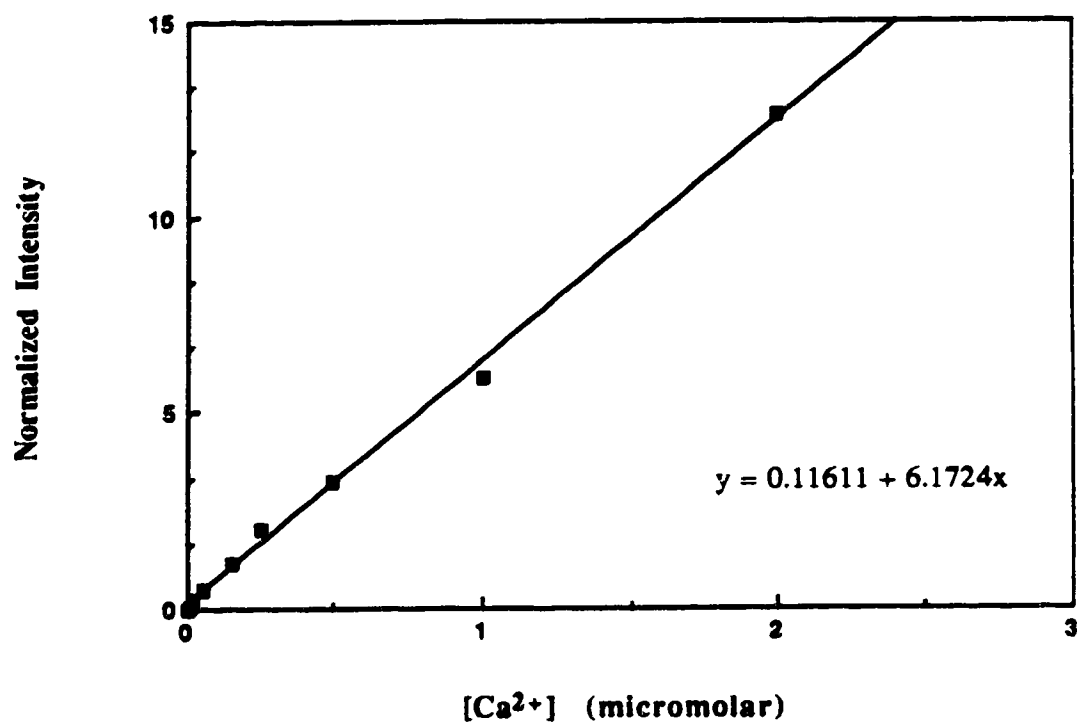


**Figure 3-6** Variation in the normalized fluorescence intensity of 1 micromolar fura-2 over a  $[Ca^{2+}]$  range of 0 to 2 micromolar at 25°C, pH 7.2 and ionic strength of 0.2. The slope of the line represents the conditional association constant of the  $Ca^{2+}$ -(fura-2) complex.

**Table 3-4** Variation in the normalized fluorescence intensity of 25 micromolar quin-2 with  $[Ca^{2+}]$  at 18, 25 and 37°C, pH 7.2 and ionic strength of 0.2.

$[Ca^{2+}]$ (micromolar)	Norm. Int. <sup>a</sup> (18°C)	RSD <sup>b</sup>	Norm. Int. (25°C)	RSD	Norm. Int. (37°C)	RSD
0.000	0.000	-	0.000	-	0.000	-
0.005	0.046	1.4	0.040	1.8	0.032	0.9
0.010	0.109	1.7	0.095	1.7	0.076	0.8
0.020	0.412	1.7	0.357	1.4	0.290	1.3
0.050	1.281	2.0	1.042	2.0	0.837	1.7
0.150	3.010	0.8	2.313	0.9	2.019	1.5
0.250	5.239	1.3	4.740	2.1	4.186	1.8
0.500	11.317	1.7	9.717	1.5	8.123	1.8
1.000	19.44	1.9	16.78	1.3	13.57	1.9
2.000	27.81	1.5	24.12	1.6	19.78	2.1
1000	-	-	-	-	-	-

<sup>a</sup> Normalized intensity;  $[(I_f - I_{f(\min)}) / (I_{f(\max)} - I_f)]$  (see the footnote for table 3-2)

<sup>b</sup> Relative standard deviation of the normalized intensity in percent, calculated by the procedure of footnote d in table 2-1.



**Table 3-5.** Variation in the normalized fluorescence intensity of 1 micromolar fura-2 with  $[Ca^{2+}]$  at 18, 25 and 37°C, pH 7.2 and ionic strength of 0.2.

$[Ca^{2+}]$ (micromolar)	Norm. Int. <sup>a</sup> (18°C)	RSD <sup>b</sup>	Norm. Int. (25°C)	RSD	Norm. Int. (37°C)	RSD
0.000	0.000	-	0.000	-	0.000	-
0.005	0.036	3.2	0.034	3.4	0.029	2.3
0.010	0.065	3.0	0.061	2.8	0.051	2.6
0.020	0.262	2.5	0.249	2.3	0.209	2.5
0.050	0.525	2.9	0.487	2.0	0.403	2.7
0.150	1.071	4.0	1.169	2.5	0.995	2.4
0.250	1.980	2.2	2.030	3.2	1.496	2.6
0.500	3.590	1.7	3.274	3.3	2.724	2.4
1.000	6.640	1.9	5.847	2.8	5.070	3.1
2.000	13.27	2.7	12.61	2.1	9.734	3.0
1000	-		-		-	

<sup>a</sup> Normalized intensity;  $[(R - R_{f(min)}) / (R_{f(max)} - R)]$  B (see the footnote for table 3-3)

<sup>b</sup> Relative standard deviation of the normalized intensity in percent, calculated by the procedure of footnote d in table 2-1.

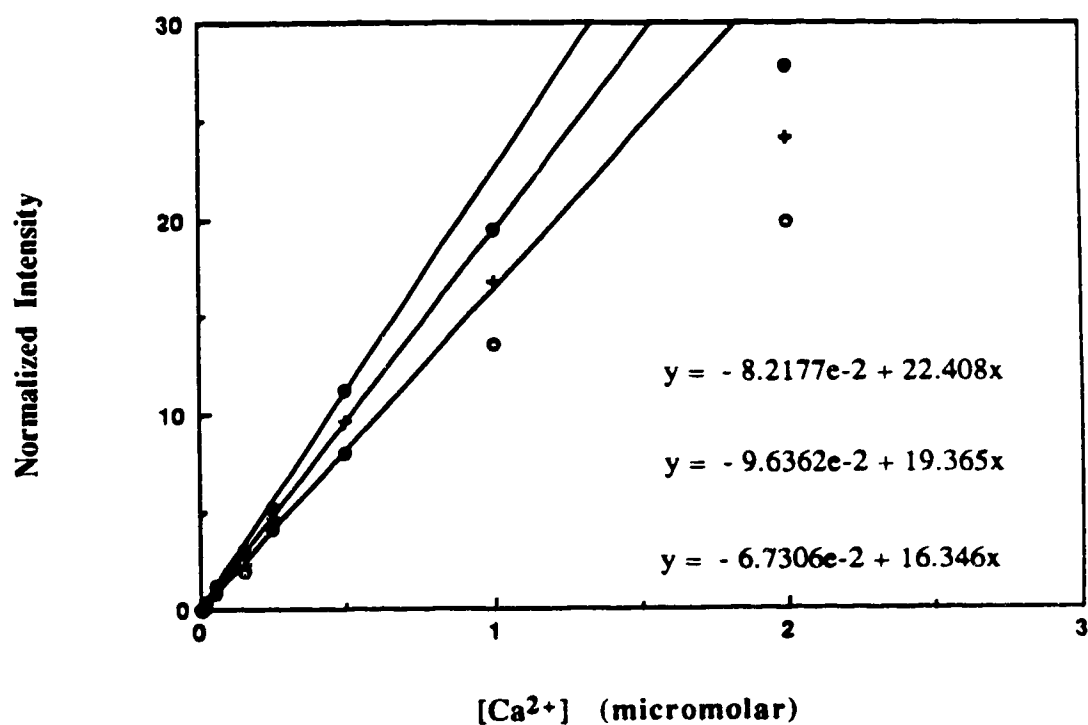


**Figure 3-7** Variation in the normalized fluorescence intensity of 25 micromolar quin-2 with  $[Ca^{2+}]$  at pH 7.2, ionic strength of 0.2 and temperatures of 18°C (•), 25°C (+) and 37°C (o). Decreasing slope indicates a decrease in the value of  $K'$  with elevation of temperature.

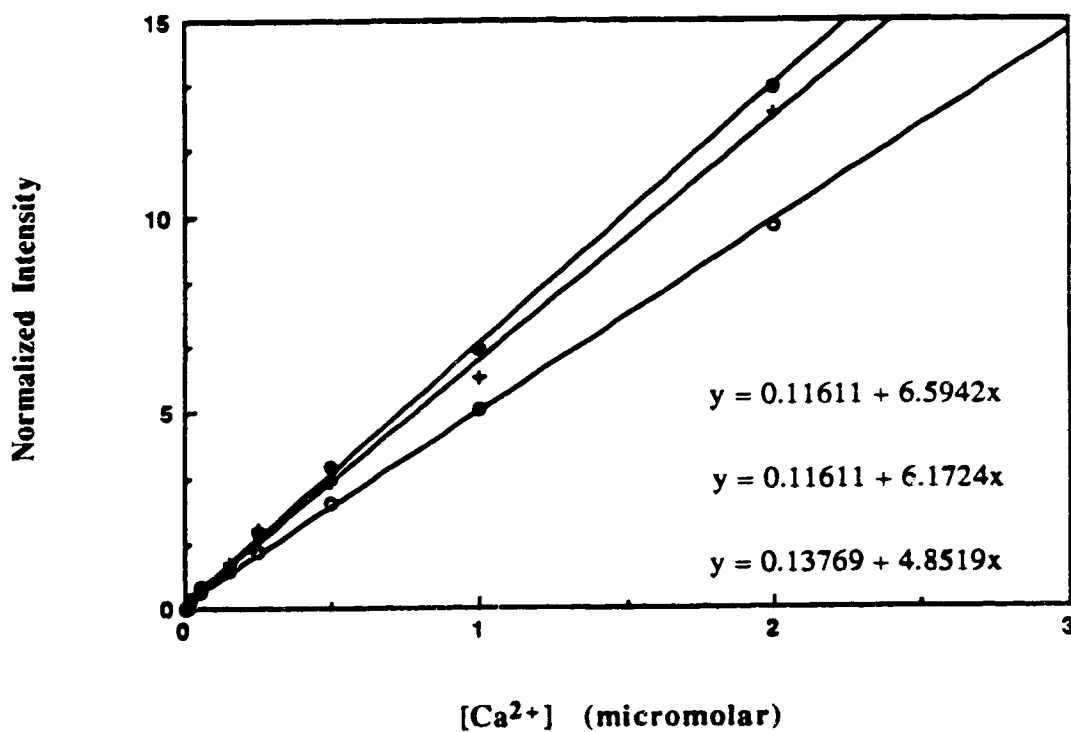


**Figure 3-8** Variation in the normalized intensity of 1 micromolar fura-2 with [Ca<sup>2+</sup>] at pH 7.2, ionic strength of 0.2 and temperatures of 18°C (•), 25°C (+) and 37°C (o). Decreasing slope indicates a decrease in the value of  $K'$  with elevation of temperature.

**Table 3-6** Variation in the normalized fluorescence intensity of 25 micromolar quin-2 with  $[Ca^{2+}]$  at 25°C, pH 6.7, 7.2 and 7.6, and ionic strength of 0.2.

$[Ca^{2+}]$ (micromolar)	Norm. Int. <sup>a</sup> (pH 6.7)	RSD <sup>b</sup>	Norm. Int. (pH 7.2)	RSD	Norm. Int. (pH 7.6)	RSD
0.000	0.000	-	0.000	-	0.000	-
0.005	0.034	2.0	0.040	1.6	0.038	1.1
0.010	0.079	1.1	0.095	1.7	0.098	1.5
0.020	0.304	0.8	0.357	1.4	0.410	1.4
0.050	0.927	1.5	1.042	1.3	0.995	2.1
0.150	2.357	1.3	2.313	0.9	2.897	2.3
0.250	4.123	1.7	4.740	2.1	4.880	1.1
0.500	8.260	2.0	9.717	1.5	9.517	1.7
1.000	14.50	1.8	16.78	1.9	17.03	1.6
2.000	20.43	1.8	24.12	1.6	23.99	1.6
1000	-	-	-	-	-	-

<sup>a</sup> Normalized intensity;  $[(I_f - I_{f(\min)}) / (I_{f(\max)} - I_f)]$  (see the footnote for table 3-2)

<sup>b</sup> Relative standard deviation of the normalized intensity in percent, calculated by the procedure of footnote d in table 2-1.

**Table 3-7** Variation in the normalized fluorescence intensity of 1 micromolar fura-2 with  $[Ca^{2+}]$  at 25°C, pH 6.7, 7.2 and 7.6 and ionic strength of 0.2.

$[Ca^{2+}]$ (micromolar)	Norm. Int. <sup>a</sup> (pH 6.7)	RSD <sup>b</sup>	Norm. Int. (pH 7.2)	RSD	Norm.Int. (pH 7.6)	RSD
0.000	0.000	-	0.000	-	0.000	-
0.005	0.040	3.0	0.034	2.5	0.038	2.9
0.010	0.066	2.7	0.061	2.5	0.059	2.6
0.020	0.223	2.4	0.249	3.4	0.251	2.4
0.050	0.455	1.7	0.487	2.9	0.481	2.2
0.150	1.146	1.9	1.169	2.0	1.190	1.9
0.250	2.121	4.1	2.030	2.8	1.950	2.0
0.500	3.050	2.7	3.274	2.8	3.343	3.3
1.000	5.637	2.9	5.847	2.4	6.335	2.4
2.000	11.97	2.5	12.61	2.6	12.87	2.7
1000	-	-	-	-	-	-

<sup>a</sup> Normalized intensity;  $[(R - R_{f(min)}) / (R_{f(max)} - R)] \cdot D$  (see the footnote for table 3-3)

<sup>b</sup> Relative standard deviation of the normalized intensity in percent, calculated by the procedure of footnote d in table 2-1.

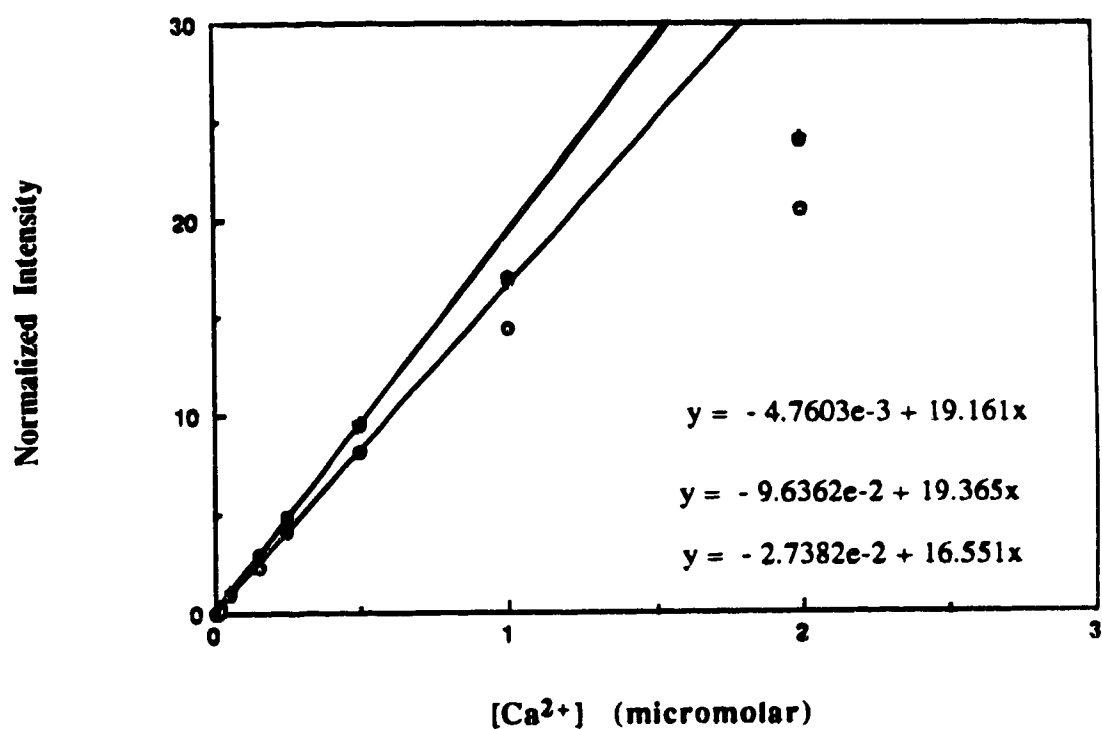


**Figure 3-9** Variation in the normalized intensity of 25 micromolar quin-2 with  $[Ca^{2+}]$  at 25°C, ionic strength 0.2 and pH 7.6 (•), 7.2 (+) and 6.7 (o)

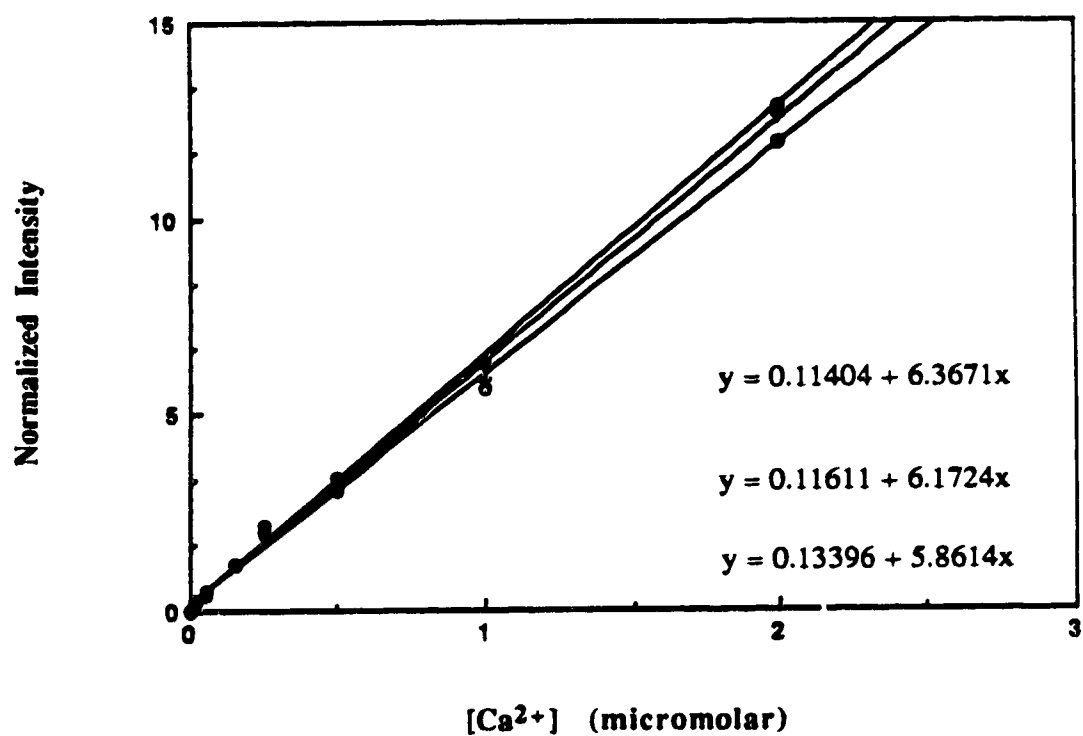


**Figure 3-10** Variation in the normalized intensity of 1 micromolar fura-2 with  $[Ca^{2+}]$  at 25°C, ionic strength 0.2 and pH 7.6 (•), 7.2 (+) and 6.7 (o)

**Table 3-8** Variation in the normalized intensity of 25 micromolar quin-2 with  $[Ca^{2+}]$  at 25°C, pH 7.2 and ionic strengths of 0.1, 0.2 and 0.4

$[Ca^{2+}]$ (micromolar)	Norm. Int. <sup>a</sup> ( $\mu = 0.1$ )	RSD <sup>b</sup>	Norm. Int. ( $\mu = 0.2$ )	RSD	Norm. Int. ( $\mu = 0.4$ )	RSD
0.000	0.000	-	0.000	-	0.000	-
0.005	0.049	0.7	0.040	1.7	0.036	1.4
0.010	0.115	1.5	0.095	0.9	0.086	1.1
0.020	0.445	1.3	0.357	2.0	0.323	1.5
0.050	0.281	1.5	1.042	1.1	0.962	2.0
0.150	3.043	1.7	2.313	1.8	2.268	1.9
0.250	5.707	1.6	4.740	1.5	4.261	1.1
0.500	11.59	2.2	9.717	1.7	8.979	1.8
1.000	20.78	1.9	16.78	2.0	15.32	1.6
2.000	27.50	1.9	24.12	2.3	21.86	1.7
1000	-	-	-	-	-	-

<sup>a</sup> Normalized intensity;  $[(I_f - I_{f(\min)}) / (I_{f(\max)} - I_f)]$  (see the footnote for table 3-2)

<sup>b</sup> Relative standard deviation of the normalized intensity in percent, calculated by the procedure of footnote d in table 2-1.



**Table 3-9** Variation in the normalized intensity of 1 micromolar fura-2 with  $[Ca^{2+}]$  at 25°C, pH 7.2 and ionic strengths of 0.1, 0.2 and 0.4

$[Ca^{2+}]$ (micromolar)	Norm. Int. <sup>a</sup> ( $\mu = 0.1$ )	RSD <sup>b</sup>	Norm. Int. ( $\mu = 0.2$ )	RSD	Norm. Int. ( $\mu = 0.4$ )	RSD
0.000	0.000	-	0.000	-	0.000	-
0.005	0.043	2.6	0.034	2.9	0.031	2.0
0.010	0.086	2.9	0.061	3.0	0.060	2.1
0.020	0.224	3.6	0.249	2.3	0.161	2.8
0.050	0.509	2.4	0.487	2.6	0.361	2.5
0.150	1.230	2.9	1.169	2.9	0.888	2.5
0.250	2.098	3.7	2.030	2.8	1.507	2.5
0.500	4.190	3.0	3.274	2.5	2.978	2.4
1.000	8.240	2.7	5.847	1.8	5.823	2.7
2.000	15.94	2.4	12.61	1.9	11.46	2.6
1000	-	-	-	-	-	-

<sup>a</sup> Normalized intensity;  $[(R - R_{f(\min)}) / (R_{f(\max)} - R)] B$  (see the footnote for table 3-3)

<sup>b</sup> Relative standard deviation of the normalized intensity in percent, calculated by the procedure of footnote d in table 2-1.

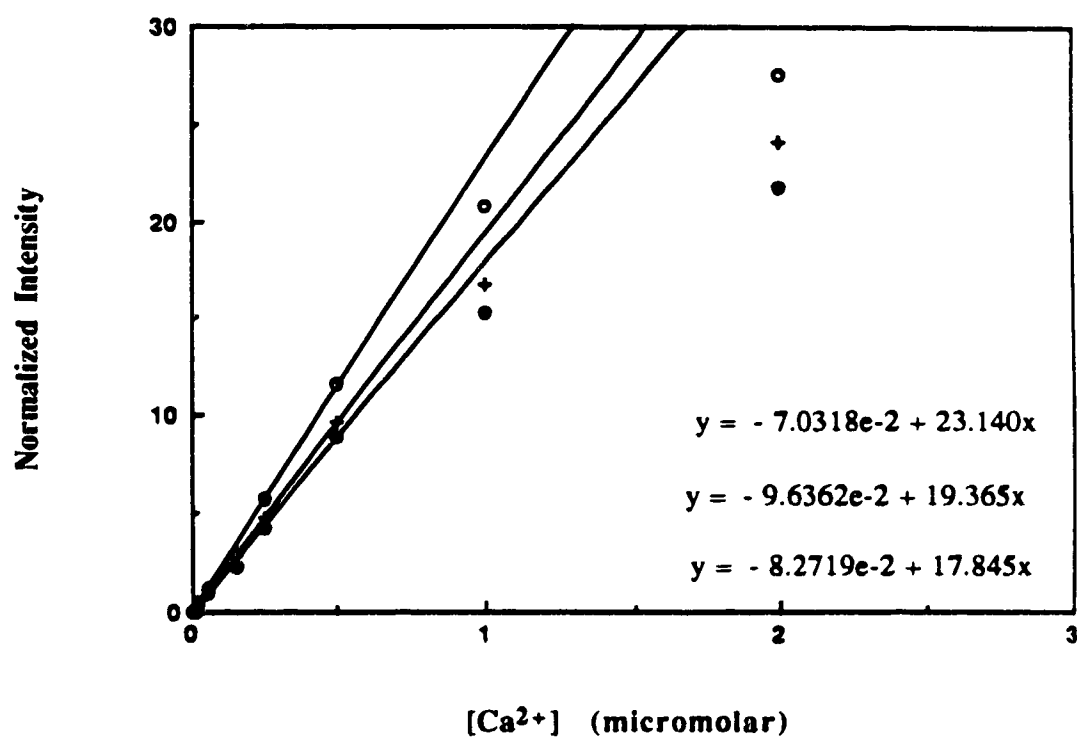


**Figure 3-11** Variation in the normalized fluorescence intensity of 25 micromolar quin-2 with  $[Ca^{2+}]$  at 25°C, pH 7.2 and ionic strength of 0.4 (•), 0.2 (+) and 0.1 (o)

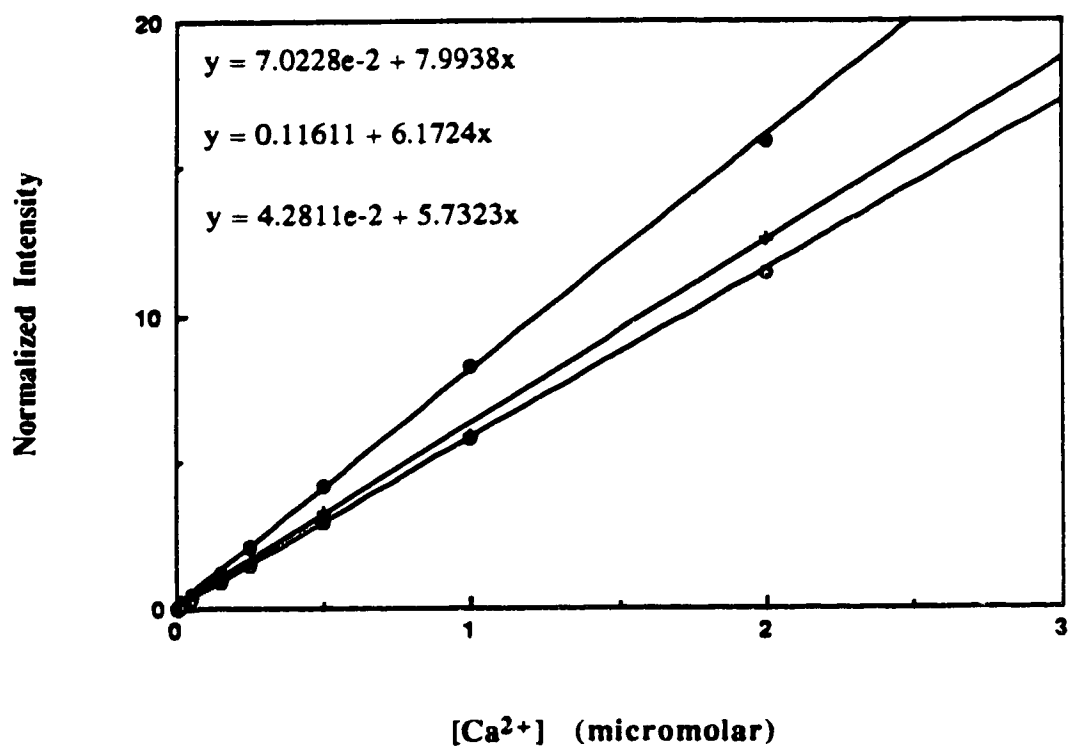


**Figure 3-12** Variation in the normalized fluorescence intensity of 1 micromolar fura-2 with [Ca<sup>2+</sup>] at 25°C, pH 7.2 and ionic strength of 0.1 (•), 0.2 (+) and 0.4 (o)

**Table 3-10** Calculated values for the activity coefficient of a tetravalent ion as a function of ionic strength

$\mu$	$\gamma$
0.050	0.04251
0.080	0.02476
0.100	0.01910
0.150	0.01217
0.200	0.00921
0.250	0.00772
0.300	0.00696
0.340	0.00665
0.360	0.00656
0.380	0.00652
0.400	0.00651
0.420	0.00659
0.440	0.00659
0.460	0.00667
0.480	0.00678
0.500	0.00691
0.550	0.00737

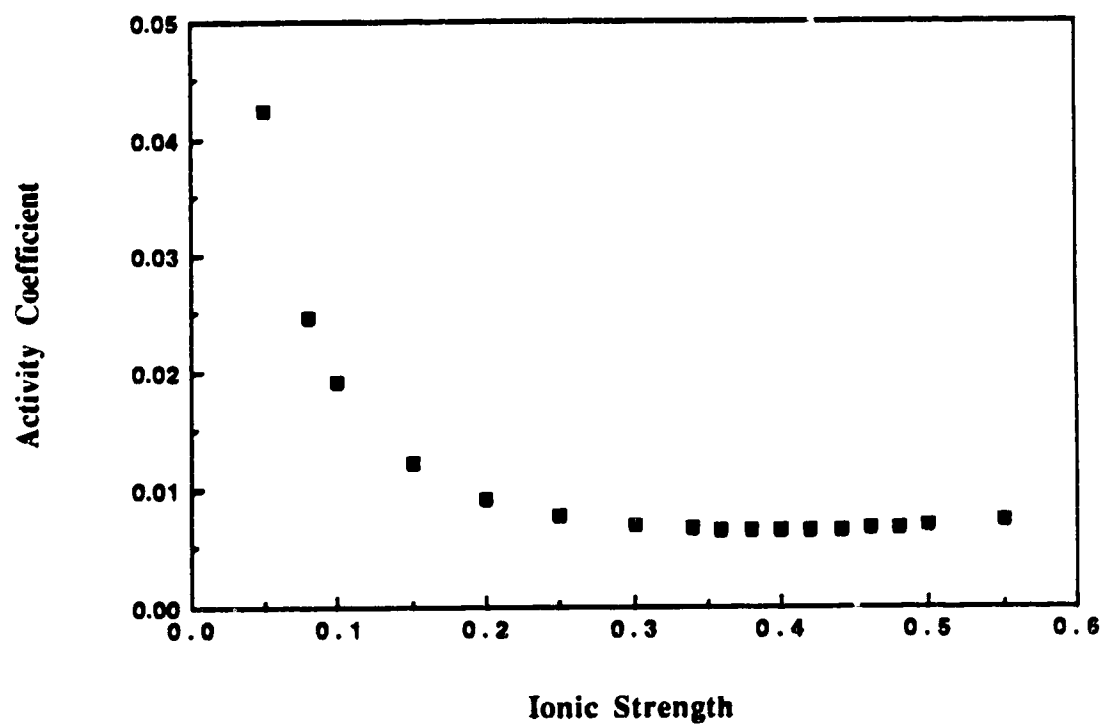


**Figure 3-13** Variation in the activity coefficient of a tetravalent ion with ionic strength in the range of 0.05 to 0.55

**Table 3-11** Variation in the normalized fluorescence intensity of 25 micromolar quin-2 and 1 micromolar fura-2 with  $[Ca^{2+}]$  at 25°C, pH 7.2 and ionic strength of 0.2 M in the presence of 1 millimolar  $Mg^{2+}$

$[Ca^{2+}]$ (micromolar)	Norm. Int. <sup>a</sup> (quin-2)	RSD <sup>b</sup>	Norm. Int. <sup>c</sup> (fura-2)	RSD
0.000	0.000	-	0.000	-
0.005	0.039	1.4	0.038	2.7
0.010	0.090	1.6	0.088	2.6
0.020	0.260	1.7	0.196	1.9
0.050	0.683	1.6	0.324	1.8
0.150	1.332	1.9	0.807	3.1
0.250	2.382	2.0	1.123	2.9
0.500	4.213	2.1	2.318	2.3
1.000	8.365	2.0	4.204	2.8
2.000	14.43	1.5	8.254	2.7
1000	-	-	-	-

<sup>a</sup> Normalized intensity;  $[(I_f - I_{f(\min)}) / (I_{f(\max)} - I_f)]$  (see the footnote for table 3-2)

<sup>b</sup> Relative standard deviation of the normalized intensity in percent, calculated by the procedure of footnote d in table 2-1.

<sup>c</sup> Normalized intensity;  $[(R - R_{f(\min)}) / (R_{f(\max)} - R)]$  B (see the footnote for table 3-3)

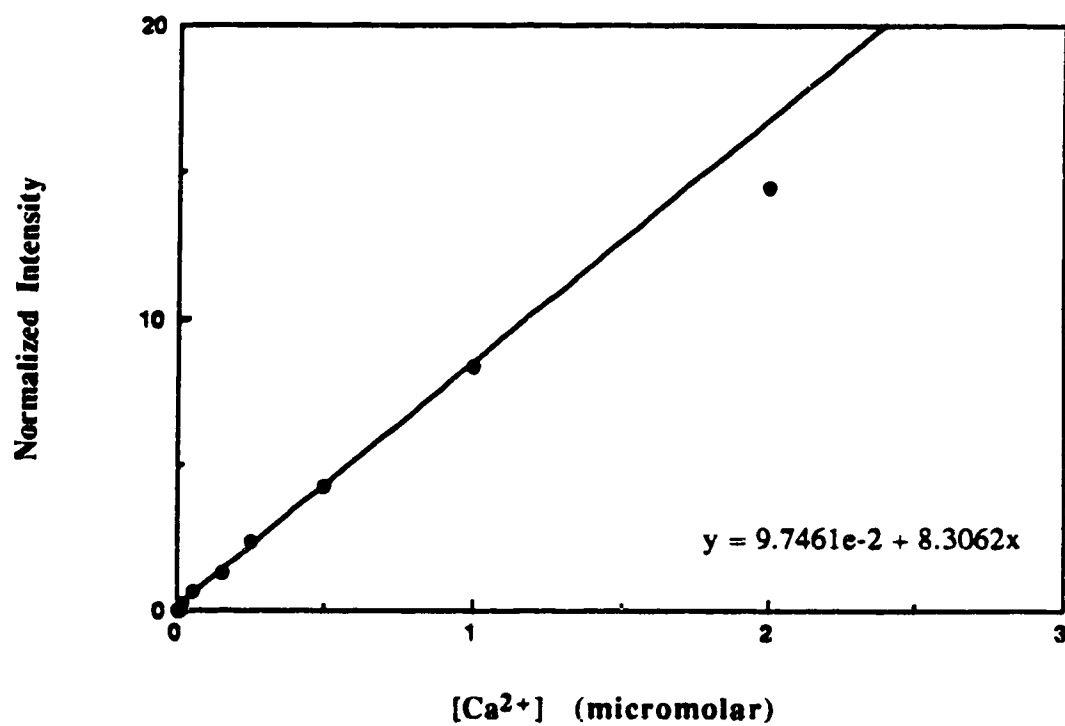


**Figure 3-14** Variation in the normalized fluorescence intensity of 25 micromolar quin-2 with  $[Ca^{2+}]$  at 25°C, pH 7.2 and ionic strength of 0.2, in the presence of 1 millimolar  $Mg^{2+}$

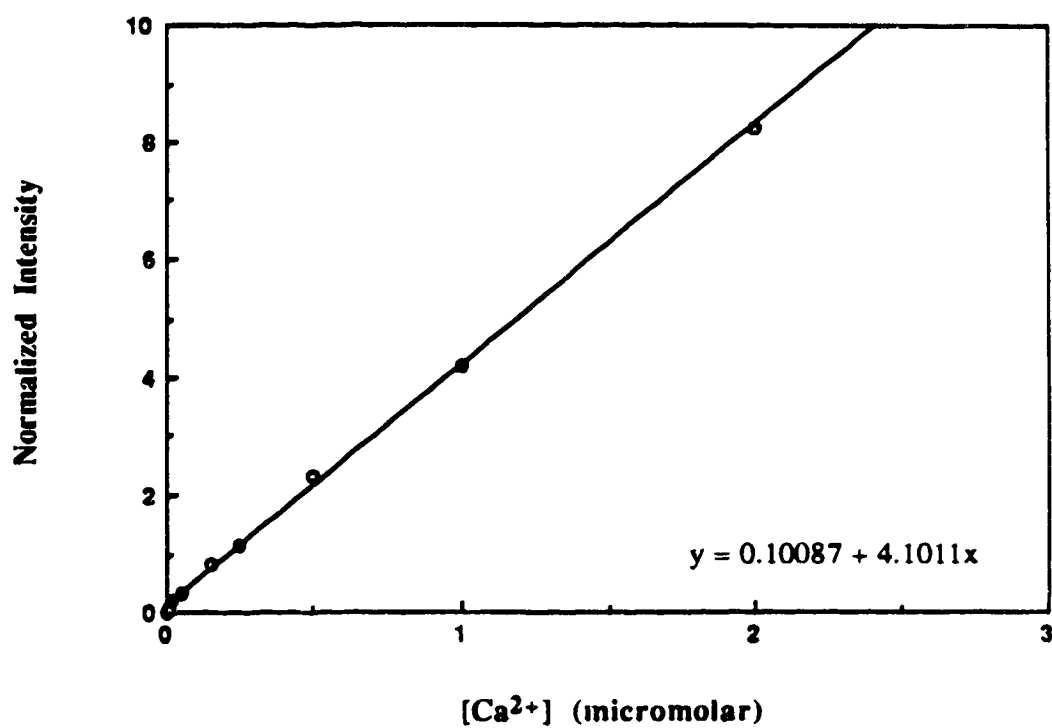


**Figure 3-15** Variation in the normalized fluorescence intensity of 1 micromolar fura-2 with  $[Ca^{2+}]$  at 25°C, pH 7.2 and ionic strength of 0.2, in the presence of 1 millimolar  $Mg^{2+}$



## **Chapter 4**

### **Fluorometric Determination of Calcium in Milk Diffusate Using Quin-2 and Fura-2**

#### **1. Background**

##### **1.1. Measurement of extra-cellular ionic calcium**

So far the use of quin-2 and fura-2 has been limited to the determination of intracellular free calcium which exists in the submicromolar concentration range. Because of the greater affinity of these dyes for calcium,  $[Ca^{2+}]$  greater than  $1 \times 10^{-5}$  M cannot be detected easily.

In extra-cellular media (i.e. biological fluids) ionic calcium exists at the millimolar level, hence direct employment of quin-2 and fura-2 in these systems for calcium measurement is not satisfactory. Since these dyes show a great sensitivity to 0.1-0.5 micromolar free calcium, a strong chelator such as EGTA or EDTA can be added to sample with millimolar levels of calcium to tie up most of the calcium, leaving the free calcium in submicromolar concentration range. Then by addition of quin-2 or fura-2 to the sample and measuring the excitation spectra, one can estimate the free calcium concentration using dye-calcium calibration curves obtained at optimum conditions of the system. Then knowing the added amount of the chelator and the conditional association constant of chelator with calcium one can calculate the original concentration of the calcium in the sample.

$$K' = \frac{[\text{calcium-chelator complex}]}{[Ca^{2+}][\text{free chelator}]} \quad (4.1)$$

$$[\text{Chelator}]_{\text{total}} = [\text{free chelator}] + [\text{calcium-chelator complex}] \quad (4.2)$$

$$K' = \frac{[\text{calcium-chelator complex}]}{[\text{Ca}^{2+}][\text{chelator}]_{\text{total}} - [\text{calcium-chelator complex}]} \quad (4.3)$$

$$[\text{Calcium}]_{\text{total}} = [\text{Ca}^{2+}] + [\text{calcium-chelator complex}] \quad (4.4)$$

This is the same as making a Ca-EGTA or Ca-EDTA buffer with the difference that the total calcium concentration is unknown, hence one would not know how much of the chelator needs to be added in order to obtain the desired  $[\text{Ca}^{2+}]$ . Therefore, one should take a few portions of the sample and add different amount of the chelator to each portion and make the measurements till the free calcium concentration falls in the linear region of the calibration curve.

This method is applicable only under ideal conditions where there are no other ligands or complexes in the system, otherwise addition of a chelator with a high affinity for calcium and other divalent ions can disturb the system's equilibria. Also, if magnesium exists in the system, it will interfere with complexation of the dye with calcium, i.e., the chelator may partially bind magnesium and causes some error in the results.

We applied this method to the determination of total calcium in milk diffusate. Because ligands such as citrate and phosphate form complexes with calcium and magnesium, addition of strong chelators interfere with these complexes. Therefore one will not be able to add enough amount of the chelator to complex the free calcium without disturbing the equilibria in the rest of the system. This makes measurement of the free calcium rather difficult. Addition of an excess amount of chelator to the system can mask the magnesium and bind to most of the calcium, leaving a small amount of free calcium in the submicromolar

range which can be detected by one of the indicator dyes. Then using equations 4.1 to 4.4, one can calculate the concentration of total calcium present. Since quin-2 and fura-2 bind magnesium 4 to 5 orders of magnitude less strongly than they bind calcium, the exact amount of the magnesium in the sample need not be known. The approximate amount of  $Mg^{2+}$  in the sample can be estimated from the literature or be measured by other analytical techniques.

For the purpose of this work EDTA appears to be a more suitable chelator than EGTA. This is due to the fact that the binding affinity of EGTA for magnesium is quite comparable to those of citrate and phosphate, whereas EDTA binds magnesium about five orders of magnitude more strongly than citrate and phosphate.<sup>65</sup> Hence addition of EDTA to the milk diffusate can not only buffer calcium but also mask most of the magnesium.

## **1.2. Calcium in milk**

Calcium in milk exists in both colloidal and soluble forms. In a typical cow's milk about two-thirds of the total calcium is colloidal, mainly as a calcium phosphate complex with casein and as calcium bound directly to casein.<sup>72</sup> The soluble calcium and about half of the inorganic phosphate are diffusable.<sup>72,73</sup> In a milk ultrafiltrate or diffusate the univalent ions  $Na^+$ ,  $K^+$  and  $Cl^-$  exist largely as free ions, while the proton and multivalent ions such as  $Ca^{2+}$ ,  $Mg^{2+}$ ,  $PO_4^{3-}$  and  $Cit^{3-}$  are partially in the ionic form, and partially in the form of complexes such as  $HPO_4^{2-}$ ,  $CaCit^-$  and  $MgHPO_4$ .<sup>73,74</sup>

The soluble calcium is present in milk mainly in the forms of the free ion,  $CaCit^-$  and  $CaHPO_4$ .<sup>73,74</sup> Citrate binds strongly to calcium at the pH of milk to form a relatively soluble 1:1 calcium-citrate complex,  $CaCit^-$ , which has a much greater association constant than the less soluble calcium-phosphate complex

$\text{CaHPO}_4$ .  $\text{CaCit}^-$  is the largest component of the soluble calcium (about two-thirds). Complexes with sulfate and carbonate exist in very small amounts ( $< 0.005$  millimolar) in the diffusate. Variations in pH and temperature can affect the concentration of the complexes and the free ions.<sup>73,75</sup>

## **2. Experimental**

### **2.1 Solutions and reagents**

**Bulk skim milk.** Six 1 liter portions of fresh skim milk (Nu-maid) were mixed and divided into 2 portions of 2L and 2 portions of 1L for dialysis against DDW.

**0.0703 EDTA solution.** 6.603 g of disodium ethyldiamine tetraacetate (Fisher Scientific Company) was dissolved in DDW and diluted to 250 ml. The resulting solution was standardized against 0.1027 M  $\text{Ca}(\text{NO}_3)_2$  using 0.02 percent calcein solution as indicator.

**Standard solution of Na, K, Mg and Ca.** 0.1173g of NaCl, 0.3001g KCl, 12 ml of 0.025 M  $\text{MgCl}_2$ , and 22.8 ml of 0.0439 M  $\text{CaCl}_2$  were dissolved in DDW and diluted to 100 ml to make a solution of 20.0 millimolar  $\text{Na}^+$ , 40.0 millimolar  $\text{K}^+$ , 3.0 millimolar  $\text{Mg}^{2+}$  and 10.0 millimolar  $\text{Ca}^{2+}$ .

Solutions of quin-2, fura-2, calcium chloride, potassium chloride, MOPS, hydrochloric acid and potassium hydroxide were prepared the same way as in chapter 2 and chapter 3.

### **2.2 Apparatus**

All pH measurements were made to  $\pm 0.01$  with a Fisher -Accumet (model 520 digital) pH/Ion meter equipped with an Accu-pHast combination electrode.

Fluorescence spectra were obtained using a Shimadzu RF-5000 spectrofluorophotometer. The temperature of the fluorometer sample compartment was controlled to  $\pm 0.1$  degree with a K-4/RD Lauda/Brinkmann circulating water bath. Total Na, K, Mg and Ca concentrations in the milk diffusate samples were measured with an ARL 34000 multielement ICP-AES. The instrument was used under the following conditions: incident power of 1.15 KW, the coolant argon pressure of 32 psi, plasma argon pressure of 32 psi, nebulizer argon flow rate of 0.55 L/min and nebulizer uptake flow rate of 1 ml/min.

### **2.3 Procedure**

Samples of milk diffusate were prepared by dialysis of a volume of DDW against a much larger volume of skim milk, using water to milk ratios of 1:20 and 1:40 for a period of 48 hours at 4°C with constant stirring. Each dialysis process was done in duplicate. The containers were covered during the whole period to avoid water evaporation and contamination with the particles in air. Dialysis tubes (Spectra/Por, recorder number:132720) containing 50 ml of DDW were immersed in 1L of skim milk for the ratio of 1:20 and in 2L for the ratio of 1:40. At the end of 48 hours each tube contained about 30 ml of the diffusate, i.e., some water was lost through osmosis, hence a correction for the change of volume and concentration of the diffusable calcium in milk was necessary. Facilities in Dr. M. Palcic's laboratories were used for the preparation of these diffusate samples.

The diffusates were suctioned through a 0.2 micron membrane filter to remove any colloidal particles that entered the diffusate during dialysis. A small portion of each diffusate sample was analyzed for total magnesium, sodium, and potassium by ICP using a solution of 20 millimolar NaCl, 40 millimolar KCl, 3 millimolar MgCl<sub>2</sub> and 10 millimolar CaCl<sub>2</sub> as standard. The pH of the samples

were measured to  $\pm 0.01$  at  $37^{\circ}\text{C}$  and the ionic strength was estimated from the results obtained by ICP analysis and the literature values of citrate, phosphate and calcium obtained from typical milk diffusates at about the same pH.<sup>73,75</sup>

About 3 millimolar EDTA, 25 micromolar quin-2, and 10 millimolar MOPS buffer was added to 5 ml of each diffusate sample and the solution was diluted to 25 ml. The pH of the solutions were adjusted to  $6.68 \pm 0.01$  at  $37^{\circ}\text{C}$  and the ionic strength was adjusted to 0.065 by addition of the required amount of KCl. Since this analysis was for total calcium and not the ionic fraction, disturbance of the system equilibria by dilution and addition of KCl does not affect the results.

Standard calibration solutions of quin-2/calcium were prepared with 1 micromolar quin-2 and free calcium levels ranging from 0 to 0.5 micromolar at  $37^{\circ}\text{C}$  with no added magnesium, an ionic strength of 0.065, and a pH of 6.68. Similar sets of standards and sample solutions were prepared for fura-2 using 1 micromolar fura-2. Fluorescence spectra were collected with the RF-5000 fluorometer; each solution was filtered, deoxygenated, and adjusted to  $37^{\circ}\text{C}$  before measurements. All measurements were made in triplicate.

The amount of EDTA added was based on the estimated concentrations of magnesium and calcium obtained from ICP measurements and literature values. At the end the diffusate samples were analyzed for calcium directly by ICP using the 10 millimolar calcium standard solution, to verify the results obtained using EDTA and the indicator dyes.

### **3. Results and discussion**

Table 1-4 presents the results of the ICP analysis for total Na, K, Mg and Ca in milk diffusate. The measurements for the first three elements were made

after collecting the diffusate samples, in order to estimate the ionic strength of the system. The calcium was, however, measured by this technique after the fluorometric analysis to compare the results.

In figures 4-1 and 4-2 the calibration curves for the determination of the total calcium in milk diffusate are presented. The points shown with black dots represent the samples that are prepared by addition of enough EDTA to five-fold diluted milk diffusate samples. The added EDTA masks most of the magnesium and makes a calcium-EDTA buffer that leaves about 0.22 to 0.25 micromolar free calcium which is detectable by both quin-2 and fura-2. From the calibration curves one can estimate the amount of the free calcium detected by the indicator dye, then, knowing the conditional stability constant of Ca-EDTA,<sup>65</sup> the concentration of the added EDTA and the total magnesium in the solution (which would be one-fifth of the amount in the diffusate), one can calculate the total calcium in the diffusate.

$$K' = \frac{[\text{CaEDTA}]}{[\text{Ca}^{2+}] [[\text{EDTA}]_{\text{total}} - [\text{MgEDTA}] - [\text{CaEDTA}]]} \quad (4.5)$$

$$[\text{CaEDTA}] = \frac{K' [\text{Ca}^{2+}] [[\text{EDTA}]_{\text{total}} - [\text{MgEDTA}]]}{1 + K' [\text{Ca}^{2+}]} \quad (4.6)$$

The term  $[\text{Ca}^{2+}]$  can be ignored in equation 4.4, hence  $[\text{Calcium}]_{\text{total}} \approx [\text{CaEDTA}]$ . Since the diffusate is five fold diluted this value has to be multiplied by 5 to give the  $[\text{Calcium}]_{\text{total}}$  in the diffusate.

During the 48 hour period of dialysis about 20 ml of the water in the dialysis tube has entered the bulk milk. Changes of the volume from 1 liter to 1.02 liter and from 2 liter to 2.02 liter make the concentration of the calcium in the diffusate different from that of the actual diffusable calcium. The diffusable

calcium which would be in 1 and 2 liters rather than 1.02 and 2.02 liters was calculated and these values are shown in tables 4-3 and 4-4.

The values of total calcium measured by ICP-AES are very close to those obtained by the fluorometric technique. No major difference was observed in the calcium concentration of the diffusate samples obtained from the 1:20 and 1:40 water to milk ratio dialysis processes.



**Table 4-1** Concentrations of total sodium, total potassium, total magnesium and the total calcium in samples of milk diffusate obtained with ICP measurements.

Sample <sup>a</sup>	Na (mM)	RSD <sup>b</sup>	K (mM)	RSD	Mg (mM)	RSD	Ca (mM) <sup>c</sup>	RSD
1	19.51	1.6	34.85	0.7	2.83	0.8	9.47	1.2
2	19.83	1.1	35.01	2.0	2.90	1.2	9.55	1.2
3	19.46	1.3	35.18	1.4	2.85	1.8	9.38	1.6
4	19.77	0.9	34.92	1.1	2.79	0.9	9.45	0.9

<sup>a</sup> Samples 1 & 2 are obtained from the dialysis of 1 portion of DDW against 20 portions of skim milk, and samples 3 & 4 are the results of the dialysis of 1 portion of water against 40 portions of skim milk.

<sup>b</sup> Relative standard deviation in percent.

<sup>c</sup> Calcium measurements with ICP were made at the end of the experiment to verify the values obtained by the fluorometric technique.

**Table 4-2** Variation of the normalized fluorescence intensity of 25 micromolar quin-2 and 1 micromolar fura-2 with  $[Ca^{2+}]$  in the concentration range of 0 to 0.5 micromolar at 37°C, pH 6.68 and ionic strength of 0.065.

$[Ca^{2+}]$ (micromolar)	Norm. Int. <sup>a</sup> (quin-2)	RSD <sup>b</sup>	Norm. Int. <sup>c</sup> (fura-2)	RSD
0.000	0.000	-	0.000	--
0.010	0.103	0.8	0.093	1.8
0.020	0.405	1.1	0.201	2.0
0.050	1.073	1.4	0.447	2.3
0.150	3.654	1.7	1.140	2.7
0.250	5.421	2.0	1.930	1.6
0.500	10.55	0.9	3.880	2.1
1000	-	-	-	-

<sup>a</sup> Normalized intensity;  $[(I_f - I_{f(\min)}) / (I_{f(\max)} - I_f)]$  (see the footnote for table 3-2)

<sup>b</sup> Relative standard deviation of the normalized intensity in percent, calculated by the procedure of footnote d in table 2-1.

<sup>c</sup> Normalized Intensity;  $[(R - R_{\min}) / (R_{\max} - R)]$  B (see the footnote for table 3-3)

**Table 4-3 Results of the analysis of milk diffusate samples for calcium using fluorometric technique and quin-2 dye.**

Sample	Normalized Intensity <sup>a</sup>	RSD <sup>b</sup>	[Ca <sup>2+</sup> ] <sup>c</sup> (micromolar)	[Ca] <sub>T</sub> (diffusate) <sup>d</sup> (millimolar)	[Ca] <sub>T</sub> (diffusable) <sup>e</sup> (millimolar)
1	4.920	2.1	0.228	9.05	9.50
2	5.240	1.5	0.243	9.14	9.60
3	5.010	2.2	0.232	9.08	9.31
4	5.149	1.1	0.239	9.19	9.51

<sup>a</sup> Normalized intensity;  $[(I_f - I_{f(\min)}) / (I_{f(\max)} - I_f)]$  (see the footnote for table 3-2)

<sup>b</sup> Relative standard deviation of the normalized intensity in percent, calculated by the procedure of footnote d in table 2-1.

<sup>c</sup> The concentration of the free calcium in the solutions containing milk diffusate and EDTA, obtained from the fluorometric measurements.

<sup>d</sup> Total calcium in the diffusate samples

<sup>e</sup> Total diffusable calcium in the bulk milk. A correction was made for volume change in milk during the dialysis process. The total moles of calcium in the diffusate (30 ml) was added to the total calcium in the bulk milk (1020 ml for samples 1 & 2 and 2020 ml for samples 3 & 4) and divided by 1000 for samples 1 & 2 and 2000 for samples 3 & 4) to obtain the total diffusable calcium in milk

**Table 4-4** Results of the analysis of the milk diffusate samples for calcium using fluorometric technique and fura-2 dye.

Sample	Normalized Intensity <sup>a</sup>	RSD <sup>b</sup>	[Ca <sup>2+</sup> ] <sup>c</sup> (micromolar)	[Ca] <sub>T</sub> (diffusate) <sup>d</sup> (millimolar)	[Ca] <sub>T</sub> (diffusable) <sup>e</sup> (millimolar)
1	1.710	2.8	0.219	8.96	9.41
2	1.850	3.0	0.238	9.10	9.55
3	1.771	2.7	0.227	9.02	9.49
4	1.839	2.4	0.235	9.15	9.75

<sup>a</sup> Normalized Intensity;  $[(R - R_{\min}) / (R_{\max} - R)]B$  (see the footnote for table 3-3)

<sup>b, c, d, e</sup> See the footnote for table 4-3

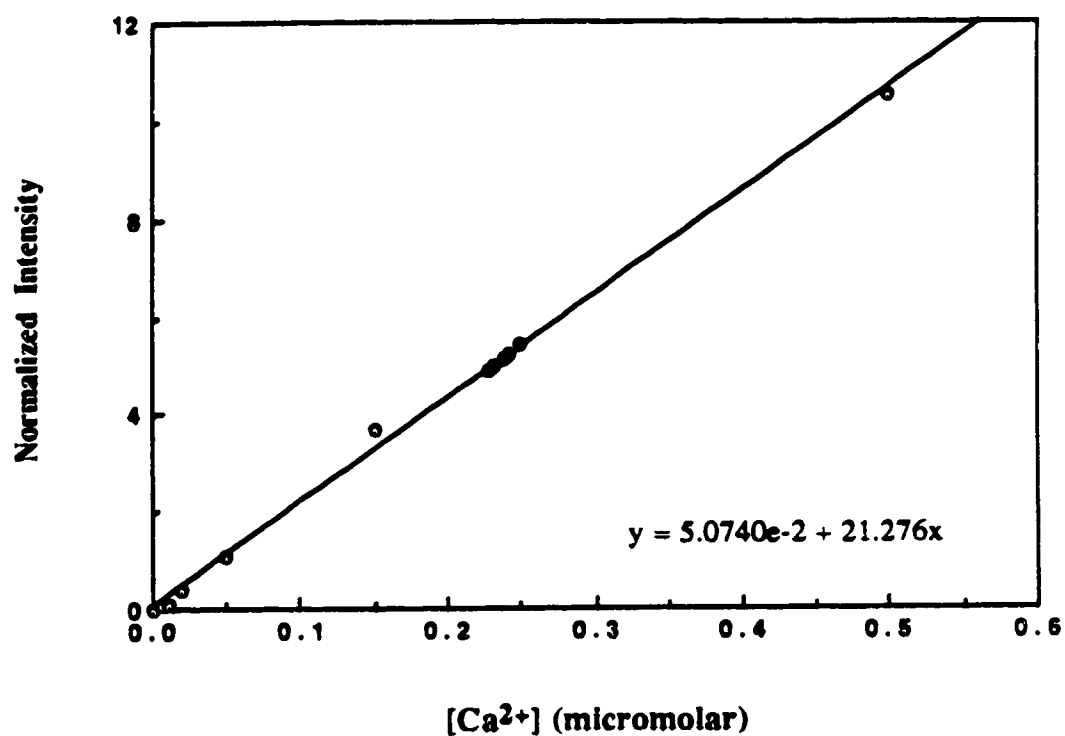


**Figure 4-1** Calibration curve for the determination of [Ca<sup>2+</sup>] in solutions containing milk diffusate samples using quin-2 indicator dye. (o) represents the standard calibration solutions and (•), the sample solutions.

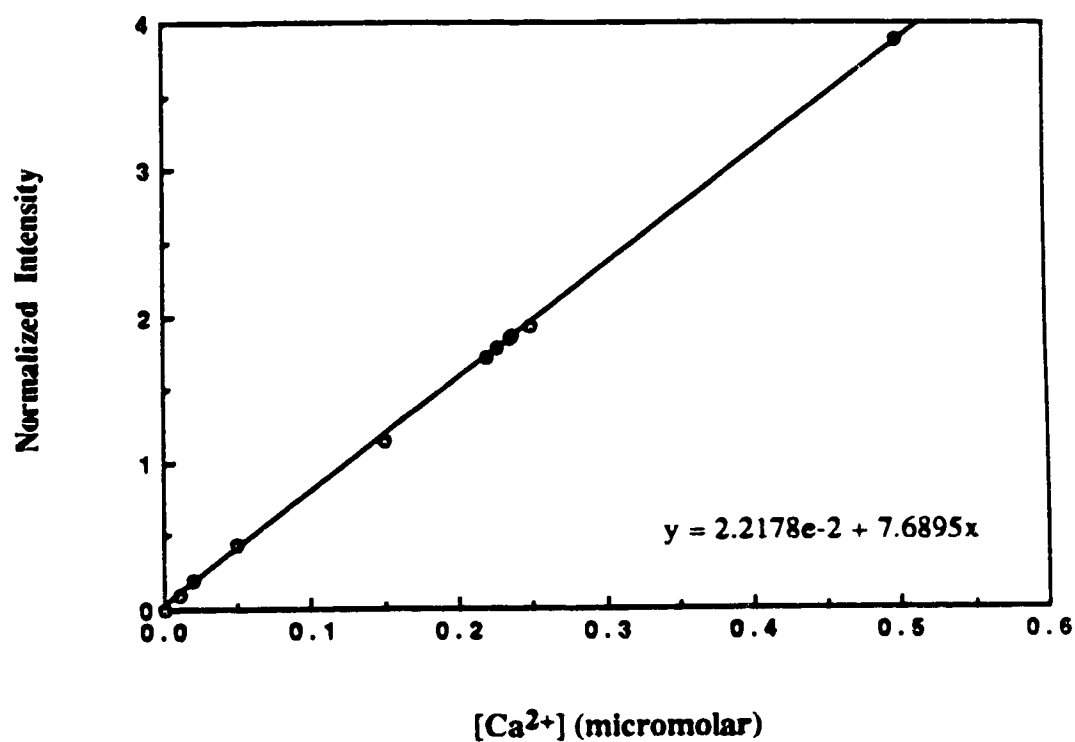


**Figure 4-2** Calibration curve for the determination of [Ca<sup>2+</sup>] in solutions containing milk diffusate samples using fura-2 indicator dye. (○) represents the standard calibration solutions and (●), the sample solutions.

## **Chapter 5**

### **Conclusions and Future Work**

#### **1. Conclusions**

The fluorometric determination of calcium using quin-2 and fura-2 indicator dyes is a very sensitive technique. It also has great selectivity for calcium over magnesium, and the experimental data show good reproducibility of the results. The main disadvantage of this technique for many applications is however, insensitivity of the dyes to  $[Ca^{2+}]$  greater than  $1 \times 10^{-5}$  M which limits the use of these indicators for calcium determinations in biological fluids. Another drawback in the use of these dyes is the fact that they are quite expensive, and are not very stable on storage.

In a comparison between quin-2 and fura-2 as calcium indicators one may find fura-2 preferable because: ( 1 ) it has a higher degree of stability against energetic radiation, temperature and oxygen quenching. ( 2 ) The fluorescence intensity of fura-2 is about 25 times greater than that for quin-2, which means that only 1 micromolar fura-2 is required to obtain the same sensitivity as 25 micromolar quin-2. ( 3 ) Because fura-2 has a lower affinity for calcium compared to quin-2, it is able to detect calcium at larger concentrations. ( 4 ) Binding of fura-2 to  $Ca^{2+}$  alters the excitation wavelengths as well as the peak intensity. When using this dye, therefore, one can take the ratio of intensities at two different wavelengths rather than making the measurements at only one wavelength. This eliminates the effects of many other factors such as dye concentration and emission efficiency.

## **2. Future Work**

In the present study the use of quin-2 and fura-2 dyes for the determination of ionic calcium at submicromolar levels and total calcium at millimolar levels was shown. For direct measurement of millimolar calcium without disturbing the equilibria of a system the dyes need to be modified in such a way that they have a lower affinity for calcium and even less for magnesium than the present forms do.

Becker and Fay<sup>76</sup> examined the spectral properties of fura-2 and its sensitivity to calcium after exposure to excitation light for some time. The dye appeared to partially decompose to an intermediate product that could bind to calcium in the millimolar concentration range. This study was not explored further and the photobleached fura-2 was not investigated in physiological samples.

The main problem with the use of such a product would be that the variation of the fluorescence signal between the sample with 0.05 millimolar free calcium and the one with 50 millimolar free calcium is only about 8%, while that for 5 and 50 millimolar is about 4%. Hence the system is not sensitive enough to small variations in  $[Ca^{2+}]$ . Also the sensitivity of this product for calcium in the presence of magnesium was not examined.

Further research in this line may, however, lead to modifications of these dyes in such a way that they become sensitive to millimolar free calcium and at the same time less responsive to magnesium.



## **Bibliography**

1. Wasserman et al. *Calcium-Binding Proteins and Calcium Function*; North-Holland: New York, 1977
2. Urban, P.; Buchmann, G.; Scheidegger, D. *Clin. Chem.* **1985**, *31*, 264.
3. Hodgkinson, A.; Nordin, B. E. C. *Proceedings of the Renal Stone Symposium*; Churchill: London, 1968
4. Dalquist, R. L.; Knoll, J. W. *Appl. Spect.* **1978**, *32 (1)*, 1.
5. Olesik, J. W. *Anal. Chem.* **1991**, *63 (1)*, 12A.
6. Trudeau, L. D.; Freier, E. F. *Clin. Chem.* **1967**, *13*, 101.
7. Grunbaum, B. W.; Pace, N. *Microchem. Journal.* **1970**, *15*, 666.
8. Perrin, D. D. *Masking and Demasking of Chemical Reactions*; Wiley & Sons: New York, 1970
9. Harris, W. E.; Kratochvil, B. *An Introduction to Chemical Analysis*; Saunders College: Philadelphia, 1981
10. Gaur, S. S.; Nancollas, G. H. *Kidney Int.* **1984**, *26*, 767.
11. Ladenson, H.; Bowers, G. N. *Clin. Chem.* **1973**, *19*, 575.
12. Robertson, W. G.; Marshall, R. W. *CRC Crit. Rev. Clin. Lab. Sci.* **1981**, *15*, 85.
13. Selwyn, J. R.; Barkeley, J.; Loken, H. F. *Clin. Chem.* **1984**, *30*, 304.
14. Thode, J.; Holmegard, S. N.; Transbol, J.; Anderson, N. F.; Anderson, O. S.; *Clin. Chem.* **1990**, *36*, 541.
15. Umemoto, M.; Tani, W.; Kuwa, K.; Ujihira, Y. *Anal. Chem.* **1994**, *66(6)*, 352A.
16. Thode, J.; *Scand. J. Clin. Lab. Invest.* **1985**, *45*, 327.
17. Yatzidis, H. *Clin. Nephrol.* **1985**, *23*, 63.
18. Nordin, B. E. C. *The Lancet* **1962**, *1*, 409.

19. Robertson, W. G.; Peacock, M.; Nordin, B. E. C. *Clin. Sci.* 1968, 34, 579.
20. Cham, B. E. *Clin. Chim. Acta* 1972, 37, 5.
21. Robertson, W. G. *Ann. Clin. Biochem.* 1976, 13, 540.
22. Hewavitharana, A. K. *Study of Ionized Calcium and Magnesium Measurements by Ion Exchange/Atomic Absorption*; Ph.D. Thesis, Department of Chemistry, University of Alberta, 1991
23. Bronner, F. *Intracellular Calcium Regulation*; Wiley-Liss: 1990
24. Ciba Foundation Symposium 122; *Calcium and the Cell*; Wiley & Sons: Chichester, 1983
25. Tsien, R. Y. *Annu. Rev. Biophys. Bioeng.* 1983, 12, 101.
26. Oehme, M.; Kessler, M.; Simon, W. *Chimia.* 1976, 30, 204.
27. Tsien, R. Y. *Annu. Rev. Biophys. Bioeng.* 1983, 12, 103.
28. Blinks, J. R.; Prendergast, F. G.; Allen, D. G. *Pharmacol. Rev.* 1976, 28, 1.
29. Blinks, J. R.; Mattingly, P. H.; Jewell, B. R.; Leewen, M.; Harrer, G. C.; Allen, D. G. *Methods Enzymol.* 1978, 57, 292.
30. Tsien, R. Y. *Annu. Rev. Biophys. Bioeng.* 1983, 12, 104.
31. Brown, J. E.; Brown, P. K.; Pinto, L. H. *J. Physiol. (London)* 1977, 267, 299.
32. Tsien, R. Y. *Annu. Rev. Biophys. Bioeng.* 1983, 12, 105.
33. Tsien, R. Y.; Pozzan, T.; Rink, T. J. *J. Cell Biol.* 1982, 94, 325.
34. Garestier, T. M. Dafilho, M. D.; Devynck, M. A. *Cell Calcium* 1988, 9, 167.
35. LuK'acs, G. L.; Kapus, A. *Biochem. J.* 1987, 248, 609.
36. Hesketh, T. R.; Smith, G. A.p; Moore, J. P.; Taylor, M. V.; Metcalfe, J. C. J. *Biol. Chem.* 1983, 258(8), 4876.
37. Komada, H.; Nakabayashi, H.; Nakano, H.; Hara, M.; Yoshida, T.; Takanari, H.; Izutsu, K. *Cell Struc. Func.* 1989, 14, 141.
38. Ross, J. W. *Science* 1967, 156, 1378.

39. Freaney, R.; Egan, T.; McKenna, M. J.; Doolin, M. C.; Muldowney, F. P. *Clin. Chim. Acta* 1986, 158, 129.
40. Hansen, A. C.; Engel, K.; Kilderberg, P.; Wamberg, S. *Clin. Chim. Acta* 1977, 79, 507.
41. Baker, J.M.; Gehrke, C. W.; Affsprung, H. E. *J. Dairy Sci.* 1954, 37, 1409.
42. Christianson, G.; Jenness, R.; Coulter, S. T. *Anal. Chem.* 1954, 26, 1923.
43. Muldoon, P. J.; Liska, B. J. *J. Dairy Sci.* 1969, 52, 460.
44. Brown, H. M.; Pemberton, J. P.; Owen, J. D. *Anal. Chim. Acta* 1976, 85, 261.
45. Shimomura, O.; Johnson, F. H.; Saiga, Y. *J. Cell Comp. Physiol.* 1962, 59, 223.
46. Shimomura, O.; Johnson, F. H.; Saiga, Y. *Science* 1963, 140, 1339.
47. Ashley, C.C.; Ridgway, E. B. *Nature (London)*, 1968, 219, 1168.
48. Ashley, C.C.; Ridgway, E. B. *J. Physiol. (London)* 1970, 209, 105.
49. Borle, A. B.; Snowdowne, K. W. *Science* 1982, 217, 252.
50. Hallet, M. B.; Cambell, A. K. *Nature* 1982, 295, 155.
51. Rios, E.; Schneider, M. F. *Biophys. J.* 1981, 36, 607.
52. Thomas, M. V. *Biophys. J.* 1979, 25, 541.
53. GrynKiewicz, G.; Poenie, M.; Tsien, Y. *J. Biol. Chem.* 1985, 260, 3440.
54. Tsien, R. Y.; *Biochemistry*, 1980, 19, 2396.
55. Ewing, G. N. *Instrumental Methods of Chemical Analysis*; McGraw-Hill: New York, 1985; p. 124.
56. Miller, J. N. *Standards in Fluorescent Spectrometry*; Chapman and Hall: London, 1981
57. Schenk, G. H.; *Absorption of Light and Ultraviolet Radiation*; Allyn and Bacon: Boston, 1973; p. 124.

58. Guilbault, G. G. *Practical Fluorescence, Theory, Methods and Techniques*; Marcel Dekker: New York, 1973
59. Skoog, D. A.; West, D. M. *Principles of Instrumental Analysis*; Saunders College: Philadelphia, 1980
60. Harris, D. C. *Quantitative Chemical Analysis*; Freeman: New York, 1991
61. Robinson, K. A. *Chemical Analysis*; Little and Brown: Boston, 1987
62. Olsen, E.D. *Modern Optical Methods of Analysis*; McGraw-Hill: New York, 1975; p. 381.
63. Parker C. A. *Photoluminescence of Solutions*; Elsevier: Amsterdam, 1968
64. Diehl, H. *Calcein, Calmagite, and O,O'-Dihydroxyazobenzene. Titrimetric, Colorimetric, and Fluorometric Reagents for Calcium and Magnesium*; G. F. Smith Chemical Company: columbus, 1964; p. 28.
65. Smith, R. M.; Martell, A. E. *Critical Stability Constants*; Plenum: New York, 1975
66. Melhuish, W. H. *J. Opt. Soc. Amer.* **1961**, *51*, 278.
67. Weast, R. C. *Hand Book of Chemistry and Physics*; CRC: Cleveland, 1972-1973, p. E-209.
68. Blinks, J. R.; Wier, W. G.; Hess, P.; Prendergast, F. G. *Prog. Biophys. Mol. Biol.* **1982**, *40*, 109.
69. Atkins, P. W. *Physical Chemistry*; Freeman: New York, 1990; p. 141.
70. Tsien, R. Y.; Poenie. M. *Trends in Biochemical Sciences.* **1986**, *11*, 450.
71. Tsien, R. Y.; Rink, T. J.; Poenie, M. *Cell Calcium.* **1985**, *6*, 145.
72. Holt, C. J. *Dairy Sci.* **1980**, *64*, 1958.
73. Fox, P.F. *Developement in Dairy Chemistry-3*; Elsevier Applied Science Publishers: London, 1982; p. 143
74. Holt, C.; Muir, D. J. *Dairy Res.* **1979**, *46*, 433.

- 75. Davis, D. T.; White, C. D. *J. Dairy Res.* **1960**, *27*, 171.
- 76. Becker, P.L.; Fay, F. S. *Am. J. Physiol.* **1987**, *253*, C613.

## **Appendix A**

In order to maintain the desired  $[Ca^{2+}]$  a calcium metal ion buffer system using EGTA was set up. To prepare such a buffer solution one must know the conditional association constant ( $K'$ ) of Ca-EGTA under the conditions of the experiment, so that one can estimate the amount of  $K_2H_2EGTA$  and  $CaCl_2$  that need to be added. The pertinent equation is

$$K' = \frac{[CaEGTA]}{[Ca^{2+}][EGTA_T - CaEGTA]} \quad (A.1)$$

where  $EGTA_T$  is the total EGTA in the system. Charges on all the species have been omitted for simplicity.

### **Calculation of $K'$ for Ca-EGTA**

The thermodynamic association constants for EGTA at 20°C and ionic strength ( $\mu$ ) of 0.1 are shown in table A-1. The value of  $K'$  for Ca-EGTA at 25°C, pH 7.2 and  $\mu$  of 0.2 can be calculated in three steps:

Step 1 - Calculation of  $K_{HEGTA}^H$ ,  $K_{H_2EGTA}^H$ ,  $K_{CaEGTA}^{Ca}$  and  $K_{CaHEGTA}^{Ca}$  at 25°C and  $\mu$  of 0.1:

According to equation 3.1,

$$\log K_{25^\circ C} = \log K_{20^\circ C} + \frac{\Delta H}{2.303R} \left( \frac{1}{293} - \frac{1}{298} \right) \quad (A.2)$$

hence at 25°C,

$$K_{HEGTA}^H = 2.49 \times 10^9$$

$$K_{CaEGTA}^{Ca} = 7.39 \times 10^{10}$$

$$K_{H_2EGTA}^H = 5.98 * 10^8$$

$$K_{CaHEGTA}^{Ca} = 1.58 * 10^5$$

Step 2 - Calculation of  $K_{HEGTA}^H$ ,  $K_{H_2EGTA}^H$ ,  $K_{CaEGTA}^{Ca}$  and  $K_{CaHEGTA}^{Ca}$  at 25°C and  $\mu$  of 0.2:

According to equation 3.3,

$$K^\circ = K \left( \frac{\gamma_{ML}}{\gamma_M \gamma_L} \right)$$

Also, based on equation 3.4,

$$K_{0.2} = K_{0.1} \left( \frac{\gamma_{ML}}{\gamma_M \gamma_L} \right)_{0.1} \left( \frac{\gamma_M \gamma_L}{\gamma_{ML}} \right)_{0.2} \quad (A.3)$$

The activity coefficients at each ionic strength are calculated using the Davies equation (equation 3.5).

$$\begin{aligned} (\gamma^{\pm 1})_{0.1} &= 0.781 & (\gamma^{\pm 1})_{0.2} &= 0.746 \\ (\gamma^{\pm 2})_{0.1} &= 0.372 & (\gamma^{\pm 2})_{0.2} &= 0.310 \\ (\gamma^{\pm 3})_{0.1} &= 0.108 & (\gamma^{\pm 3})_{0.2} &= 0.072 \\ (\gamma^{\pm 4})_{0.1} &= 0.019 & (\gamma^{\pm 4})_{0.2} &= 0.009 \end{aligned}$$

Hence,

$$(K_{HEGTA}^H)_{0.2} = (K_{HEGTA}^H)_{0.1} \left( \frac{\gamma^{\pm 3}}{\gamma^{\pm 1} \gamma^{\pm 4}} \right)_{0.1} \left( \frac{\gamma^{\pm 1} \gamma^{\pm 4}}{\gamma^{\pm 3}} \right)_{0.2} = 1.73 * 10^9$$

$$(K_{H_2EGTA}^H)_{0.2} = (K_{H_2EGTA}^H)_{0.1} \left( \frac{\gamma^{\pm 2}}{\gamma^{\pm 1} \gamma^{\pm 3}} \right)_{0.1} \left( \frac{\gamma^{\pm 1} \gamma^{\pm 3}}{\gamma^{\pm 2}} \right)_{0.2} = 4.57 * 10^8$$

$$(K_{CaEGTA}^{Ca})_{0.2} = (K_{CaEGTA}^{Ca})_{0.1} \left( \frac{\gamma^{\pm 2}}{\gamma^{\pm 2} \gamma^{\pm 4}} \right)_{0.1} \left( \frac{\gamma^{\pm 2} \gamma^{\pm 4}}{\gamma^{\pm 2}} \right)_{0.2} = 3.58 * 10^{10}$$

$$(K_{CaHEGTA}^{Ca})_{0.2} = (K_{CaHEGTA}^{Ca})_{0.1} \left( \frac{\gamma^{\pm 1}}{\gamma^{\pm 2} \gamma^{\pm 3}} \right)_{0.1} \left( \frac{\gamma^{\pm 2} \gamma^{\pm 3}}{\gamma^{\pm 1}} \right)_{0.2} = 9.19 \times 10^4$$

Step 3 - Calculation of  $K'$  for Ca-EGTA at 25°C,  $\mu$  of 0.2 and pH 7.2:

According to equations 3.8 and 3.15,

$$K' = K'_{CaEGTA} + K'_{CaHEGTA} \quad (A.4)$$

$$K'_{CaEGTA} = K_{CaEGTA}^{Ca} \left( \frac{1}{1 + K_{HEGTA}^H [H^+] + K_{HEGTA}^H K_{H_2EGTA}^H [H^+]^2} \right) \quad (A.5)$$

$$K'_{CaHEGTA} = K_{CaHEGTA}^{Ca} \left( \frac{K_{HEGTA}^H [H^+]}{1 + K_{HEGTA}^H [H^+] + K_{HEGTA}^H K_{H_2EGTA}^H [H^+]^2} \right) \quad (A.6)$$

hence,

$$K' = 1.10 \times 10^7 \text{ M}^{-1} + 3.08 \times 10^3 \text{ M}^{-1} = 1.10 \times 10^7 \text{ M}^{-1}$$

The contribution of the monoprotonated species to  $\text{Ca}^{2+}$  binding is negligible, therefore the second term in equation A.4 can be ignored.

#### Estimation of the total amount of EGTA and calcium present in system

The non-bound or the free EGTA is 2 millimolar, so the total EGTA and calcium can be given as:

$$[\text{EGTA}]_T = [\text{CaEGTA}] + 2 \times 10^{-3} \quad (A.7)$$

$$[\text{Calcium}]_T = [\text{CaEGTA}] + [\text{Ca}^{2+}] \quad (A.8)$$



Equation A.1 can be written as:

$$[\text{CaEGTA}] = 2 * 10^{-3} K' [\text{Ca}^{2+}] \quad (\text{A.9})$$

and substituting in equations A.7 and A.8,

$$[\text{EGTA}]_T = 2 * 10^{-3} K' [\text{Ca}^{2+}] + 2 * 10^{-3} \quad (\text{A.10})$$

$$[\text{Calcium}]_T = 2 * 10^{-3} K' [\text{Ca}^{2+}] + [\text{Ca}^{2+}] \quad (\text{A.11})$$

For solutions containing 1 millimolar  $\text{Mg}^{2+}$ , the  $K'$  of Mg-EGTA must also be calculated in order to make a Ca-Mg-EGTA buffer.

Step 1 - The absolute association constants of Mg-EGTA at 25°C and  $\mu$  of 0.1 are calculated using the information in table A-1.

$$K_{\text{MgEGTA}}^{\text{Mg}} = 1.87 * 10^5 \quad K_{\text{MgHEGTA}}^{\text{Mg}} = 2.90 * 10^3$$

Step 2 - The absolute association constants are calculated at 25°C and  $\mu$  of 0.2.

$$(K_{\text{MgEGTA}}^{\text{Mg}})_{0.2} = 9.07 * 10^4 \quad (K_{\text{MgHEGTA}}^{\text{Mg}})_{0.2} = 1.69 * 10^3$$

Step 3 - The apparent association constant for Mg-EGTA at 25°C,  $\mu$  of 0.2 and pH of 7.2 is:

$$\begin{aligned} K' &= K_{\text{MgEGTA}}^{\text{Mg}} + K_{\text{MgHEGTA}}^{\text{Mg}} \\ &= 27.83 + 56.53 = 84.36 \end{aligned} \quad (\text{A.12})$$

In order to have 1 millimolar free magnesium and 2 millimolar free EGTA, one must use the  $K'$  values for Ca-EGTA and Mg-EGTA to calculate the total amounts of magnesium, calcium and EGTA that need to be added to the system. Therefore,

$$[\text{Magnesium}]_T = 1.17 \times 10^{-3} \text{ M}$$

$$[\text{EGTA}]_T = [\text{CaEGTA}] + 2.17 \times 10^{-3} \text{ M}$$

$$= 2.17 \times 10^{-3} K' [\text{Ca}^{2+}] + 2.17 \times 10^{-3} \text{ M}$$

$$[\text{Calcium}]_T = 2.17 \times 10^{-3} K' [\text{Ca}^{2+}] + [\text{Ca}^{2+}]$$

**Table A-1** Thermodynamic association constants for EGTA at 20°C and ionic strength of 0.1.<sup>65,68</sup>

<u>Association constant expression</u>	<u>log K</u>	<u>ΔH (KJ/mole)</u>
$K_{CaEGTA}^{Ca} = \frac{[CaEGTA^{2-}]}{[Ca^{2+}][EGTA^{4-}]}$	10.97	-33.89
$K_{CaHEGTA}^{Ca} = \frac{[CaHEGTA^{1-}]}{[Ca^{2+}][HEGTA^{3-}]}$	5.30	-33.89
$K_{MgEGTA}^{Mg} = \frac{[MgEGTA^{2-}]}{[Mg^{2+}][EGTA^{4-}]}$	5.21	20.92
$K_{MgHEGTA}^{Mg} = \frac{[MgHEGTA^{1-}]}{[Mg^{2+}][HEGTA^{3-}]}$	3.40	20.92
$K_{HEGTA}^H = \frac{[HEGTA^{3-}]}{[H^{1+}][EGTA^{4-}]}$	9.47	-24.27
$K_{H_2EGTA}^H = \frac{[H_2EGTA^{2-}]}{[H^{1+}][HEGTA^{3-}]}$	8.85	-24.27